Selenoproteins in Cancer Etiology

BY

Dede N. Ekoue

B.S., University of Illinois at Urbana-Champaign, Urbana-Champaign, 2007

THESIS

Submitted as a partial fulfillment of requirements

for the degree of Doctor of Philosophy in Pathology

in the Graduate College of the

University of Illinois at Chicago, 2016

Chicago, Illinois

Defense Committee:

Alan M. Diamond, Advisor

Maarten Bosland, Chair

Andre Kajdacsy-Balla

Marcelo Bonini, Medicine

Jeremy Johnson, Pharmacy Practice

Cette rédaction est dediée à mon Seigneur et Sauver qui a été toujours à mes côtés tout le long de ma carière academique en tant qu'étudiante en doctorat mais aussi les deux dernières années pendant lesquelles j'ai véçue une période émotionellement bouleversante et de peur. Il est la raison pour laquelle je peux sourire et regarder positivement vers l'avenir.

ACKNOWLEDGEMENTS

I would like to express my sincere gratitude to my mentor Dr. Alan M. Diamond for his guidance and unwavering support throughout the course of this work. I came to the Diamond lab a shy soft-spoken Togolese woman and can now confidently leave with an expanded perspective and greatly improved scientific thought.

I am also grateful to my thesis committee professors Dr. Maarten Bosland, Dr. Andre Kadjacsy-Balla, Dr. Marcelo Bonini and Dr. Jeremy Johnson for their support and suggestions. I would like to also thank my collaborators Dr. Vincent Freeman, Mr. Matthew Picklo, Dr. Peter Gann and Ryan Deaton for their patience, help, and suggestions. A special thanks to Dr. Klara Valyi-Nagy for her willingness to help and for ensuring a one day turnaround time for every tissue sample I needed for optimization studies.

I admire Dr. Emmanuel Ansong who was my first rotation trainer in laboratory research and the driving force behind me becoming confident and boosting my morale and productivity during the numerous times I doubted myself as a scientist. He is genuinely an exceptional scientist and friend who has positively impacted me in more ways than one. I am forever indebted.

I am very fortunate to have colleagues whose support I have enjoyed throughout these past years. Thank you Dr. Soumen Bera and Dr. Frank Weinberg for making the initial observations which inspired critical elements of my project, and helping me with continuing your work. I thank Dr. Peter Hart for his training and his genuine friendship. Even after graduating, he is still extending his support. Thank you to Dr. Emily Reinke for her training and support as well as to Dr. Sofia Zaichick for her many contributions.

I would also like to thank my family for always supporting my academic adventures. My deepest gratitude to my mother Catherine who has sacrificed a lot to ensure my academic success, to my father Jacob whose dream of immigrating to the US has traced the path for the academic success of his children, to my sister Florence and brother Wilfrid for their support. I would like to thank my brother in law Simon, my nephews Samuel and Josias for their monthly calls and concerns as to when will I actually start making money as a scientist to buy them all the toys they desire.

To my extended family members, Mrs. Meryl Diamond and Mrs. Janice Ansong for their moral support as well as for always making sure that I am not alone nor without food. I am also appreciative of the Ayite and Lassey family for their support and prayers.

Finally, I would like to thank Laurent for his understanding and encouragement. I thank him for everything big and small he's done for me these past years. I know that it has been an emotional rollercoaster these past two years but having him by my side has made all the difference. I am so blessed to have him in my life and thank him from the bottom of my heart.

ACKNOWLEDGEMENT OF CONTRIBUTIONS

This thesis project was designed and performed by the author, Dede N. Ekoue. Other collaborators have provided conceptual and technical guidance for all aspects of the project and these are described below.

Chapter II. Methods

Generation of MCF-7 GPx-1 and MnSOD cell lines-Soumen Bera

VECTRA quantitative imaging analysis-Ryan Deaton and Emmanuel Ansong

Chapter III. Results

Figure 4: Soumen Bera and Frank Weinberg- Cell culture and western blotting analysis

Figures 12 and 16: -Sofia Zaichick-Quantification of nuclear Nrf2

Figures 15 and 16- Peter C. Hart-CMXROS assay

Table 3: Alan M. Diamond- Table design

Figures 19, 20 and 21: Andy Hall and Rami Hayajneh-Immunohistochemistry

Figure 22 and Table 6: Ryan Deaton and Li C. Liu-Statistical analysis

Tables 4 and 5: Ryan Deaton and Rawan Al-Lozi-Statistical analysis

Figure 27: Alan M. Diamond-Figure design

Appendix: Emmanuel Ansong-Table design

TABLE OF CONTENTS

TABLE OF CONTENTS

LIST OF TABLES

LIST OF FIGURES

LIST OF FIGURES

FIGURES PAGE

LIST OF ABBREVIATIONS

Se- selenium

Sec- selenocysteine

ROS - reactive oxygen species

H_2O_2- hydrogen peroxide

MnSOD - manganese superoxide dismutase

GPx1 - glutathione peroxidase-1

Nrf-2 - nuclear factor (erythroid–derived 2)-like 2

E-Cadherin–epithelial Cadherin

Akt–protein kinase B

p-Akt–Ser473 phosphorylated Akt

Sirt3–NAD-Dependent Deacetylase Sirtuin-3

Bcl-2–B-Cell CLL/Lymphoma 2

OCR - oxygen consumption rate

ECAR - extracellular acidification rate

Sep15–Selenoprotein 15

SEPP1, SelP- Selenoprotein P

SBP1- Selenium binding protein 1

GAPDH- Glyceraldehyde 3-phosphate dehydrogenase

UGGT- UDP-glucose: glycoprotein glucosyl transferase

NPC- Nutritional Cancer Prevention Trial

SELECT- Selenium and Vitamin E Cancer Trial

SUMMARY

Selenium (Se) exerts its effect on human health in part through its incorporation into selenoproteins in the form of selenocysteine (Sec), which is encoded by a UGA codon. Sec is present at the active site of selenoproteins glutathione peroxidase-1 (GPx-1) and selenoprotein 15 (Sep15).

Reactive oxygen species are implicated in the etiology of cancer and are controlled by antioxidant proteins manganese superoxide dismutase (MnSOD) and glutathione peroxidase-1 (GPx-1). The conversion of superoxide into H_2O_2 and its subsequent detoxification into water is catalyzed by MnSOD and GPx-1 respectively. The current study provides evidence for the existence of a molecular interaction between polymorphic variants of these antioxidant enzymes, and elucidates their combined effects in modulating ROS, and the levels proteins implicated in cancer. Although critical pathways are altered by these antioxidant enzymes, their expression was not an indicator of biochemical recurrence after radical prostatectomy.

Sep15 has been reported to be located in the endoplasmic reticulum (ER), and occurs in a complex with UDP-glucose: glycoprotein glucosyltransferase (UGGT). It is suspected to be involved in ensuring the structural fidelity of N-linked glycoproteins. This study describes a novel subcellular localization of the protein to the plasma membrane in human prostate tissue and reports that this location is different in cancers compared with benign tissue. Allelic variations in the Sep15 gene that have been associated with decreased Sep15 levels and increased prostate cancer mortality were confirmed to be more prevalent in African American men than Caucasians. It was also shown that Sep15 levels in prostate carcinomas do not predict prostate cancer recurrence, but identifying men carrying the functional genetic variant that is associated

with lower Se levels may allow stratifying individuals at risk of prostate cancer who may benefit from Se supplementation.

I. INTRODUCTION

This thesis project is divided into two studies investigating the role of selenium-containing proteins GPx-1 and Sep15 in cancer etiology. First, the molecular interaction between polymorphic variants of GPx-1 and MnSOD in modulating the levels of proteins implicated in cancer were investigated, as well as whether GPx-1 and MnSOD protein levels are predictive of biochemical recurrence of prostate cancer. The second study addressed the association between Sep15 levels and prostate cancer biochemical recurrence, and the prevalence of a functional polymorphism in the African-American population.

A. Selenium and cancer

Selenium (Se), named after Selene the Greek goddess of the moon in 1817 by Swedish chemist Jons Jacob Berzelius, is an essential micronutrient required for human health [1]. It was considered a toxic agent and a suspected carcinogen as result of its role in neurological conditions observed in livestock [2-4]. However, this historical perspective has undergone a radical shift in many ways. Today, Se is recognized for its biological function through the expression of Se containing proteins or selenoproteins [5]. Dietary Se intake is dependent on the Se concentration in soil on which consumed plants were grown as wells as in animal products and water. Se levels in soil varies greatly across the world, and Se deficiency can occur in regions where plants are grown in Se deficient soil [6]. The low dietary intake of Se is a contributing factor to Keshan disease, a disorder originally reported in a low-Se region of China [7-9]. The prevalence of Keshan disease in this region was successfully reduced by Se supplementation [10]. In the United States, the recommended dietary intake of Se is 55 ug/day for adults and children 14 and older with an increase of 5-15 ug/day for pregnant and

breastfeeding women [11]. Although symptomatic Se deficiency is not common, an individual's dietary intake may be below what is optimal for health.

Se was first implicated in the etiology of cancer in 1943 by its ability to promote liver cancer in rats [12]. This seminal study was followed by other reports of its role in promoting cancer as well as its ability to inhibit cancer cell growth in animal models, indicating that Se can either prevent or promote cancer [13]. The first study addressing the relationship of Se and human cancer was conducted in the 1960's and theorized that Se intake was inversely associated with risk and mortality of several cancers; specifically, cancer mortality was lower in regions where Se content in forage crop was high compared to regions of low Se [13]. These studies were followed by several epidemiological studies indicating an association of Se and cancer. One meta-analysis of prospective observational studies included individuals with high or low serum or toenail Se levels who were followed over time to assess whether or not they developed cancer. The results indicated an inverse relationship with higher Se levels and cancer incidence (OR 0.69, 95% CI 0.53-0.91, N=8) and mortality (OR 0.60, 95% CI 0.39 -0.93, N=6) [14]. The most significant decreases in risk of cancers were seen stomach, bladder and prostate cancers [14].

Supplementation studies indicate that there is no association between Se intake and cancer incidence. Supplementation trials were carried out to assess whether or not an association exists between Se and cancer risk. Initial results lead to claims that Se supplementation may reduce cancer risk and mortality. The Nutritional Cancer Prevention Trial (NPC) was the first double-blind placebo-control Se intervention trial involving over 1300 subjects [15]. It was designed to assess whether Se supplementation would reduce basal cell and squamous cell skin cancer. The primary outcome of the NPC trial indicated that 200 ug/day supplementation of Se (in the form of selenized yeast) non-significantly increased the risk of squamous cell carcinoma

(RR 1.14, 95% CI, 0.93-1.39) and total non-melanoma skin cancer (RR 1.10, 95% CI 0.95-1.28) [15]. Analysis of secondary end points indicated reduced total cancer mortality, total cancer incidence and the risk of total cancers. Remarkably, prostate and colon-rectum cancer risk was reduced by more than 60% in the lowest tertile of selenium status prior to supplementation, indicating that baseline selenium status likely modulates the response to supplementation [16]. However, the NPC trial had many limitations: it was initially designed to investigate the role of Se in skin cancer, only risk factors for that specific population of patients who had prior of skin cancer were considered, and the small number of subjects who participated in the study [15]. The NPC trial led to widespread claims that taking Se supplementation could prevent carcinogenesis, and propelled the much larger trial Selenium and Vitamin E Cancer Trial (SELECT), a clinical trial that assessed whether supplementation of Se, vitamin E or a combination of both could prevent prostate cancer. The trial included 35,533 healthy men over the age of 55 (greater than 50 years if African American) with prostate specific antigen (PSA) levels of less than 4 ng/mL and normal digital rectal exams (DRE) who were randomized to 200 ug/day selenomethionine, 40 IU/day vitamin E or a combination of the two supplements or placebo for 7-12 years [17, 18]. No protective effect of Se against prostate cancer was found in SELECT with either the Se (HR, 1.13; 99% CI, 0.95-1.35), vitamin E (HR, 1.04; 99% CI, 0.87-1.24) nor Se+ vitamin E (HR, 1.05; 99% CI, 0.88-1.25) arms compared to placebo [18]. Secondary analysis revealed that Se supplementation alone increased cancer risk in men with high Se status but had no significant effects on men with low Se status. In addition, an elevated prostate cancer risk (17%) was observed in men given vitamin E, however this risk was attenuated in subjects with low baseline Se levels who were given both Se and vitamin E [19]. Although the findings from SELECT were unexpected, plausible explanations exist. It is possible that the form of Se used in the NPC,

selenized yeast, was more efficacious than selenomethionine, used in SELECT. Studies have shown that the two forms of Se distribute differently in the body, therefore, the levels of Se achieved in the prostate during supplementation may differ [20, 21]. However, the possibility that the two forms of administered Se are not equally efficacious was corroborated when a study investigating prostate specific responses to selenomethionine or selenized yeast in a randomized controlled feeding trial of elderly beagle dogs, the only species besides humans to develop prostate cancer [22, 23], found no significant difference in toenail or intraprostatic Se concentration. Additionally, there was no observed difference in DNA damage, proliferation, apoptosis or levels of intraprostatic dihydrotestosterone, testosterone or the ratio between these hormones when either selenized yeast or selenomethionine was used [24]. Higher baseline Se status was also observed in the SELECT population compared to NPC, which could have contributed to the discrepancies observed between the two trials [16, 18]. Perhaps a more compelling argument can be made that individual genetic variations which impact the ability to metabolize nutrients, such as functional single nucleotide polymorphisms (SNPs) in selenoproteins implicated in cancer were not considered and may have affected response to dietary Se supplementation [25, 26]. Therefore, genotyping study participants for these SNPs would allow for analysis that may clarify the conflict observed between observational and clinical studies as well as the relationship between Se, the expression of selenoproteins as a result of genetic variation, and the risk of cancer. Although the results of the previous epidemiological and clinical studies were inconsistent, a systematic review was conducted to assess whether there is an association between selenium exposure and cancer risk. The review included 55 prospective studies in which adults classified as having low or high baseline Se levels were monitored over time to determine whether they developed cancer, and 8 clinical trials in which subjects were

randomized to receive either Se supplements or placebo. The study concluded that there was no convincing evidence for supplementation of Se reducing risk of cancer (RR 0.90, 95% CI 0.70-1.17), cancer-related mortality (RR 0.81, 95% CI 0.49-1.32) or prostate cancer risk (RR 0.90, 95% CI 0.71-1.14) [27, 28].

B. Selenoproteins: synthesis and function

Se has been shown to prevent cancer in animal models, and is associated with reduced cancer risk in observational studies [15, 29, 30], including prostate cancer [31]. Although the mechanism by which Se may reduce tumor development is not well understood, it is proposed that Se exerts its cancer preventive potential within mammalian systems primarily through its incorporation into selenoproteins. Twenty-five selenoproteins have been identified in the human genome in which Se is present in the form of selenocysteine (Sec), the 21st naturally occurring amino acid [32-35]. The list of selenoproteins includes the glutathione peroxidase family (GPx) that have redox or antioxidant functions, thioredoxin reductases (TrxR) having oxidoreductase function, iodothyronine deiodinases (DIO) that carry oxidoreductase reactions in the metabolism of thyroid hormones, methionine sulfoxide reductases (Msr) and several selenoproteins that are not well characterized [36]. Selenoproteins may be localized in several different subcellular compartments [36].

The co-translational incorporation of Se into selenoproteins employs a unique and complex mechanism that involves the decoding of a UGA codon, normally a translation termination codon, which determines the position of Sec insertion [37, 38]. The recognition of UGA codon requires one or more stem loop structures in the 3' untranslated region (3'UTR) of the mRNA called selenocysteine insertion sequence (SECIS) and accessory proteins [37]. The

biosynthetic process requires multiple features and accessory proteins such as the specific elongation factor EFSec and the SECIS binding protein 2 (SBP2) [39, 40]. Briefly, serine is attached to $tRNA^{Sec}$ by $tRNA^{[Ser]Sec}$ synthetase forming a complex which is then phosphorylated by phosphoseryl-tRNA kinase [41]. The phosphate is replaced with Se by selenophosphate synthetase 2 resulting in selenocysteyl-$tRNA^{[Ser]Sec}$. Selenocysteyl-$tRNA^{[Ser]Sec}$ is subsequently deliver Sec to a growing polypeptide chain as a result of SBP2 binding to the SECIS element and recruiting the specific elongation factor EFSec. EFSec binds selenocysteyl-$tRNA^{[Ser][Sec]}$ and delivers it to the ribosome [41].

Selenoprotein synthesis is highly regulated and involves many specialized factors which are modified by Se [41]. The levels of $tRNA^{[Ser]Sec}$ are modified by Se levels and the availability of $tRNA^{[Ser]Sec}$ impacts UGA read-through [42-44]. In low Se conditions, eukaryotic initiation factor 4a3 (eIF4a3), a selenium regulated RNA binding protein, competes for SBP2 binding of the SECIS element, essentially inhibiting the synthesis of selenoproteins [45]. In addition, Se deficiency targets the mRNAs of certain selenoproteins for degradation by the nonsense-mediated mRNA decay pathway [46, 47] . Se availability regulates the expression of Se containing proteins and leads to a selenoprotein hierarchy where the mRNAs of some selenoproteins are more stable than others in a selenium deficiency background (GPx-1<D1<TR1<SEPP1<GPx-4) [48-50] .

C. Glutathione peroxidase-1 and its role in cancer

Se availability regulates the expression of the selenoprotein glutathione peroxidase-1 (*GPx-1*) and since the levels of GPx-1 diminish rapidly under conditions of Se deficiency, it can be hypothesized that the biological effect of Se supplementation is modulated through GPx-1 [51]. GPx-1, a member of the Se containing family of proteins and the first characterized selenoprotein, functions in the detoxification of hydrogen peroxide and lipid peroxides, using reducing equivalents from glutathione [52, 53]. Immunohistostaining of mitochondria, nuclei and cytosol of rat hepatocytes with anti-rat GPx-1 antibody indicated that GPx-1 was localized in both the cytoplasm and mitochondria, despite lacking a mitochondrial localization sequence [54, 55]. GPx-1 in the mitochondria it detoxifies H_2O_2, the dismutase product of manganese superoxide dismutase (MnSOD), to water [56]. GPx-1 is ubiquitously expressed in epithelial tissue of prostate, breast and other organs [57].

Many studies have linked GPx-1 to carcinogenesis. The human *GPx-1* gene is located on chromosome 3p21, a locus that is often associated with loss of heterozygosity (LOH) in cancers. LOH of *GPx-1* is observed in breast, lung, colon and head and neck cancers [58, 59]. Although GPx-1 is implicated in the etiology of these cancers, its levels are not reduced in all cancer types, but is reduced in many [60, 61]. In fact, studies where *GPx-1* is over-expressed indicate that GPx-1 plays a role in both the promotion and the suppression of tumorigenesis. Over-expression of *GPx-1* decreased the growth of cancer cell lines in culture, decreased tumor growth following injection of these cells into nude mice [62], reduced UV-induced DNA damage measured by micronuclei formation, and increased survival of mice following UV irradiation [63, 64]. However, over-expression of *GPx-1* in a transgenic mouse model of skin cancer with a 1-fold increase in *GPx-1* expression compared to non-transgenic mouse resulted in fast growing tumors

and more tumors per mouse [65]. *GPx-1* knockout mice are not embryonic lethal but are more susceptible to toxicity from ROS generating agents [66], and mice with double knockout of *GPx-1* and glutathione peroxidase-2 (GPx-2) develop spontaneous tumors indicating that other selenoproteins compensate for the loss of *GPx-1* [67, 68].

Two common genetic variations in the *GPx-1* gene, one resulting in a leucine (*Leu*) instead of a proline (*Pro*) at position 198 (*Pro*198*Leu*) and the other involving 5, 6 or 7 alanine *(Ala)* repeats have been identified and associated with elevated cancer risk (Figure 1) [69]. The *GPx-1* alleles encoding the *Ala* repeats are associated with risk of prostate and breast cancer [70]. A case control study investigating whether the *GPx-1* alleles encoding the *Ala* repeats variant is associated with risk of early onset prostate cancer found no association between the two, but an increased frequency of the allele with six *Ala* repeats was observed in prostate cancer cases compared to the control individuals with similar mean age to cases and were spouses of patients in a population study of colorectal cancer [70]. Additional studies have investigated the consequences of the *Pro198Leu* polymorphism on the expression and activity of the protein and its role in cancer. Using MCF-7 breast cancer cells that were engineered to express the *Pro* or *Leu* alleles by transfection of allele specific *GPx-1* constructs, it was demonstrated that the cells expressing the *Leu* allele were less responsive to Se supplementation in media inducing GPx-1 activity compared to *Pro* expressing MCF-7 cells [58]. In addition, increased GPx-1 activity is associated with increased plasma Se levels in individuals homozygous for *Pro/Pro* genotype compared to those with *Leu/Leu* genotype in a study of over 400 human subjects [71]. The *Pro*198*Leu* polymorphism has been investigated in several types of malignancies such as lung cancer [72-74], breast cancer [75], and liver cancer [76]. A meta-analysis consisting of 31 publications including 14,372 cases and 18,081 controls examining the relationship between

*GPx-1 Pro*198*Leu* genotypes and overall cancer risk indicated an increased cancer risk in individuals who carried the *Leu* allele [77]. Although studies indicate that the *Pro* variant was protective, others have shown that the *Leu* variant was also protective in various cancer types, indicating that nutrition and genetics may interact to confer risk or protection and this interaction may be modulated by lifestyle choices such as smoking and diet [78]. In addition, *GPx-1 Leu* allele polymorphism interact with the *MnSOD Ala* allele to increase risk of breast cancer. GPx-1 levels may be modulated by or other selenoproteins such as selenoprotein P (SelP), a selenoprotein present mainly in the plasma and is responsible for transporting Se within the body and delivering it to tissues, and this interaction may modulate GPx-1 activity and its association with cancer risk [79, 80].

GPx-1 is regulated at the translational level by the incorporation of Sec. However, very little is known about the post translational regulation of GPx-1. GPx-1 can be phosphorylated by the c-Abl and Arg tyrosine kinases which enhances GPx activity [81]. GPx-1 was also found to be hyper-acetylated in livers of ethanol fed mice and this resulted in a 2.8 fold increase in acetylation of the protein [82]. Additionally, GPx-1 was hyper-acetylated in livers of mice lacking nicotine adenine dinucleotide (NAD+)-dependent mitochondrial deacetylase Sirtuin 3 (Sirt3) which deacetylates MnSOD upstream of GPx-1 [83]. Mitochondrial fractions isolated from livers of Sirt3 knock-out mice were subjected to 2D gel electrophoresis and mass spectrometry was used to identify GPx-1 hyper-acetylation which was subsequently verified by immunoprecipitation [83]. These observations indicate that GPx-1 is regulated at the post translational level and that GPx-1 is a target of the mitochondrial deacetylase. The localization of GPx-1 to the mitochondria where MnSOD resides as well as the presence of functional

polymorphisms in MnSOD that modulates its enzymatic activity also indicate that the two enzymes may interact to modulate the effect of their expression on carcinogenesis [56, 84].

Figure 1. *Allelic variations in GPx-1*. Two common variations are present in the GPx-1 gene, one resulting in a leucine (*Leu*) instead of a proline (*Pro*) at position 198 and the other involving 5, 6 or 7 alanine (*Ala*) repeats in the coding sequence.

D. Interaction of GPx-1 and MnSOD and its role in cancer

MnSOD is the first line anti-oxidant defense in the mitochondria against superoxide generated as a byproduct of oxidative phosphorylation [85]. MnSOD detoxifies superoxide by reducing it to the less toxic hydrogen peroxide (H_2O_2) which is subsequently catalyzed to H_2O by glutathione peroxidase-1 [85, 86].

MnSOD is important in the maintenance of mitochondrial function. Mice deficient in MnSOD are embryonic lethal and heterozygotes exhibited cardiomyopathy [87]. MnSOD is nuclear encoded, mitochondrially localized and is activated by a myriad of environmental and biological factors such as alcohol, smoking, ROS and cytokines [88-90]. MnSOD is translated with a signal peptide that targets the protein into the mitochondria [91]. A polymorphism in the mitochondrial targeting sequence resulting in a substitution of an alanine (*Ala*) for a valine (*Val*) in codon 16 (Figure 2) targets the enzyme more efficiently into the mitochondria, and results in increased MnSOD mRNA stability [92]. Although the consequences of this polymorphism are

not well understood, it is suggested to alter the secondary structure of the protein from a beta sheet (*Val*) to alpha helix (*Ala*) which affects its import into the mitochondrial membrane [92]. These observations indicate that homozygotes expressing the *Ala/Ala* genotype have higher MnSOD activity than individuals with *Val/Val* genotype.

High levels of MnSOD may be beneficial, however, data obtained using cultured cells and animal models suggesting that the levels of MnSOD in tumors can be lower or higher than those observed in the corresponding normal tissue, indicating that the benefits or harmful effects of reduced or elevated MnSOD levels may be context specific [93-97]. Recently, it was shown that high levels of MnSOD increased H_2O_2 production, resulting in the metabolic shift to glycolysis via the sustained activation of AMP-activated kinase (AMPK) [98]. Epidemiological studies have indicated an elevated cancer risk is associated with the *Ala/Ala* genotype and low intake of dietary antioxidants [99, 100]. Finnish men that are heavy smokers and are homozygous for the Ala allele had a 3-fold increased risk of developing high grade cancers and 70% higher risk for total prostate cancer compared to individuals with *Val/Val and Val/Ala* genotype [101]. In addition, other studies examined the impact of the *Val16Ala* polymorphism on breast cancer risk with two showing an increase in risk [102, 103] while other studies report no association or reduced risk [104-106] among women homozygous for the *Ala/Ala* genotype. Breast cancer risk was elevated for premenopausal women who are homozygous for the *Ala/Ala* genotype and had low intake of dietary antioxidants [105]. Furthermore, the *Ala* polymorphism has been associated with an impressive 10-fold increase in aggressive prostate cancer risk between men with the lowest level of dietary anti-oxidant intake [100], with those individuals consuming the lowest levels of Se and/or other dietary antioxidants having the greatest risk dietary compared to the individuals with the highest levels of dietary antioxidants, including Se

[100]. In addition, a 3-fold increase in aggressive prostate cancer was observed in men homozygous for *Ala/Ala* genotype and low dietary carotenoid status (CI 1.37-7.02, P=0.02) [99]. These studies indicated that it is possible that increased mitochondrial transport of MnSOD is beneficial when antioxidant activity is high and H_2O_2 generated by MnSOD is reduced to water [100]. Antioxidant status can be modulated by dietary intake and/or genetics [100]. In the context of MnSOD, a low antioxidant status could result in increased H_2O_2 which can undergo Fenton mechanism to form a hydroxyl radical, thus contributing to the peroxidase activity of MnSOD which can lead to carcinogenesis by directly oxidizing cellular DNA and protein [107]. Taken together, antioxidant status can influence whether allele variants of *MnSOD* can be beneficial or detrimental.

The genetic polymorphisms in *MnSOD* and *GPx-1* interact to elevate breast cancer risk [79]. While there was no association between the at-risk *Leu* allele of GPx-1 and risk of breast cancer in participants of the Nurse's Health Study [108], a follow-up nested case control study from the same study population reported that there was indeed a significant increased risk for breast cancer when *MnSOD* genotypes were considered [79]. Individuals homozygous for both the *Ala/Ala* and the *Leu/Leu* genotypes were at greater risk of breast cancer (OR 1.87, CI 1.09-3.19) [79]. This indicates that an interplay between MnSOD and GPx-1 in modulates cancer risk. In addition, men homozygous for Se carrier *SEPP1 Ala234* polymorphism who were also homozygous for the *MnSOD Ala* allele had a higher risk of prostate cancer (OR, 1.43; 95% CI, 1.17-1.76) and aggressive prostate cancer (OR, 1.60; 95% CI, 1.22-2.09) compared to those who were homozygous for the *MnSOD Val* allele [109].

Figure 2.Functional polymorphism in MnSOD. A polymorphism in the mitochondrial targeting sequence (MTS) of the *MnSOD* gene results in a substitution of *Ala* for *Val* at codon 16.

In this thesis, the molecular mechanisms behind the epidemiological observation that genotypes in the *GPx-1* gene modify elevated risk of cancer associated with *MnSOD* genotypes were examined by manipulating the genotypes and levels of MnSOD and GPx-1 in MCF-7 breast cancer cells that are null for GPx-1 and have negligible levels of endogenous MnSOD [58, 110, 111]. These cells were used to exclusively express *GPx-1* and *MnSOD* by transfection of allele specific *GPx-1* and *MnSOD* expression constructs. The molecular consequences of polymorphisms in the antioxidant enzymes were investigated to determine outcomes related to cellular signaling, oxidative stress response, and mitochondrial potential.

E. Selenoprotein 15 (Sep15) expression is regulated by dietary selenium

Sep15 is a selenoprotein implicated in cancer etiology. The *Sep15* gene is located on chromosome 1 locus p 31 and encodes a 15 kDa selenoprotein which contains Se in the form of Sec at its active site. Dietary Se has been shown to regulate the expression of selenoproteins, including Sep15 [112]. Sep15 is an endoplasmic reticulum (ER) resident protein, and was first identified in the rat prostate [113]. Subsequently, it was identified in a human T cell line as a protein of unknown function that was labeled with Se^{75} and was expressed at high levels in the human prostate, liver and kidney [114, 115]. Se deficiency in the kidney and the liver resulted in a significant reduction of Sep15 levels, however the changes observed were less pronounced than those previously observed with GPx-1 [112].

F. Sep15 interacts with UDP-glucose: glycoprotein glucosyltransferase

Sep15 was reported to reside in the ER lumen after identification of an ER localization signal in its peptide [114]. The protein lacks the typical ER retention sequence found in ER resident proteins, but it complexes with UDP-glucose: glycoprotein glucosyltransferase (UGGT), a chaperone protein and regulator of the calnexin cycle that senses the folding status of glycoproteins [116, 117]. Sep15 may therefore play an important role in disulfide bond formation and protein quality control in the ER [116, 117]. Protein folding occurs in the ER of mammalian cells and is comprised of a complex network of chaperone proteins and thiol-disulfide oxidoreductases, enzymes that catalyze the formation of disulfide bonds, as well as the machinery that ensures proper folding of newly synthesized polypeptides [118]. The interaction of Sep15 with UGGT and its proposed function as a disulfide isomerase of glycoproteins that are targeted by UGGT is evidenced by the possession of a thioredoxin-like active site motif (CGU),

enabling it to play an important role in the folding of glycoproteins, specifically N-linked glycoproteins [116, 117]. The folding of N-linked glycoproteins containing a sugar moiety attached to an asparagine residue is assisted by an ER localized chaperone protein calnexin (CNX) [119, 120]. CNX binds to monoglycosylated glycoproteins and recruits the ER resident oxidoreductase, ER Resident protein (ERp57) to catalyze disulfide bond formation [119, 120]. Glucosidase II then cleaves the last glucose resulting in the release of the peptide from CNX. UGGT monitors the folding state of the released proteins from the CNX-Erp57 complex and facilitates the transfer of a glucose moiety from UDP-glucose to the partially folded or misfolded nascent protein for re-entry into the CNX-Erp57 pathway for proper folding [119, 120].

G. Sep15 expression and the unfolded protein response (UPR)

When there is an accumulation of misfolded or unfolded proteins in the ER, the unfolded protein response (UPR) is activated [118]. UPR is a signaling pathway that leads to the increased expression of chaperone proteins such as binding immunoglobulin protein BiP, inositol requiring 1 (IRE1), and activating transcription factor 6 (ATF6), which facilitate proper protein folding or removal of misfolded proteins [118]. In addition, UPR inhibits protein translation when protein kinase RNA-like endoplasmic reticulum kinase (PERK) is activated and when the response is prolonged it leads to the initiation of apoptosis [118]. The UPR has been repeatedly implicated in carcinogenesis [121-123], specifically the expression of BiP protein, which is associated with increased tumor aggressiveness and worse patient prognosis [124-126], is elevated in several cancer types[127-129]. Sep15 contains a thioredoxin-like fold (Cystine-X-Sec motif), allowing it to form a 1:1 complex with UGGT, thus implying that it plays a role in the ability of UGGT to sense the folded state of N-linked glycoproteins. Therefore, the accumulation of proteins in the

ER and subsequent initiation of UPR may regulate the expression of Sep15 [116]. However, Sep15 was differentially regulated by ER stress and its expression is modulated by which ER stressor is utilized [116]. Examination of Sep15 levels in mouse fibroblast NIH3T3 cells in response to ER stressor indicated that the expression of Sep15 is increased in response to ER stressors tunicamycin and brefeldin A whereas ER stressors dithiothreitol and thapsigargin led to proteosomal degradation of Sep15 [116]. Surprisingly, reduced levels of Sep15 did not activate UPR, evidenced by unchanged levels of BiP, its levels which is increased when unfolded proteins accumulate in the ER [116].

H. Sep15 in cancer

Sep15 has functional polymorphisms in the 3'UTR region

Functional single nucleotide polymorphisms can have profound effects on the regulation of gene expression. In the case of selenoproteins, polymorphisms that are present in the SECIS element may impact protein levels by modulating the read-through of the UGA because of the importance of the SECIS element determining the efficiency of Sec incorporation [58, 115, 130]. *Sep15* is polymorphic at positions 811 and 1125 in the 3'-untranslated region, the location of the SECIS element that determines the recognition of in-frame UGA codons as the amino acid selenocysteine [131]. The single nucleotide polymorphisms, form a haplotype and are located at nucleotide positions *811 (C/T)* and *1125 (G/A)*. Using a specialized reporter construct that measures the ability of the *Sep15* SECIS element to promote the read-through of a UGA codon, these polymorphisms were shown to be functional and likely impact translation of the protein as a function of selenium availability [115, 131]. Specifically, transfection of constructs encoding the polymorphic variants of *Sep15* SECIS element indicated that the SECIS element encoded by

the *1125A* variant resulted in a higher read-through efficiency of UGA codon compared to the *1125G* variant [115]. The identity of nucleotides at 811/1125 may impact the levels of Sep15 in a Se dependent manner as evidenced by luciferase reporter construct containing either *1125G* transfected into NIH 3T3 mouse fibroblast cells showed higher luciferase activity when cultured in Se supplemented media compared to cells containing *1125A* cultured in the same condition [115, 131].

Sep15 TT genotype is associated with cancer risk

Loss of heterozygosity at the Sep15 locus occurred specifically among African Americans, not Caucasians in both breast and head and neck cancers [132, 133]. Two case control studies reported an association between *Sep15* polymorphisms and the risk of colorectal cancer [134, 135] as well as an interaction *Sep15* polymorphisms and polymorphisms in *SEPP1* in modulating the risk of colon cancer [135]. The expression of the homozygous *TT* at-risk allele of *Sep15* in conjunction with high plasma Se concentration is associated with low risk of lung cancer [136] whereas the expression of Sep15 does not differ between malignant and non-malignant lung tissue [137]. Studies using targeted down regulation of *Sep15* revealed an inhibition of colon carcinogenesis and metastasis in a *Sep15* knockout mouse model [138], as well as growth inhibition of human colon cancer cells in culture and protection against formation of chemically-induced aberrant crypt foci in mice [139, 140].

Sep15 TT genotype is associated with prostate cancer mortality

A nested case control study (1286 cases and 1267 controls) designed to assess the relationship between *Sep15* polymorphisms, selenium status and prostate cancer risk and survival indicated that no association exists between *Sep15* polymorphisms and prostate cancer risk [141]. However, a statistically significant association exists between polymorphisms in *Sep15*,

plasma selenium levels and prostate cancer mortality [141]. In this study, the functional *Sep15* polymorphisms that form a haplotype such that a C or T at residue 811 is always paired with a *G* or *T* at residue 1125 respectively showed a trend toward a significant association between the functional polymorphisms and prostate cancer mortality (p=0.1) [141]. The population examined in this study was self-reported Caucasian men from the Physicians Health Study and the reported allele frequency for 811 at-risk *TT* genotype was only 4.8% (n=1195) for cases and 4.6% (n=1186) for controls [141]. In contrast, in a study population of which the majority was African Americans, a much higher 6 fold frequency (31%) for the *AA* genotype among African Americans, who have both the highest incidence and mortality from prostate cancer, was also reported [130]. Therefore, Sep15 may play a role in the disparity of prostate cancer outcome observed in African Americans compared to Caucasians.

In this thesis, the role of Sep15 in prostate cancer was investigated by examining the distribution and levels of the protein using human prostatic tissue microarrays representing both Caucasians and African-American population, one with lower Se levels [142] and a higher frequency of the *AA* allele predicted to result in decreased levels of the protein [130], to determine whether Sep15 levels are associated with prostate cancer recurrence and whether the association is much stronger in this population. Genotyping studies were also conducted to assess whether an association exists between Se status, *Sep15* polymorphisms and the polymorphisms in the *SEPP1* gene.

II. METHODS

A. Cell culture- MCF-7 human breast cancer, and RWPE1, PC3 and LNCaP human prostate cells were obtained from American Type Culture Collection (ATCC) (Manassas, VA). MCF-7 cells were verified by analyzing 15 autosomal short tandem repeat loci and sex specific amelogenin locus to identify gender (Genetica DNA Laboratories, Burlington, NC). MCF-7 and MCF-7 *GPx-1* and *MnSOD* engineered to express allele specific constructs were maintained in minimum essential media (MEM, Gibco, Grand Island, NY) supplemented with 10% fetal bovine serum (FBS, Gemini Biosciences, West Sacramento, CA), 100 units/ml penicillin and 100 ug/ml streptomycin (Gibco, Grand Island, NY) and incubated at 37^{o}C with 5% CO_2. The selenium concentration of the serum used was 152 nM as determined by graphite furnace atomic absorption spectrometry resulting in a final selenium concentration of 15.2 nmol/L in media supplemented with 10% serum (Texas A&M Veterinary Diagnostic Laboratory at College station, Texas) and incubated at 37^{o}C with 5% CO_2. GPx-1 and MnSOD transfectants were generated using Lipofectamine 2000 transfection reagent (Invitrogen, Carlsbad, CA) and selected with 500 ug/mL G418 (Sigma, St. Louis, MO). The transfectants were expanded and screened for GPx activity and GPx-1 and MnSOD levels.

MCF-7 cells expressing *Sep15* (MCF-7^{Sep15}) were generated by transfection of doxycycline (Dox) inducible *Sep15* expression construct using Continuum transfection reagent (Gemini Biosciences, West Sacramento, CA) and were selected with 400 ug/mL G418 (Sigma, St. Louis, MO) and 1 ug/mL puromycin (Santa Cruz, Dallas, TX). MCF-7^{Sep15} cells were cultured in MEM media (Gibco, Grand Island, NY), and the prostate cell lines RWPE1, PC3 and LNCaP were cultured in RPMI 1640 (ATCC Manassas, VA). The media were supplemented with 10% fetal bovine serum (FBS, Gemini Biosciences, West Sacramento, CA), 100 units/ml

penicillin and 100 ug/ml streptomycin (Gibco, Grand Island, NY). The cells were incubated at 37ºC with 5% CO_2. MCF-7^{Sep15} cells were maintained in 200 ug/mL G418 (Sigma, St. Louis, MO) and 0.5ug/mL puromycin (Santa Cruz, Dallas, TX) and antibiotic selection for all transfectants was removed 3 days prior to the start of an experiment.

B. Generation of allele-specific expression constructs- *GPx-1* expression constructs encoding 5 or 7 alanine repeats at the -NH2 terminus and either a proline or leucine at codon 198 were previously generated [58] and transfected into MCF-7. Both *MnSOD Ala*16 and *Val*16 expression constructs were kindly provided by Dr. Fredrick Domann at the University of Iowa and transfected into MCF-7 cells individually using Lipofectamine 2000 transfection reagent (Invitrogen, Carlsbad, CA) and selected with 500 ug/mL G418 (Sigma, St. Louis, MO). GPx-1 and *MnSOD* double transfectants were generated by sequential transfection of *MnSOD* allele specific constructs in previously generated MCF-$7^{GPx\text{-}1}$ engineered cell lines using lipofectamine 2000 transfection reagent (Invitrogen, Carlsbad, CA) and selected with 400 ug/mL G418 (Sigma, St. Louis, MO). The MCF-7 *GPx-1* transfectants containing either 5 or 7 alanine repeat codons (A5 or A7) or either a proline (P) or leucine (L) at codon 198, these being referred to as A5L, A7L, A5P, or A7P were generated. The MCF-7 transfectants containing either *MnSOD Val* or *Ala* at codon 16 are referred to as $MnSOD^{Val}$ or $MnSOD^{Ala}$. The *MnSOD* and *GPx-1* MCF-7 combined transfectants containing GPx-1 A5P are referred to as $MnSOD^{Val}$ GPx-1, $MnSOD^{Ala}$ GPx-1 A5P and the double transfectants containing GPx-1 A7L are referred to as $MnSOD^{Val}$ $GPx\text{-}1^{A7L}$, or $MnSOD^{Ala}$ $GPx\text{-}1^{A7L}$. The control MCF-7 cell line was transfected with control pLNCX plasmid and is referred to as C for "controls".

Dox-inducible Sep15 expression construct was generated by the insertion of the *Sep15* open reading frame generated by PCR amplification using cDNA from the PC3 prostate cancer cell line as the template and ligated into the pRetroX-Tight-Pur vector (Clontech, Mountain View, CA). For amplification, two oligonucleotides synthesized containing forward *NotI* (5'-gcagcagcggccgcgatcaggctctggagtggac-3') and reverse *MluI* (5'-gcagcaacgcgtgagcaggcaatctgttgagg-3') primers were used, the amplification product was digested with NotI and MluI restriction enzymes and ligated into pRetroX-Tight-Pur vector containing a Tet-On transactivator gene that codes for a protein that binds to the promoter region of the plasmid to induce transcription of *Sep15* by activation of a tetracycline-responsive promoter in response to Dox. *Sep15* was induced with a Dox concentration of 1 ug/mL.

C. GPx activity assay- GPx enzyme activity was determined on whole cell lysates using a coupled spectrophotometric assay that determines the GPx dependent consumption of NADPH [143]. Enzyme activity was expressed as nmole oxidized NADPH per min per milligram of total protein. For all experiments, the cells were plated in triplicate and maintained in G418, which was removed from culture media 3 days before analysis to reduce impact of antibiotic supplementation on selenoprotein synthesis [144, 145].

D. Western blot analyses- Adherent cells collected from plates by scraping were reconstituted in Cell Lysis Buffer (Cell Signaling, Danvers MA) with 1 mM phenylmethanesulfonyl fluoride (PMSF, Sigma, St. Louis, MO) protease inhibitor and lysed on ice for 30 min. Lysates were centrifuged at 14,000 rpm at 4^{o}C for 15 min. Protein concentration of cleared lysate was determined using the Bradford assay (Bio-Rad, Hercules, CA). The protein

was prepared in NuPAGE lithium dodecyl sulfate (LDS) sample buffer (Invitrogen, Carlsbad, CA) containing NuPAGE sample reducing agent and boiled at 100^{o}C for 10 min, and analyzed by electrophoresis on NuPAGE 4-12% Bis-Tris denaturing polyacrylamide gels (Invitrogen, Carlsbad, CA) followed by transfer to polyvinylidene difluoride membranes (Millipore, Billerica, MA). The membranes were blocked in 5% nonfat milk in tris-buffered saline (TBS, Bio-Rad, Hercules, CA) for 1 hr. at room temperature, and then incubated with primary antibody [mouse anti-GPx-1 1:1000 (MBL International Corporation,Woburn, MA), rabbit anti-MnSOD, 1:2000 (Millipore, Billerica, MA), rabbit anti-Nrf2, 1:1000 (Santa Cruz, Dallas, TX), mouse anti-E Cadherin, 1:2000 (Abcam, Cambridge, MA), rabbit anti-Akt, rabbit anti-Phosphorylated-Akt S473 (p-Akt), 1:1000 (Cell Signaling, Danvers, MA), rabbit anti-Bcl-2, 1:1000 (Cell Signaling, Danvers, MA) and rabbit anti-Sirt3, 1:1000 (Aviva), rabbit anti-catalase, 1:1000 (Abcam, Cambridge, MA), rabbit anti-Sep15, 1:1000 (Abcam, Cambridge, MA), rabbit anti-Actin, 1:15,000 (Abcam, Cambridge, MA), mouse anti-GAPDH, Cell Signaling, Danvers, MA] in TBS + Tween (TBS-T) overnight at 4°C. After 3x15 min washes, the membranes were incubated with either the IRDye secondary antibody for rabbit/mouse, 1:5000 (LI-COR Biosciences, Lincoln, NE) or anti-rabbit/mouse IgG HRP-linked antibody, 1:1000 (Cell Signaling, Danvers, MA) for 1hr at room temperature. Membranes were washed 3x for 15 min each, and analyzed by infrared detection using the LI-COR Odyssey Imaging System or detected by enhanced chemiluminescence with ECL plus (GE life Sciences, Pittsburgh, PA) and normalized to actin band density. Protein levels were quantified by densitometry or fluorescence detection using LI-COR. Statistical analysis was performed with Graphpad Instat using paired t test, two-tailed. A value of $P<0.05$ was considered statistically significant.

E. CMXROS assay- Mitochondrial potential was performed by Peter Hart and measured using the MitoTracker Red CMXROS reagent, a red-fluorescent dye that stains the mitochondria of live cells (Thermo Fisher Scientific, Waltham, MA). The accumulation of the dye in the organelle is dependent upon mitochondrial membrane potential. Cells were grown to 80% confluence in black-walled 96-well plates. Cells were washed twice with PBS, and then incubated with CMXROS (1µg/mL) for 15 min at 37°C. Cells were then washed once with PBS and fixed with 4% paraformaldehyde (Affymetrix, Cleveland, OH) for 15 min. Cells were washed 3x with PBS and a final volume of 100µL was added to each well. CMXROS fluorescence was measured at 579ex/599em on a SpectraMax M5 spectrophotometer (Molecular Devices), and normalized to bicinchoninic acid assay (BCA, Thermo Fisher Scientific, Waltham, MA) protein concentration. Statistical analyses were performed with Graphpad Instat using paired t test. A value of $P<0.05$ was considered statistically significant.

F. Confocal microscopy- MCF-7 cells expressing Sep15, as well as benign prostate cell line RWPE-1 and the prostate cancer cell lines LNCaP and PC3, were plated onto MatTek 1.5mm glass-bottomed culture dishes (MatTek Corporation, Ashland, MA). The cells were grown to 80% confluence and washed twice with PBS and incubated with ER-Tracker Green dye (ThermoFisher Scientific, Waltham, MA) at a concentration of 1uM in Hank's Balanced Salt Solution, calcium, magnesium (HBSS/Ca/Mg) (Gibco, Grand Island, NY) at 37^{o}C/5% CO_2 for 30 min. The dishes were washed 3 x 3 min and cells and were fixed with 4% paraformaldehyde (Affymetrix, Cleveland, OH) for 15 min. After 3x3 min washes, cells were permeabilized using 100% ice cold methanol for 15 min. After permeabilization, the cells were again washed with PBS 3 x 3 min each and blocked using 5% bovine serum albumin (BSA) in 1% TBS-T for 45

min. Following the blocking step, the dishes were washed 3 x 3 min each and then incubated with rabbit anti-Sep15 primary antibody (Abcam, Cambridge, MA) at 1:100 in 1% BSA in 1% TBS-T in a humid chamber to prevent drying. Secondary antibody (Alexafluor -568) was then incubated at 1:200 in 1% BSA in 1% TBS-T for 2 hrs at room temperature in a dark humid chamber. Confocal dishes were incubated with DAPI (50 μM) for 30 min with agitation in the dark. Following DAPI incubation, the dishes were washed 3 x 3 min each, and final volume of 2mL phosphate-buffered saline (PBS) was added to the dishes. Images were obtained using a LSM510UV confocal microscope (Zeiss, Oberkochen, Germany).

MCF-7 GPx-1 and MnSOD cells were plated onto MatTek 1.5mm glass-bottomed culture dishes (MatTek Corporation, Ashland, MA). The cells were allowed to grow to 80% confluence. Cells were washed 3 x 3 min with PBS and fixed with 4% paraformaldehyde for 15 min. After 3x3 min washes, cells were permeabilized using 100% ice cold methanol for 15 min. After permeabilization, the dishes were again washed with PBS 3 x 3 min each and blocked using 5% BSA in 1% TBS-T for 45 min. Following the blocking step, the dishes were washed 3 x 3 min each and then incubated with rabbit anti-Nrf2 primary antibody (Santa Cruz, Dallas, TX) at 1:100 and mouse anti-GAPDH (Abcam, Cambridge, MA) in 1% BSA in 1% TBS-T overnight in a humid chamber to prevent drying. The dishes were washed 3 x 3 min with TBS-T and incubated with secondary antibody (Alexafluor -488, -568) at 1:200 dilution in 1% BSA in 1% TBS-T for 2 hrs at room temperature in a dark humid chamber. The dishes were washed 3 x 3 min with TBS-T and incubated with DAPI (50 μM) for 30 min with agitation in the dark. Following DAPI incubation, the dishes were washed 3 x 3 min each, and a final volume of 2mL PBS was added to the dishes. Images were obtained using a LSM510UV confocal microscope (Zeiss, Oberkochen, Germany).

G. Quantification of Nrf2 fluorescence- Nrf2 fluorescence quantification was performed by Sofia Zaichick. Relative fluorescent units (RFU) using≥3 selected images with ≥50 cells total were determined using corrected total cell fluorescence (CTCF). CTCF was calculated as the integrated density of selection – (area of selection x mean background integrated density) using ImageJ (FIGI). The area was kept constant for each image analyzed and 3 background samples taken per selection. CTCF was calculated for both nuclear and cytoplasmic region of individual cells. Average nuclear-to-cytoplasmic ratio for MCF-7 GPx-1 and MnSOD cell lines was reported (± SEM, $n \geq 50$) and statistical analysis performed using ANOVA followed by a post-hoc (Tukey's Multiple Comparison Test).

H. Sources of clinical samples- Prostate cancer outcome tissue microarrays were obtained from the Cooperative Prostate Cancer Tissue Resource (CPCTR), a multi-institutional consortium to bank prostatectomy tissue, as well as relevant patient data including demographics, surgical pathology and follow-up history, under a set of uniform guidelines. The CPCTR has collected more than 6,000 prostate cancer and control samples, the largest collection of this type of tissue available in this country with clinical and pathological outcomes [146, 147]. The arrays used in this study include tissue cores of 0.6 mm diameter, in quadruplicate, from 202 men ("cases") who experienced biochemical recurrence (a single post-surgery prostate specific antigen (PSA) value above 0.4 ng/ml or two consecutive PSAs above 0.2 ng/ml) after prostatectomy and 202 non-recurrent controls matched on age at surgery (+/- 5 years), year of surgery, race, Gleason score (both primary and secondary) and pathological stage.

In addition, as a collaboration with Dr. Vincent Freeman at UIC, 129 DNA obtained from white blood cells and serum samples were obtained from a previously described cohort which

consisted of self-reported African-American and Caucasian men diagnosed with prostate adenocarcinoma from 4 Chicago medical centers between January 1986-December 1990 [148]. The demographic information for the prostate cancer patients was not provided. Thirty breast cancer tissue samples were also obtained from the UIC Cancer Center Core (demographic information for the breast cancer patients is found in the Appendix). Genomic DNA from these breast tissues was generated using complete DNA and RNA Purification Kits (Epicentre, Madison, WI).

I. Immunohistochemistry- Patient sample analysis by tissue micro-array: MnSOD/GPx-1 immunofluorescence was performed by the UIC Histology Core Facility. Sections were dried in a 60^{o}C oven for 60 min. Deparaffinization and antigen retrieval (pH8; 30 sec; 121^{o}C; 15 psi) was performed using a commercial buffer Target Retrieval Trilogy (Cell Marque Corporation, Rocklin, CA). The sections were then cooled at room temperature for 10 min and subsequently rinsed with deionized water and placed in wash buffer (Leica Biosystems, Buffalo Grove, IL). Target antigens were unmasked by incubation in serum free protein blocking for 30 min (BioCore Medical Technologies, Elkridge, MD). Following the blocking step, immunostaining on the BOND RX automated immunostainer (Leica Biosystems, Buffalo Grove, IL) for the primary antibodies for GPx-1 (1:500) plus pan-cytokeratin (pan-CK, EMD Millipore, Billerica, MA, 1:250) or MnSOD (1:500) plus pan-cytokeratin (pan-CK, EMD Millipore, Billerica, MA, 1:250) was performed by incubating the slides with primary antibody for 60 min at room temperature . Following primary antibody incubation, tissue sections were washed with wash buffer (Leica Biosystems, Buffalo Grove, IL) and incubated with anti-rabbit Alexa fluor 555 polymer (ThermoFisher Scientific, Waltham, MA) or anti-mouse 488 (ThermoFisher Scientific,

Waltham, MA) for 60 min at room temperature. Subsequently, the slides were washed and nuclei were counterstained with DAPI for 10 min, washed and mounted with hard set mounting media (Vector Laboratories Inc, Burlingame, CA). GPx-1, MnSOD and CK8/18 were detected by scanning using the Vectra quantitative imaging system (PerkinElmer, Waltham, MA).

All Sep15 and SelM immunohistochemistry was performed by the UIC Histology Core Facility using the Bond™ polymer refine detection HRP (Leica Biosystems, DS9800, Buffalo Grove, IL) method. Sections were dried in a 60^{o}C oven for 60 min. Deparaffinization and antigen retrieval (pH6; 20 min) were performed on-line using Leica Bond-Max (Leica Biosystems, Buffalo Grove, IL). The sections were washed with Bond Dewax solution (Leica Biosystems, AR9222, Buffalo Grove, IL) at 72^{o}C followed by a 100% ethanol wash. The slides were subsequently washed with bond wash solution and target antigen were unmasked by incubation in Bond ER 1 Solution (pH 6) for 20 min at 100^{o}C (Leica Biosystems, AR9640). Following a last wash with bond wash solution, immunostaining for the primary antibody Sep15 and SelM antibodies (Abcam, Cat# ab124840, # ab133681 rabbit monoclonal, Cambridge, MA) diluted 1:1000 was performed by incubating the primary antibody for 15 min at room temperature. Following primary antibody incubation, tissue sections were incubated with non-conjugated secondary rabbit anti-mouse IgG for 8 min at room temperature. Subsequently, the slides were washed and the tissue sections were incubated with HRP conjugated polymer anti-rabbit poly-HRP-IgG for 8 min at room temperature. Then, endogenous peroxidase activity was blocked with hydrogen peroxide for 5 min. Immunoreactivity was visualized with 3, 3-diaminobenzidine (DAB) chromogen for 10 min at room temperature. Finally, sections were counterstained with Mayer's hematoxylin for 5 min, dehydrated by graded alcohol to xylene and mounted and coversliped. Tissues known to express Sep15 (adjacent benign prostate tissue) were used as a

positive control. For a negative control, sections were treated as described above except the primary antibody was not included in the reaction.

J. VECTRA quantitative imaging analysis- The stained tissue slides were scanned. Each epithelial cell was digitally segmented into nuclear and cytoplasmic compartments for each protein analyzed. DAPI (MnSOD and GPx-1) or hematoxylin (Sep15) was recognized by the software as the nucleus of each cell and cytoplasmic signal was sampled using the area surrounding the nucleus. After the manual exclusion of poor quality and benign glands/cores, the expression of MnSOD, GPx-1 and Sep15 was quantified in both subcellular compartments using fluorescent intensity (MnSOD/GPx-1) or DAB staining (Sep15).

K. Data analysis- Data analyses were performed by Ryan Deaton, Li Liu and Rawan Al-Lozi at UIC. The intensities of nuclear and cytoplasmic GPx-1, MnSOD and Sep15 intensities were assessed for normality and log-transformed for statistical analysis. Patients were grouped into three categories based on their Gleason grade (Category 1 = Gleason $\leq$6, Category 2 = Gleason 7(3+4) Category 3 = Gleason 7(4+3) or $\geq$8). The association between Sep15 levels and Gleason category was assessed using the Wilcox Rank Sum test. Patient tissues were also assigned to quartiles based on GPx-1 and MnSOD intensity among the control subjects. Conditional logistic regression models were fitted to estimate odds ratios and 95% confidence intervals for the risk of biochemical recurrence for each quartile of GPx-1, MnSOD and Sep15. The conditional models incorporated adjustment for case-control matching variables: Gleason grade, stage and age at diagnosis; additional models were fit with pre-surgical PSA as a covariate, since PSA was not a matching factor.

L. Genotyping studies- Genotyping at the GPx-1, MnSOD, Sep15, and SEPP1 loci was accomplished by PCR amplification of the desired region using gene specific primers (Integrated DNA Technologies, Coralville, IA) and sequence analysis across the polymorphic region. PCR and sequencing primers used in the analysis as well as the size of the amplicon are found in Table 1. All sets of PCR reactions included a non DNA template control. The anticipated sizes of the PCR products were assessed by electrophoresis using a 1% agarose gel and bands were visualized with ethidium bromide (Bio-Rad, Hercules, CA). Sequencing was performed by the UIC DNA Core. Single-nucleotide heterozygosity was apparent when 2 peaks are visualized at the same location on the chromatogram that corresponded to the polymorphism of interest.

Genotyping Primers							
Gene	Chromosome Location	rs#	Nucleotide Identity/Location	Amino Acid Identity	PCR Primers	Size (bp)	Sequencing primers
GPx-1	3p21.3	rs1050450	C/T, codon 198	*Pro/Leu*	F: 5'cgccaccgcgcttatg 3' R: 5'gaaaacccccccgagac 3'	256	5' gaccccaagctcatcacctg 3'
GPx-1 Ala repeats	3p21.3	NA		*Ala*	F: 5'cctgcactgccggtaacat 3' R: 5'gcgccgagaaggcataca 3'	509	5' gcactctccagccttttcc 3'
MnSOD	6q25.3	rs4880	T/C, codon 16	*Val/Ala*	F: 5'gtagcaccagcactagcagcat 3' R: 5'gcgttgatgtgaggttccag 3'	500	5' cgcggcgctgactga 3'
Sep15	1p31	rs5859	G/A, 3'UTR position 1125		F: 5'cagacttgcggttaattatg 3' R: 5'gccaagtatgtatctgatcc 3'	413	5'cagacttgcggttaattatg 3'
SEPP1	5p12	rs3877899 rs7579	G/A, codon 234 A/G, 3'UTR	Ala/Thr	F:5' cacgcattattcctatctctataagcttg3 ' R:5'ggaaatgaaattgtgtctagacta aattgg3'	722	5'cacgcattattcctatctctataagc ttg 3'

Table 1. Genotyping primers. The polymorphisms, primers used for PCR and sequencing, and the amplicon size (size) are listed.

M. Selenium analysis- The tissue and serum selenium analyses were performed at the USDA-ARS Grand Forks Human Nutrition Research Center (Grand Forks, ND). For tissue analysis, an aliquot of solid sample is accurately weighed or measured for sample processing. For total recoverable analysis of a solid or an aqueous sample containing undissolved material, analytes are first solubilized by gentle refluxing with nitric and hydrochloric acids. After cooling, the sample is made up to volume and is mixed and ready for analysis. The samples are then analyzed on a Perkin Elmer ICPMS Nexion 350D (Perkin Elmer Corp., Wellsley, MA). Samples are validated against three digestion blanks and three National Institute of Standards and Technology (NIST) SRM 1577b Bovine Liver per set along with a CCV Continuing Calibration Verification (CCV) and a Continuing Blank Verification (CCB) every 10 samples.

30µL serum samples were diluted with 20µL of 18 megohm Reverse Osmosis and deionized water and 150µL of modifier, 0.09% PdCl (Palladium Chloride, Alfa Aesar, Ward Hill Ma.) and 1.5%NiNO3 (Nickel nitrate hexahydrate, Alfa Aesar, Ward Hill Ma.) for analysis. 20µL of sample mix, 5µL of 3% Hydroxylamine hydrochloride (Eastman Kodak Company, Rochester NY) and 5µL of 18 megohm Reverse Osmosis and Deionized water are auto sampler transferred to the graphite furnace tube of the Perkin Elmer PinAAcle 900T instrument (Perkin Elmer Corp., Wellsley, MA). Samples are normalized to the Trace Elements Normal Range Serum Toxicology Control (UTAK Laboratories, Inc., Valencia, CA) every 10 samples.

III. RESULTS

A. GPx-1 and MnSOD Overview

Increased cancer risk among individuals homozygous for *MnSOD*^{Ala} was associated with the presence of polymorphisms in the GPx-1 and selenium transport protein SEPP1 genes [79, 109]. The main objective of this study was to gain an understanding of the molecular mechanisms underlying the interaction of *GPx-1* and *MnSOD* polymorphisms in cancer etiology using a cell culture model. Studies were conducted manipulating the genotypes and levels of GPx-1 and MnSOD in MCF-7 breast cancer cells, which are null for GPx-1 and have negligible levels of endogenous MnSOD [58, 110, 111]. These cells were used to exclusively express *GPx-1* and *MnSOD* by transfection of allele specific *GPx-1* and *MnSOD* expression constructs. The molecular consequences of polymorphisms in the genes of *MnSOD* and *GPx-1* were investigated to determine outcomes related to cellular signaling, antioxidant response, and mitochondrial membrane potential.

In order to determine whether GPx-1 and MnSOD levels can be predictive of clinical outcome, 400 human prostate tissue cores from the CPCTR, half of which came from men whose cancer recurred and half of which didn't experience biochemical recurrence were assessed by immunohistochemistry [147]. In addition, serum Se quantification and genotyping studies were conducted to assess whether there is an association between Se levels and genotypes of *SEPP1* and GPx-1, as well as to determine whether there is an interaction between *GPx-1*, *MnSOD* and *SEPP1* genotypes with Se levels.

B. GPx-1 is differentially localized to the cytoplasm and mitochondria.

GPx-1 distributes to both the cytosol and the mitochondria, despite lacking a canonical mitochondrial localization sequence [149]. The two common variants in the GPx-1 gene, *Pro198Leu* and *Ala* codon repeats, have been well described, but much less is known about the molecular consequences of these variants. Hypothetically, the variants may modulate the localization of the protein between the cytoplasm and the mitochondria. To elucidate whether *GPx-1* allelic variants affect localization of the protein, the cellular location of GPx-1 encoded by allelic variants, 5 or 7 *Ala* codon repeats (A5 or A7) and either a *Pro* or *Leu* at codon 198 (A5P and A7L) was examined by ectopically expressing these genes in GPx-1 null MCF-7 cells. GPx-1 was localized to the cytoplasm and mitochondria. Allelic identity affects GPx-1 localization and the A7L version of the protein partitioned to the greatest extent in the cytoplasm compared to the other alleles examined (Figure 3) [150].

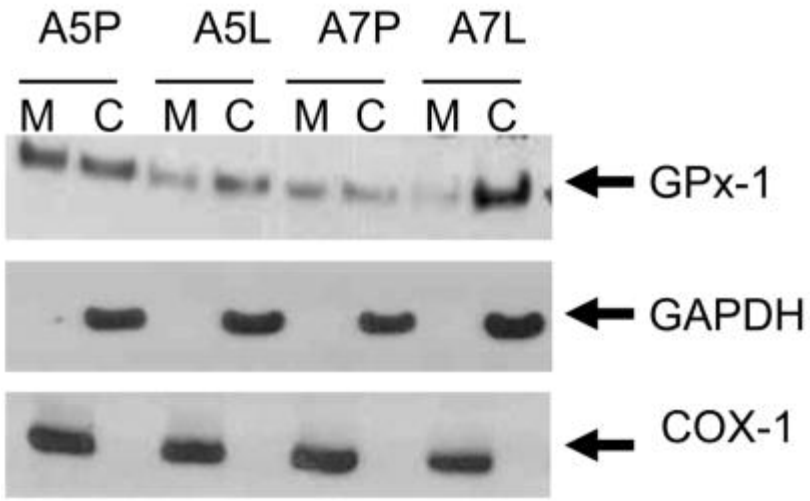

Figure 3. The cellular distribution of GPx-1 between the cytoplasm (C) and mitochondria (M) is affected by the expression of GPx-1 functional polymorphisms. MCF-7 cells expressing allele specific *GPx-1* were separated into cytoplasm and mitochondria fractions and protein levels were assessed by Western blotting with anti GPx-1 antibodies. Glyceraldehyde-3-phosphate

dehydrogenase (GAPDH) and cytochrome c oxidase subunit 1 (Cox-1) were used as markers of cytoplasmic and mitochondrial proteins, respectively.

C. *GPx-1* and *MnSOD* expression in MCF-7 cell lines.

Genetic variations in *GPx-1* impacted the localization of the GPx-1, resulting in the partitioning of the protein equally in the cytoplasm and mitochondria with the allele coding for *Pro*-198 and 5 *Ala* repeats (A5P) and to the greatest extent in the cytoplasm with the allele coding for the *Leu*-198 polymorphism and 7 *Ala* repeats (A7L) [150]. The subsequent analyses focused on these two variants because of their distinct localization. The cells expressing the A5P genotype are referred to as GPx-1 and the *A7L* cells are GPx-1^{A7L}.

Individuals homozygous for the *GPx-*1^{Leu} and *MnSOD*^{Ala} genotypes had increased risk of breast cancer compared to the other alleles examined [79], and since localization of GPx-1 is impacted by genetic variations it was hypothesized that the localization of GPx-1 in the mitochondria will alter the MnSOD-dependent effect on signaling proteins implicated in cancer. In order to investigate this hypothesis, cells were engineered to express *GPx-*1^{A5P} (hereafter referred to as *GPx-1*), that resides in both the mitochondria and cytoplasm, and *MnSOD Val* or *Ala* polymorphic constructs using MCF-7 cells because they are null for GPx-1 and express negligible levels of MnSOD [110]. GPx enzyme activity and MnSOD levels were assessed using protein extracts derived from cells transfected with either *GPx-1* or *MnSOD* allele-specific constructs or the combination of *GPx-1* and different alleles of *MnSOD* genes. GPx enzyme activity was determined by a coupled spectrophotometric assay that determines the GPx dependent consumption of NADPH (GPx-1) and MnSOD levels were assessed by western blotting using anti-MnSOD antibodies (MnSOD). Examination of GPx enzyme activity in these

cells showed significantly higher GPx activity in all transfected cell lines than in control MCF-7 cells (C) and MCF-7 cells expressing *MnSOD*^{Val} or *MnSOD*^{Ala} (Figure 4A). Immunoblotting of lysates from these cell lines showed that MnSOD is expressed in all cell lines except control cells and *GPx-1* expressing MCF-7 cells (Figure 4B).

4A

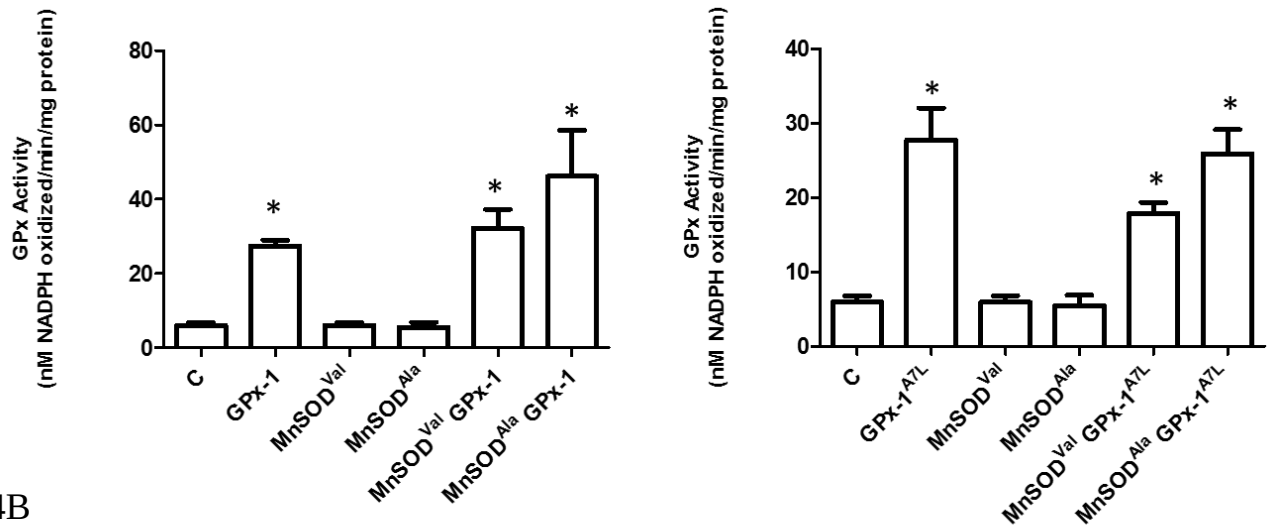

4B

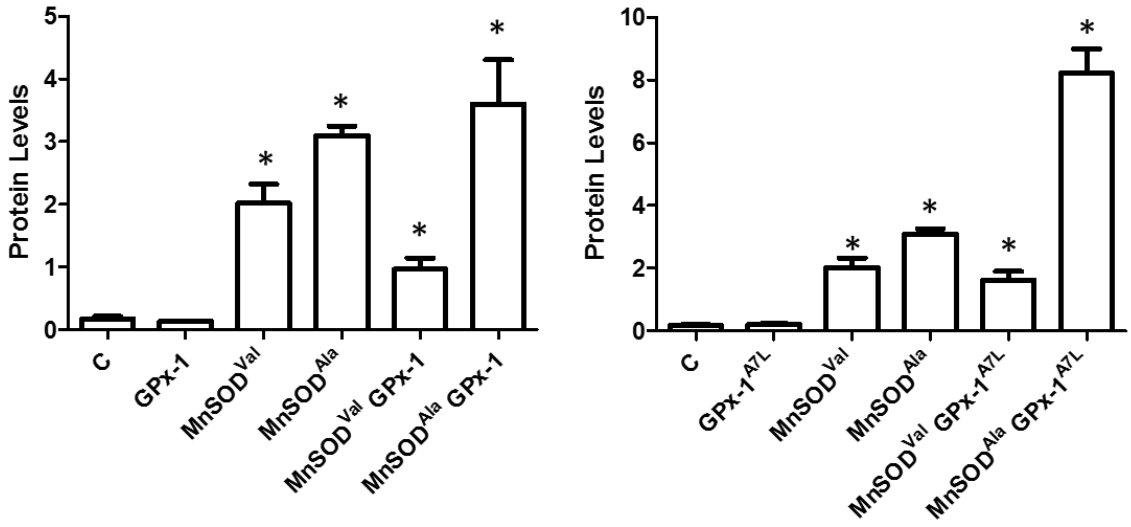

Figure 4. Successful transfection of expression constructs. A. GPx activity in all transfected cell lines. Lysates from MCF-7 (C), MCF-7 GPx-1, MCF-7 MnSOD^{Val} and MCF-7 MnSOD^{Ala} cell

lines were used to determine GPx enzyme activity. *B. Protein expression of MnSOD variants that were successfully transfected into MCF-7 cells.* Lysates from MCF-7, GPx-1, $MnSOD^{Val}$, and $MnSOD^{Ala}$ cells were analyzed for MnSOD protein levels by western blot using anti-MnSOD antibodies. β-Actin was used as an endogenous protein loading control. Protein levels were quantified using fluorescence detection and normalized to β-Actin. Error bars indicate the standard deviation (n=3) (* = $p<0.05$).

D. GPx-1 modulates the MnSOD-dependent effect of signaling proteins.

Signaling molecules involved in the redox signaling pathway, cell growth, metabolism, and cell-cell adhesion, may be differentially affected by the GPx-1 and MnSOD proteins encoded by specific alleles. Given the association of *GPx-1* and *MnSOD* genotypes with increased cancer risk [79], the effect of the expression of *GPx-1* and *MnSOD* gene variants on the levels of signaling proteins implicated in cancer such as E-Cadherin, phosphorylated-Akt (p-Akt) Serine 473, Bcl-2, Sirt3 and Nrf-2 were studied by immunoblotting and confocal imaging (Nrf2) using protein specific antibodies. The expression of *GPx-1* and $MnSOD^{Val}$ increased the levels of p-Akt and Sirt3 while the expression of *GPx-1* and $MnSOD^{Ala}$ decreased the levels of Nrf-2, p-Akt, Sirt3 and Bcl-2.

An inverse relationship exists between MnSOD levels and expression of E-cadherin, a calcium-dependent cell-cell adhesion molecule with roles in tissue formation and tumor metastasis [151-154]. In addition, H_2O_2, the product of the reaction catalyzed by MnSOD and the substrate of GPx-1, mediates the epidermal growth factor induced down regulation of E-cadherin [155]. In order to assess whether allelic variations in *GPx-1* and *MnSOD* modulate the

expression of E-cadherin, whole cell lysates were obtained from the generated MCF-7 cell lines and analyzed by western blotting with anti-E-cadherin monoclonal antibodies and anti-β-actin antibodies. MCF-7 cells transfected with *GPx-1* and *MnSOD^{Val} GPx-1* have significantly less E-Cadherin levels compared to MCF-7 cells (C) (Figure 5). *MnSOD^{Val}*, *MnSOD^{Ala}* and *MnSOD^{Ala} GPx-1* do not change the levels of E-Cadherin compared to the non-transfected control cells (C).

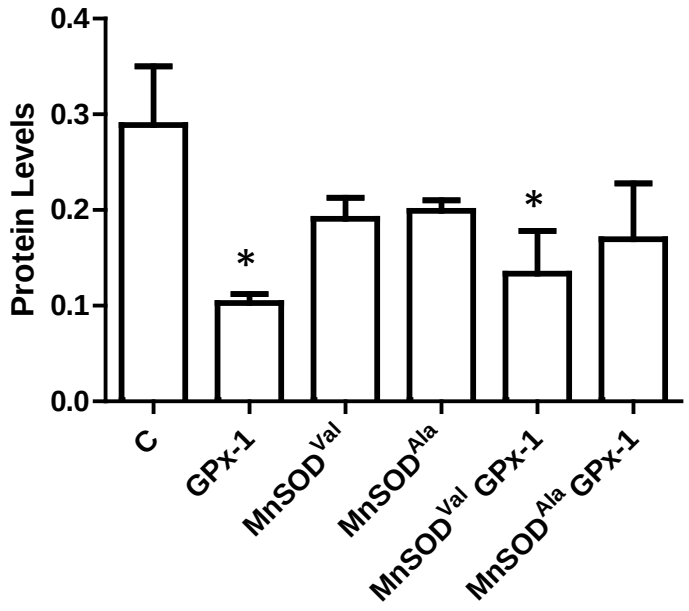

Figure 5. GPx-1 and MnSOD^{Val} GPx-1 MCF-7 cells have decreased E-Cadherin levels compared to controls (C). Lysates from MCF-7, *GPx-1*, *MnSOD^{Val}*, *and MnSOD^{Ala}* transfected cells were analyzed for MnSOD protein levels by western blot using anti-E-Cadherin antibodies. β-Actin was used as an endogenous protein loading control. Protein levels were quantified using fluorescence detection and normalized to β-Actin. Error bars indicate the standard deviation (n=3) (* = $p<0.05$).

Over-expression of *GPx-1* in Chang liver cells by transfection of *GPx-1* construct results in decreased activation of Akt whereas phosphorylation of Akt was reduced in neurons of *GPx-1* Knock-out mice [86, 144, 156]. This indicates that *GPx-1* expression has pleotropic effects on the activation of pro-survival and growth protein kinase, Akt, a predictor of poor clinical outcome in prostate cancer [157-160] MnSOD down-regulation is mediated by increased Akt activation [161]. In order to determine whether *GPx-1* and *MnSOD* allelic variations modulate the expression of p-Akt Ser 473, whole cell lysates were obtained from the generated MCF-7 cell lines and analyzed by western blotting using anti-p-Akt Ser 473 and anti-β-actin antibodies. *GPx-1* plus $MnSOD^{Val}$ MCF-7 cells have increased p-Akt levels compared to $MnSOD^{Val}$ MCF-7 cells (Figure 6). Cells expression either *GPx-1*, $MnSOD^{Val}$, $MnSOD^{Ala}$ or the combination of $MnSOD^{Ala}$ *and GPx-1* have the same levels of p-Akt when compared to the controls (C) (Figure 6).

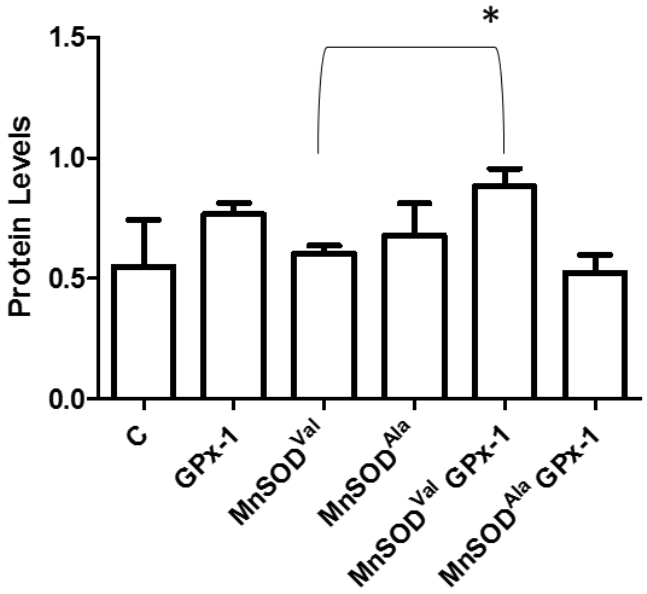

Figure 6. GPx-1 and $MnSOD^{Val}$ expression increased p-Akt levels. Lysates from MCF-7, GPx-1, $MnSOD^{Val}$, and $MnSOD^{Ala}$ cells were analyzed for MnSOD protein levels by western blot using

anti-p-Akt antibodies. β-Actin was used as an endogenous protein loading control. Protein levels were quantified by densitometry and normalized to β-Actin. Error bars indicate the standard deviation (n=3) (* = $p<0.05$).

Depending on the level of oxidative stress in cells, ROS are known to differentially regulate cell death [162]. Anti-apoptotic protein Bcl-2, which is implicated in cancer, regulates cell death by changing mitochondrial membrane permeability [163-165] and both GPx-1 and MnSOD have been shown to up-regulate the expression of Bcl-2 to promote a more anti-apoptotic environment [86, 98]. In order to investigate whether *GPx-1* and *MnSOD* expression affect Bcl-2 levels, whole cell lysates were obtained from the generated MCF-7 cell lines and analyzed by western blotting using anti-Bcl-2 and anti-β-actin antibodies. Cells expressing either *GPx-1* or genotypes of *MnSOD have* decreased Bcl-2 levels compared to the control (C) (Figure 7A). $MnSOD^{Ala}$ interacted with *GPx-1* to further decrease Bcl-2 compared to $MnSOD^{Ala}$ alone (Figure 7B), but $MnSOD^{Ala}$ plus *GPx-1* did not further reduce Bcl-2 (Figure 7A) when compared to $MnSOD^{Val}$.

7A 7B

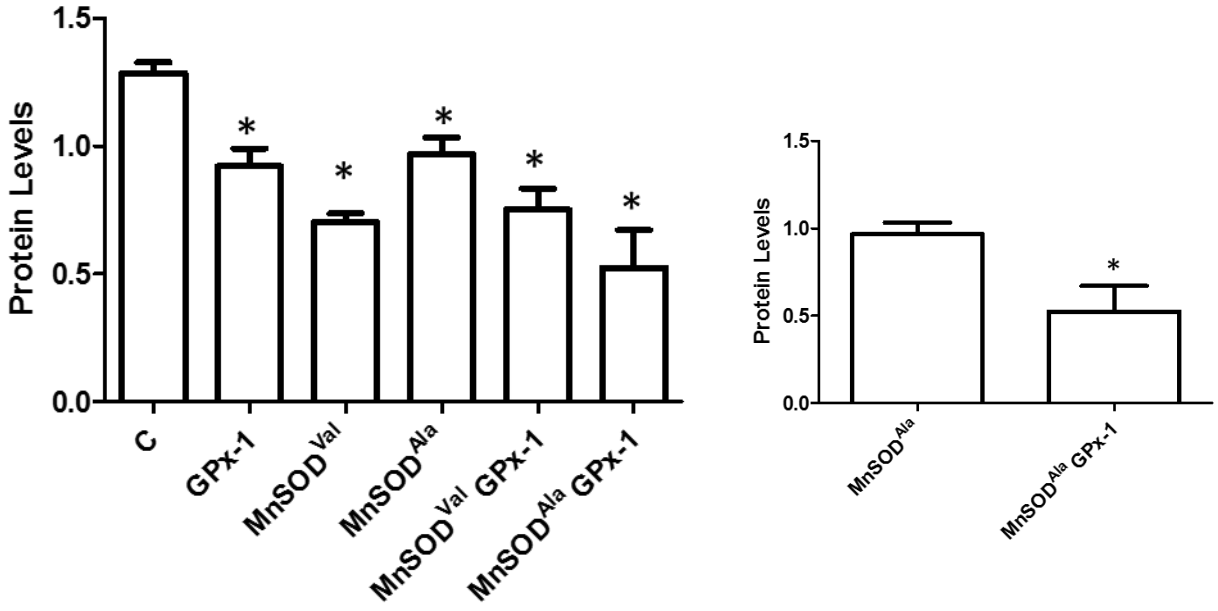

Figure 7. GPx-1, MnSOD and the combination of GPx-1 and MnSOD^{Ala} decreased Bcl-2 levels (A) and GPx-1 plus MnSOD^{Ala} significantly decreased Bcl-2 levels when compared to GPx-1 or MnSOD^{Ala} (B). Lysates from MCF-7, *GPx-1, MnSOD^{Val}, and MnSOD^{Ala}* MCF-7 cells were analyzed for Bcl-2 protein levels by western blot using anti-Bcl-2 antibodies. β-Actin was used as an endogenous protein loading control. Protein levels were quantified by densitometry and normalized to β-Actin. Error bars indicate the standard deviation (n=3) (* = $p<0.05$).

Sirt3 is a member of the mammalian sirtuin family of protein that functions as a mitochondrially localized deacetylase and has been implicated as a tumor suppressor [166-168]. Given that Sirt3 mediated deacetylation of MnSOD at lysine 122 upregulates MnSOD enzyme activity [169] and Sirt3 ablation leads to hyper-acetylation of mitochondrial and cytoplasm localized GPx-1 in response to stress [83], we determined whether polymorphisms in the gene

for *MnSOD* and *GPx-1* influence Sirt3 levels, whole cell lysates were obtained from the generated MCF-7 cell lines and analyzed by western blotting using anti-Sirt3 and anti-β-actin antibodies. *GPx-1* and *MnSOD* cells have the same levels of Sirt3 levels compared to the control cells (C) (Figure 8). $MnSOD^{Val}$ plus *GPx-1* expression increased Sirt3 levels compared to $MnSOD^{Val}$ alone (Figure 8) while $MnSOD^{Ala}$ plus *GPx-1* non-significantly decreased Sirt3 levels when compared to $MnSOD^{Ala}$ (Figure 8).

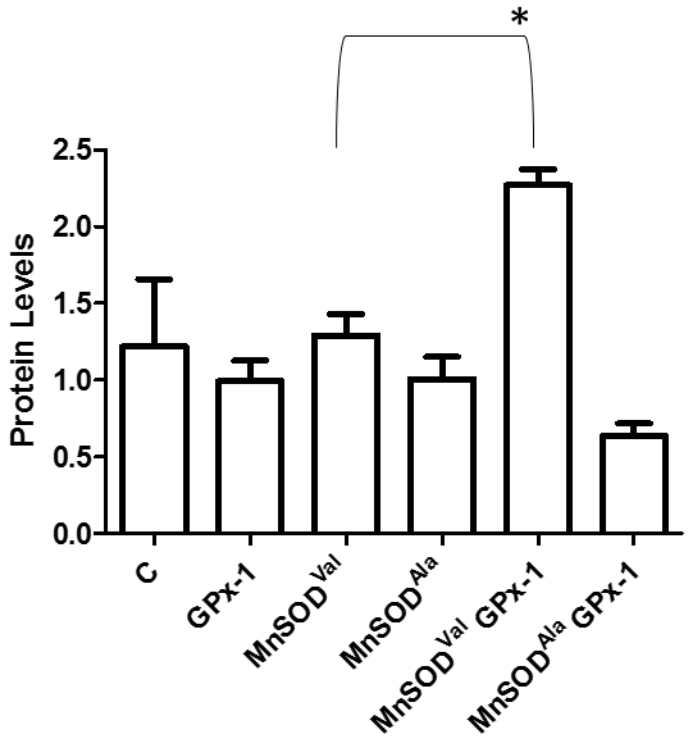

Figure 8. $MnSOD^{Val}$ GPx-1 significantly increased Sirt3 levels compared to $MnSOD^{Val}$. Lysates from MCF-7, *GPx-1, $MnSOD^{Val}$, and $MnSOD^{Ala}$* MCF-7 cells were analyzed for Sirt3 protein levels by western blot using anti-Sirt3 antibodies. β-Actin was used as an endogenous protein loading control. Protein levels were quantified by densitometry and normalized to β-Actin. Error bars indicate the standard deviation (n=3) (* = $p<0.05$).

In response to oxidative stress, the transcription factor Nrf2 translocates into the nucleus and increases the expression of antioxidant proteins MnSOD by binding to the antioxidant response element in the upstream promoter region of these genes to recruit transcription machinery [170]. In order to assess whether the expression of *GPx-1* and *MnSOD* allelic variations change the levels of Nrf2, and to investigate whether *GPx-1* and *MnSOD* expression affect Nrf2 levels, whole cell lysates were obtained from the generated MCF-7 cell lines and analyzed by western blotting using anti-Nrf2 and anti-β-actin antibodies. $MnSOD^{Ala}$ plus *GPx-1* decreased Nrf2 levels (Figure 9) compared to $MnSOD^{Ala}$, *GPx-1*, *MnSOD* and $MnSOD^{Val}$ plus *GPx-1* cells have the same levels of Nrf2 compared to controls (C) (Figure 9).

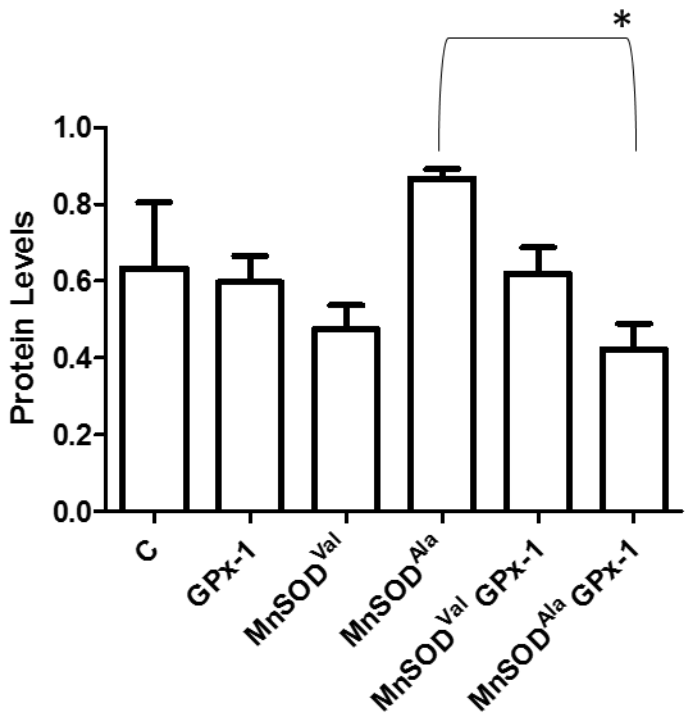

Figure 9. $MnSOD^{Ala}$ GPx-1 significantly decreased Nrf2 levels compared to $MnSOD^{Ala}$. Lysates from MCF-7, *GPx-1*, $MnSOD^{Val}$, *and* $MnSOD^{Ala}$ cells were analyzed for Nrf2 protein levels by

western blot using anti-Nrf2 antibodies. β-Actin was used as an endogenous protein loading control. Protein levels were quantified using fluorescence detection and normalized to β-Actin. Error bars indicate the standard deviation (n=3) (* = $p<0.05$).

Nrf2 is repressed by kelch-like protein Keap1 which renders it transcriptionally inactive and sequestered in the cytoplasm [171, 172]. ROS accumulation disrupts the Nrf2-Keap1 complex and facilitates the translocation of Nrf2 to the nucleus where it becomes transcriptionally active leading to the activation of various genes by binding to their antioxidant response elements (ARE) [171, 173]. In order to determine if *GPx-1* and *MnSOD* affect the translocation of Nrf2 into the nucleus, the engineered cell lines were stained with fluorescently labeled secondary antibodies following incubation with Nrf2 and GAPDH primary antibodies and analyzed by confocal microscopy. GAPDH was consistently cytoplasmic in all cell lines and Nrf2 was localized in the both the cytoplasm and nucleus. Nrf2 levels were reported as relative fluorescence units (RFU). *GPx-1* or *MnSOD* MCF-7 cells have increased nuclear Nrf2 levels compared to the control cells (C) whereas the expression of both *GPx-1* and *MnSOD* reduced the amount of Nrf2 in the nucleus compared to either *GPx-1* or *MnSOD* (Figure 10).

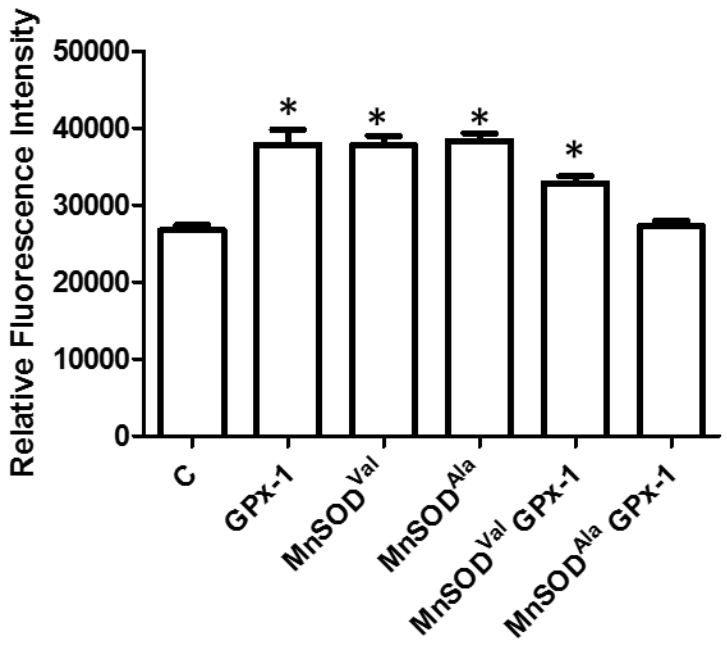

Figure 10. Levels of nuclear Nrf2 is increased in all cell lines except MnSOD^{Ala} GPx-1 cells compared to controls (C). Engineered cells were stained with anti-Nrf2 and anti-GAPDH antibodies as a cytoplasmic marker. Nuclear Nrf2 levels for the MCF-7 cell lines were determined using immunostaining/confocal microscopy and reported as relative fluorescence units. Statistical analysis was performed using ANOVA One-way analysis of variance test $p<0.0001$, Tukey's Multiple Comparison Test *= $p<0.05$. The error bars indicate the standard error of the mean ($n \geq 50$)

E. The common genetic variations in the GPx-1 gene form a haplotype

Studies investigating whether the *GPx-1* genotypes are associated with cancer focused on the *Pro*198*Leu* polymorphism, indicating the *Leu* allele most often as the at-risk allele, and in some rare cases the *Pro* allele. The variable numbers of Ala repeats in the coding region are rarely studied, and only now is the combination of these two variants being investigated. Studies were conducted to determine whether these variants are in linkage disequilibrium. DNA isolated from white blood cells of 129 men (who were diagnosed with prostate adenocarcinoma) were PCR amplified and genotyped for *GPx-1* variants. Analysis of allele distribution revealed that 5 and 7 *Ala* codon repeats are associated with 198*Pro* while 6 *Ala* codon repeats are associated with 198*Leu* (Table 2). In the studied population, 5 or 7 *Ala* repeats segregated with the *Leu* allele and 6 repeats with *Pro* allele at position 198 in only one case, indicating that although rare, these combinations exist in the population (Table 2).

	GPx-1 Genotype Frequency					
	Alanine Repeats					
	55	**56**	**57**	**66**	**67**	**77**
Pro/Pro	17.74%	-	18.55%	-	1.00%	10.48%
Pro/Leu	1.00%	29.84%	-	-	13.71%	1.00%
Leu/Leu	-	-	-	7.24%	-	-

Table 2.5 and 7 Ala repeats in GPx-1 form a haplotype with Pro198 and 6 Ala repeats segregates with Leu198. DNAs (n=129) were PCR amplified and genotyped for GPx-1 *Pro*198*Leu* and the *Ala* repeats. Genotype frequencies reported as percentage. The red color indicates the rare GPx-1 haplotype in the studied population.

F. *GPx-1*^{A7L} modulates the MnSOD-dependent effect of signaling proteins

Although a rare allele in the population, 7*Ala* repeats in *GPx-1* is found with the 198*Leu* polymorphism and when expressed in MCF-7 cells, it encodes for a GPx-1 protein that partitioned to the greatest extent in the cytoplasm [150]. In order to investigate whether the GPx-1 encoded by this allele interacts with MnSOD protein encoded by the variants to modulate the levels of signaling proteins (E-Cadherin, p-Akt, Bcl-2, Sirt3 and Nrf2), and mitochondrial potential, MCF-7 cells expressing *GPx-1*^{A7L} and *MnSOD*^{Val} or *MnSOD*^{Ala} were assessed for these endpoints by western blotting and CMXROS assay. *GPx-1*^{A7L} alone or in conjunction with *MnSOD* alleles did not change the levels of E-Cadherin and p-Akt (Figure 11A & B). *GPx-1*^{A7L} alone and *MnSOD*^{Val} plus *GPx-1*^{A7L} decreased Bcl-2 (Figure 12). *MnSOD*^{Ala} plus *GPx-1*^{A7L} decreased Sirt3 and Nrf2 (Figure 13A & B). *GPx-1*^{A7L} not only increased the nuclear translocation of Nrf2 but interacted with *MnSOD*^{Val} to further increase the translocation of Nrf2 into the nucleus (Figure 14).

A

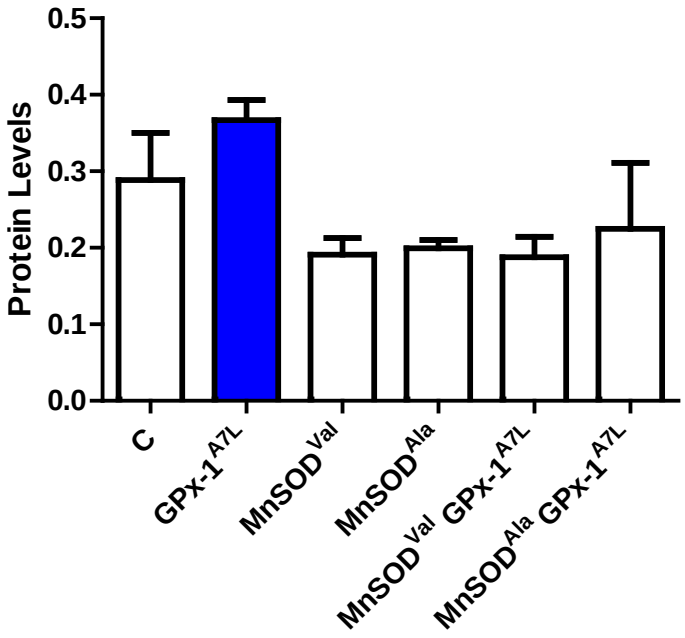

B

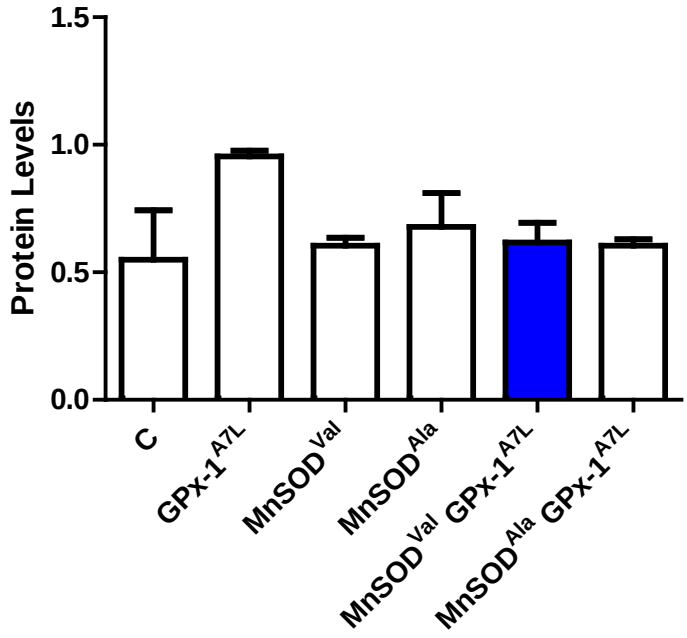

Figure 11. GPx-1^{A7L} alone and in conjunction with MnSOD alleles did not change the levels of E-Cadherin (11A) and p-Akt (11B). Lysates from MCF-7, *GPx-1^{A7L}*, *MnSOD^{Val}*, and *MnSOD^{Ala}* MCF-7 cells were analyzed for E-cadherin and p-Akt protein levels by western blot using anti-E-

Cadherin and p-Akt antibodies. β-Actin was used as an endogenous protein loading control. Protein levels were quantified using fluorescence detection (E-Cadherin) or densitometry (p-Akt) and normalized to β-Actin. The blue bar represents the changes observed when *GPx-1^{A7L}* is expressed compared to *GPx-1^{A5P}* variant. Error bars indicate the standard deviation (n=3) (* = $p<0.05$).

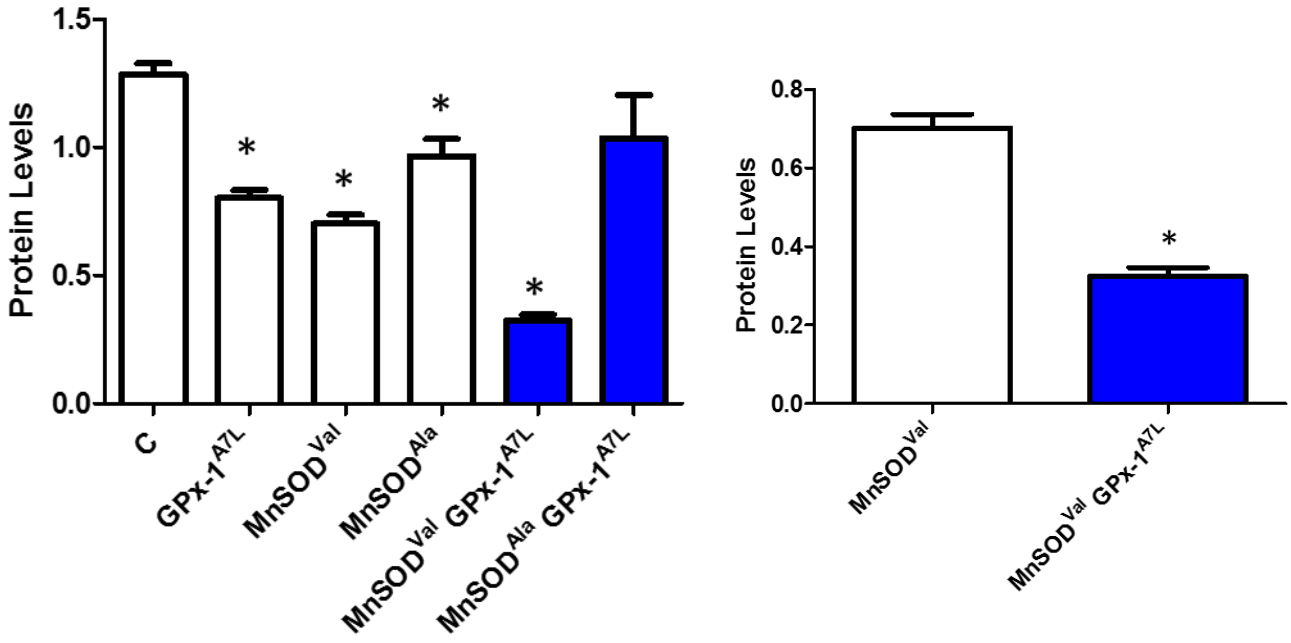

Figure 12. GPx-1^{A7L} and MnSOD^{Val} GPx-1^{A7L} decreased Bcl-2. Lysates from the cell lines were analyzed for Bcl-2 protein levels by western blot using anti-Bcl-2 antibodies. β-Actin was used as an endogenous protein loading control. Protein levels were quantified by densitometry and normalized to β-Actin. The blue bar represents the changes observed when *GPx-1^{A7L}* is expressed compared to *GPx-1^{A5P}* variant. Error bars indicate the standard deviation (n=3) (* = $p<0.05$).

A

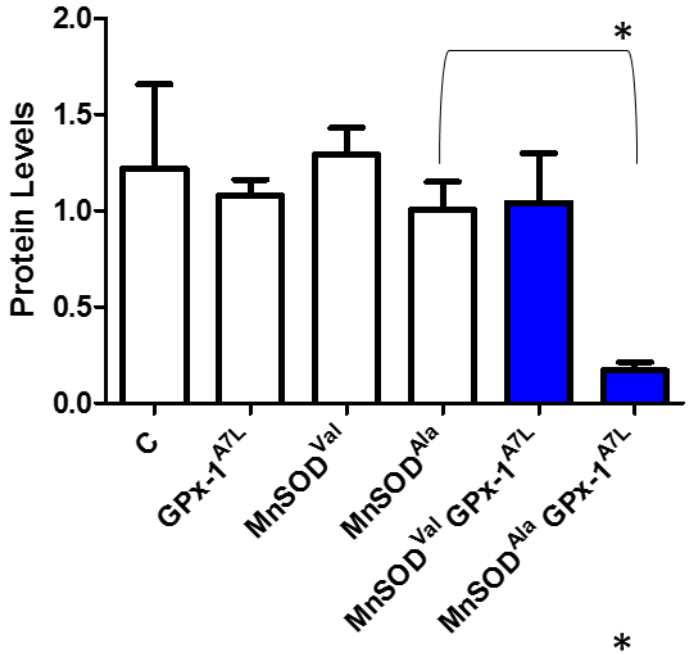

B

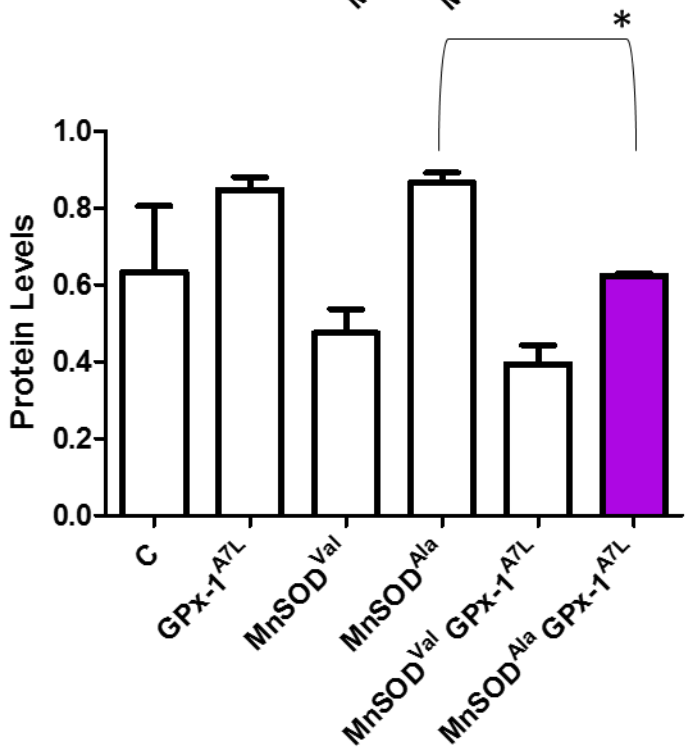

Figure 13. MnSOD^{Ala} GPx-1^{A7L} decreased Sirt3 and Nrf2. Total cell extracts were analyzed for Sirt3 (11A) and Nrf2 (11B) protein levels by western blot using anti-Sirt3 and Nrf2 antibodies. β-Actin was used as an endogenous protein loading control. Protein levels were quantified by

densitometry (Sirt3) or using fluorescence detection (Nrf2) and normalized to β-Actin. The blue bar represents the changes observed when *GPx-1^{A7L}* is expressed compared to *GPx-1^{A5P}* variant. Error bars indicate the standard deviation (n=3) (* = $p<0.05$).

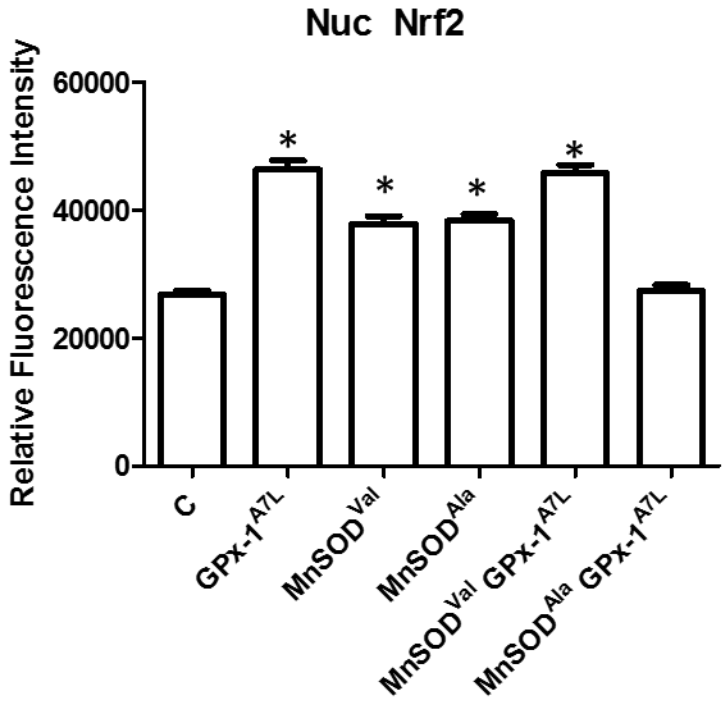

Figure 14. Nuclear Nrf2 is increased in all cells except MnSOD^{Ala} GPx-1^{A7L}. Cells were stained with anti-Nrf2 and anti-GAPDH antibodies as a cytoplasmic marker. Nuclear Nrf2 levels for the cell lines were determined using immunostaining/confocal microscopy and reported as relative fluorescence units. Statistical analysis was performed using ANOVA One-way analysis of variance test $p<0.0001$, Tukey's Multiple Comparison Test *= $p<0.05$. The error bars indicate the standard error of the mean ($n \geq 50$).

Summary of GPx-1 and MnSOD molecular interaction studies

Gene	No effect	Decrease	Increase
GPx-1^{Pro}	p-Akt	E-Cad	
	Sirt3	Bcl2	
GPx-1^{Leu}	E-Cad	Bcl2	
	p-Akt		
	Sirt3		
MnSOD^{Val}	p-Akt		
	Sirt3	Bcl2	
	E-Cad		
MnSOD^{Ala}	p-Akt		
	Sirt3	Bcl2	
	E-Cad		

Gene	No effect	Decrease	Increase
MnSOD^{Val}			p-Akt
GPx-1^{Pro}		Bcl2	Sirt3
			E-Cad
GPx-1^{Leu}	E-Cad	Bcl2	
	p-AKT		
	Sirt3		
MnSOD^{Ala}	E-Cad		
GPx-1^{Pro}	p-Akt		
	Sirt3	Bcl2	
GPx-1^{Leu}	p-Akt	Sirt3	
	E-Cad		
	Bcl2		

Table 3. GPx-1 and MnSOD genotypes interact to affect levels of proteins implicated in cancer. The table summarizes the impact of GPx-1 and MnSOD genotype on the levels of key proteins implicated in cancer as assessed by western blotting. The expression of the specific alleles either had no effect, decreased or increased the levels of E-Cad, pAkt, Bcl-2 and Sirt3. The red color indicates that allele specific effect exists and *GPx-1* and *MnSOD* gene interaction had different effects on the indicated protein compared to those labeled in blue.

G. GPx-1^{A7L} alters the MnSOD induced down-regulation of mitochondrial potential.

Mitochondria potential represents the functional status of the mitochondria, and drives the production of ATP [174]. Membrane potential regulates apoptosis by controlling the release of pro apoptotic molecules when the outer mitochondrial membrane integrity is disrupted. It was previously shown that higher levels of MnSOD increased H_2O_2 production, which then decreased mitochondrial electrochemical potential [172, 175], leading to metabolic shift to a more glycolytic state, a phenotype typical of cancer cells [98]. To investigate whether genetic variations in MnSOD differentially modify mitochondrial membrane potential or whether GPx-1 affects this, the CMXROS assay was used. The previous observation that MnSOD decreased membrane potential was recapitulated (Figure 9B), and this decrease was independent of genotype and GPx-1 did not change membrane potential from that observed in MCF-7 control cells and, it did not restore the MnSOD induced reduction to basal levels (Figure 15). However, *GPx-1^{A7L}* alone significantly decreased membrane potential and the combined expression of *GPx-1^{A7L}* with either *MnSOD^{Val}* or *MnSOD^{Ala}* significantly decreased mitochondrial membrane potential compared to the *MnSOD^{Val}* or *MnSOD^{Ala}*, respectively (Figure 16).

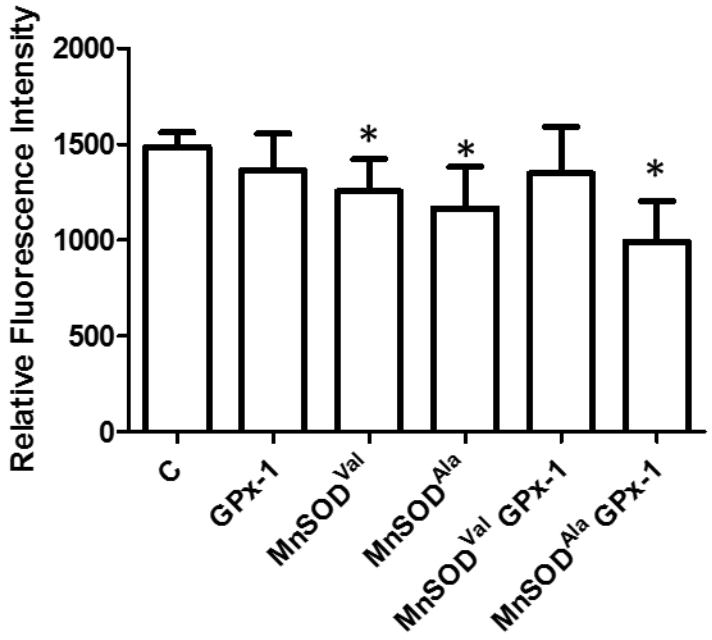

Figure 15. MnSOD^{Ala} GPx-1 and MnSOD irrespective of genotype decreased mitochondrial potential. Cells incubated in phenol red free media were treated with CMXROS (1µg/mL), an indicator of mitochondrial membrane potential. Relative fluorescence intensity was determined using a spectrophotometer and normalized to total protein concentration (BCA). Error bars indicate the standard deviation (n=9) (* = $p<0.05$).

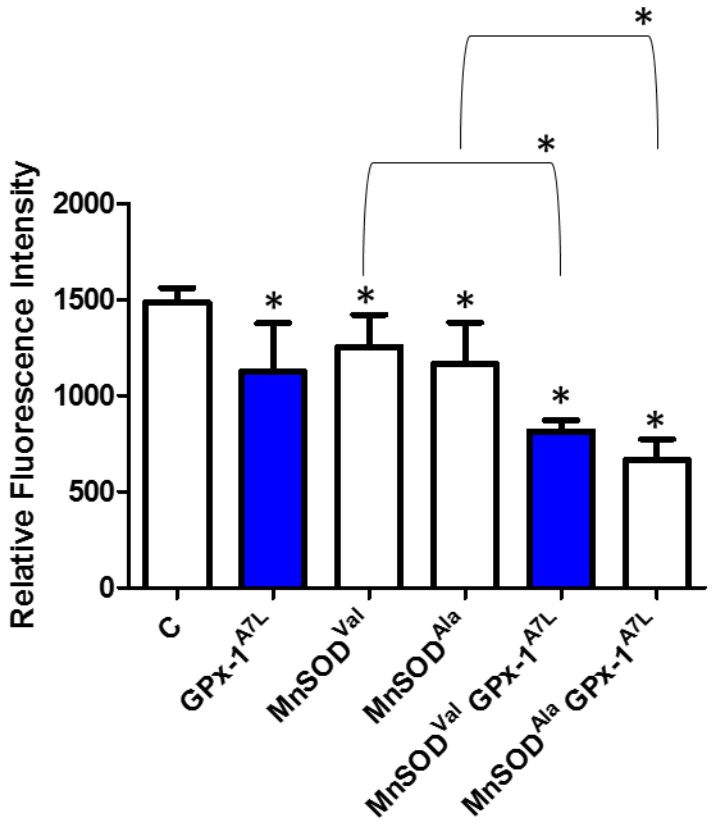

Figure 16. The expression of GPx-1^{A7L} alone and combined with either genotype of MnSOD decreased mitochondrial membrane potential. Cells incubated in phenol red free media were treated with CMXROS (1μg/mL), an indicator of mitochondrial membrane potential. Relative fluorescence intensity was determined using a spectrophotometer and normalized to total protein concentration (BCA). Error bars indicate the standard deviation (n=9) (* = $p<0.05$).

H. Genotypes in *MnSOD* are associated with its levels.

MnSOD levels and its association with genotype was assessed in human breast cells showing that there is more MnSOD protein per unit of mRNA in *Ala/Ala* MnSOD expressing cell line, ZR-75-1 [176]. To date, no studies have examined the association between genotype and the levels of MnSOD in breast tissue. In order to assess whether the MnSOD levels are associated with genotype, 21 breast cancer tissue samples were obtained from the UIC Cancer Core as a collaboration with the Diamond lab, genotyped and total lysates from tissue samples were electrophoresed and immunoblotted for MnSOD levels. *MnSOD* genotype was associated with MnSOD levels indicating that $MnSOD^{VA}$ breast cancer tissues have significantly lower MnSOD levels compared to tissues expressing the *AA* genotype. (Figure 17).

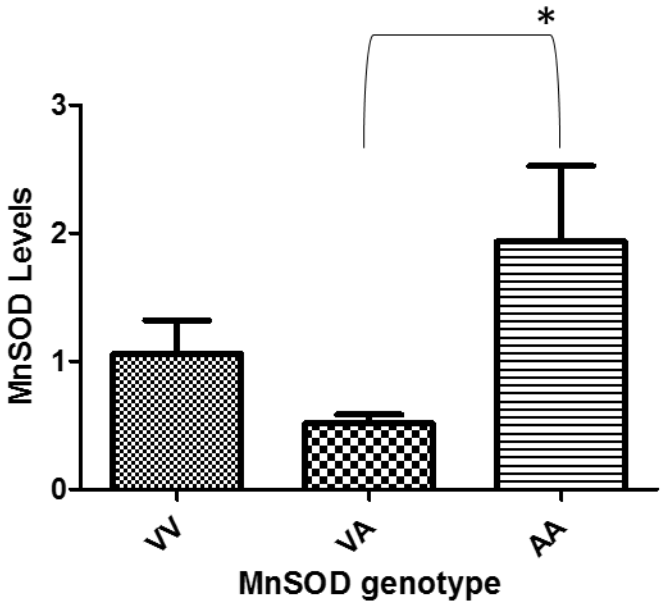

Figure 17. Breast tissues of individuals that are heterozygous for the $MnSOD^{Val}$ polymorphism have lower MnSOD levels. Breast tissue samples were genotyped and assessed by western blotting with anti-MnSOD antibodies and β -Actin as the endogenous protein loading control.

Protein levels were quantified by densitometry and normalized to β-Actin. Twenty-one samples were used, resulting in the following genotype distribution: *VV* (n=5) *VA* (n=10) *AA* (n=6). There were statistically significant differences between MnSOD levels and *MnSOD* genotype. The VA allele was associated with lower MnSOD levels in the studied population (ANOVA One-way analysis of variance test p=0.0132, Tukey's Multiple Comparison Test *= $p<0.05$).The error bars represent the standard error of the mean.

I. GPx-1 and MnSOD do not predict prostate cancer recurrence.

GPx-1 and MnSOD interact to increase risk of breast cancer. Individuals homozygous for both the $MnSOD^{Ala}$ and the $GPx\text{-}1^{Leu}$ alleles are at greater risk of breast cancer [79]. In order to assess whether GPx-1 and/or MnSOD levels are associated with aggressive prostate cancer, human prostate tissue microarray from the CPCTR was used. The tissues including both cancer and adjacent benign tissue were examined by immunohistochemistry and quantified using the VECTRA quantitative imaging system. Linear regression analysis of the interquartile odds was assessed. Although the cores contained both cancer and benign adjacent tissue, the analysis was limited to the levels of GPx-1 and MnSOD in cancer only. GPx-1 nor MnSOD levels in these tissues were not associated with prostate cancer recurrence (Table 4).

	Expression Quartile			
	1 (Low)	2	3	4 (High)
	OR (95%CI)	OR (95% CI)	OR (95% CI)	OR (95% CI)
Nuclear GPx-1	1.00	0.683 (0.363, 1.287)	0.3 (0.140, 0.641)	0.738 (0.385, 1.413)
Cytoplasmic GPx-1	1.00	0.654 (0.335, 1.277)	0.451 (0.221, 0.920)	0.807 (0.423, 1.538)
Total GPx-1	1.00	0.809 (0.415, 1.578)	0.324 (0.149, 0.703)	0.803 (0.418, 1.542)

	Expression Quartile			
	1 (Low)	2	3	4 (High)
	OR (95%CI)	OR (95% CI)	OR (95% CI)	OR (95% CI)
Nuclear MnSOD	1.00	1.199 (0.610, 2.358)	1.305 (0.660, 2.581)	1.075 (0.479, 2.411)
Cytoplasmic MnSOD	1.00	0.929 (0.465, 1.855)	0.661 (0.336, 1.298)	1.119 (0.548, 2.286)
Total MnSOD	1.00	0.756 (0.384, 1.489)	0.794 (0.409, 1.542)	0.954 (0.461, 1.974)

Table 4. GPx-1 and MnSOD levels are not associated with recurrence after radical prostatectomy, however individuals in quartile 3 of nuclear, cytoplasmic and total GPx-1 have significantly lower risk of prostate cancer recurrence. Odds ratios (OR) and 95% confidence intervals (CI) for prostate cancer recurrence by quartile of GPx-1 and MnSOD. Protein levels were measured by the VECTRA quantitative imaging system. The average of the mean GPX/MnSOD expression per cell and average of the total GPX/MnSOD expression per cell were calculated. Cases and controls were matched on race, pre-operative PSA, Gleason grade, patient age at diagnosis and pathological cancer stage. Odds ratios and p-values are from conditional logistic regression of prostate cancer recurrence adjusted for PSA. The reference group for all predictors is the First Quartile.

J. GPx-1 is located in the nucleus in benign human prostatic tissue and its levels are reduced in cancers.

GPx-1 is located in both the cytoplasm and the nucleus of breast cancer tissues, and high levels of GPx-1 in these cancers are associated with resistance to chemotherapy in patients with worse clinical outcome [177]. We assessed whether nuclear GPx-1 levels are different in low versus high grade prostate cancer. GPx-1 was localized to the nucleus in adjacent benign prostate tissue or low grade prostate cancer, but nuclear localization was frequently lost in high grade prostate cancer (Figure 18).

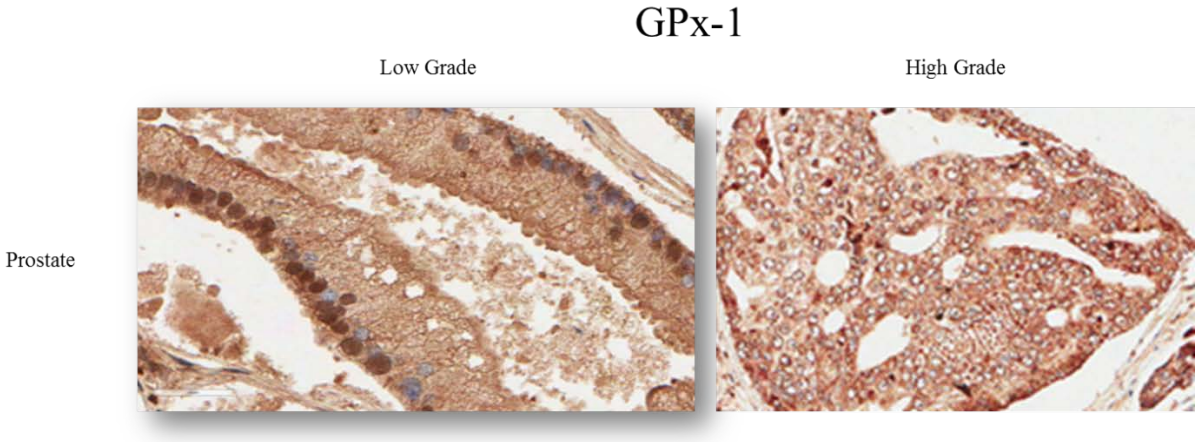

Figure 18. Nuclear localization of GPx-1 is reduced in high grade prostate cancer. An example of a core from the outcome CPCTR tissue microarray stained with anti-GPx-1 antibodies.

GPx-1 and MnSOD Summary

Although the levels of GPx-1 and MnSOD do not predict prostate cancer biochemical recurrence, *in vitro* studies indicate that there are allele-specific interactions between *GPx-1* and *MnSOD* that differentially modulate the levels of proteins implicated in cancer.

K. Sep15 Overview

The Sep15 gene is polymorphic in the 3'-UTR at positions 811 (C/T) and 1125 (G/A). The 3'-UTR is the region that determines the recognition of UGA codons as the amino acid Sec [115]. These functional genetic variations which form a haplotype may contribute to determining Sep15 levels [115, 131]. These polymorphisms in Sep15 are associated with levels of Se and prostate cancer mortality [141].The *TT* genotype is associated with increased prostate cancer mortality is 6 times more likely to exist in in African American compared to Caucasian men[133, 141]

In order to determine if Sep15 levels are associated with prostate cancer recurrence, and to investigate whether its levels differ in the cancers of African American men compared to Caucasian men, human prostate cancer tissue cores were examined by immunohistochemistry. In addition, DNA generated from 30 breast cancer tissues, and 129 white blood cells collected from prostate cancer patients were used to assess Sep15 allele distribution and its association with Se levels.

L. Sep15 expression human prostate cancer cells

Sep15 which is highly expressed in benign prostate may play a role in modifying the effects of Se in the risk of prostate cancer [112]. In order to assess the levels of Sep15 in human prostate cancer cell lines protein extracts derived from RWPE-1, benign prostate epithelium cell line, LNCaP and PC3 prostate cancer cell lines and MCF-7 doxycycline inducible Sep15 cells were assessed by western blotting using anti-Sep15 antibodies. The predicted 15 kDa Sep15 protein band was observed in all cell lines (Figure 19).

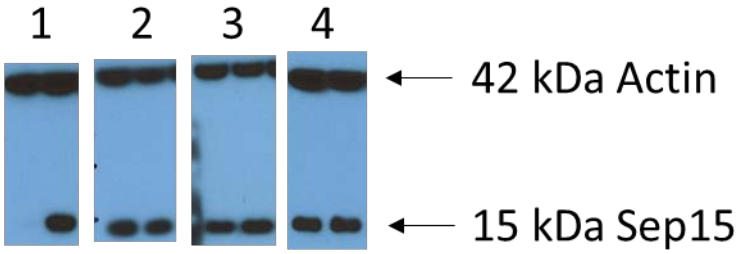

Figure 19. A 15 kDa band for the Sep15 protein is observed in all cell lines. Total cell extracts in duplicate from RWPE-1 (2), LNCaP (3), PC3 (4) prostate cell lines and total cell extract from Dox treated (#1 lane 2) or non-treated (#1 lane 1) MCF-7^{Sep15} cells were analyzed for Sep15 protein levels by western blot with anti-Sep15 and β-Actin antibodies as the endogenous control.

M. Sep15 is localized to the endoplasmic reticulum (ER) in breast and prostate cancer cells.

Sep15 is found in the ER and its localization to the ER is dependent on the presence of an ER signal peptide [115]. Localization to the ER also traditionally involves an ER retention signal, however Sep15 lacks an ER retention signal and is retained in the organelle by its association with UGGT [116, 117]. In order to confirm the cellular distribution of Sep15 in the ER, LNCaP, PC3, RWPE-1and MCF-7^{Sep15} cell lines were assessed for Sep15 localization by confocal imaging. ER-Tracker green, a fluorescent dye that specifically detects ER was used to visualize the ER in these cells. Sep15 distributes predominantly in the ER in MCF-7^{Sep15} (Figure 20A), RWPE-1 (Figure 20B) LNCaP (Figure 20B), and PC3 cells (Figure 20C), which is consistent with previously published data. However, in a very small population of PC3 cells membrane localization of Sep15 was observed (Figure 20C).

A

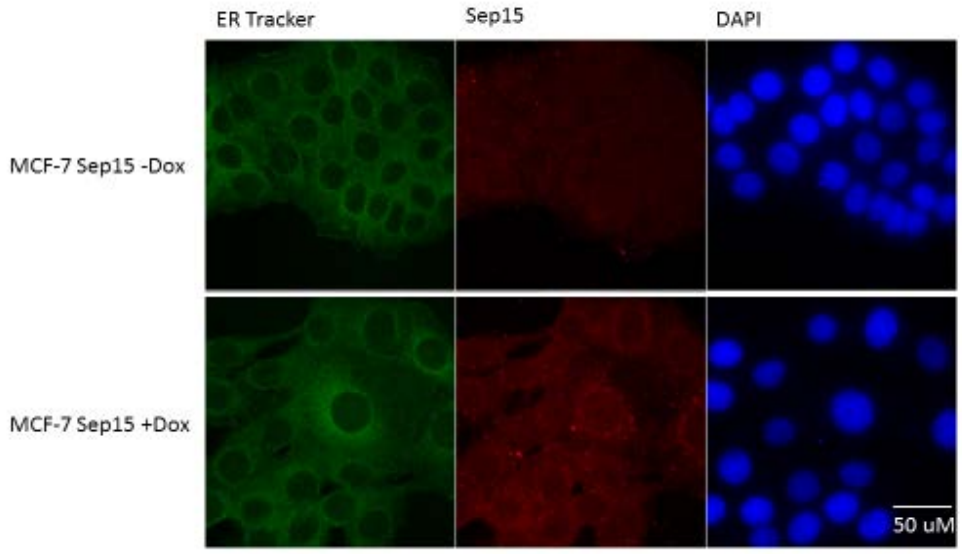
ER Tracker
Sep15
DAPI
MCF-7 Sep15 -Dox
MCF-7 Sep15 +Dox
50 uM

B

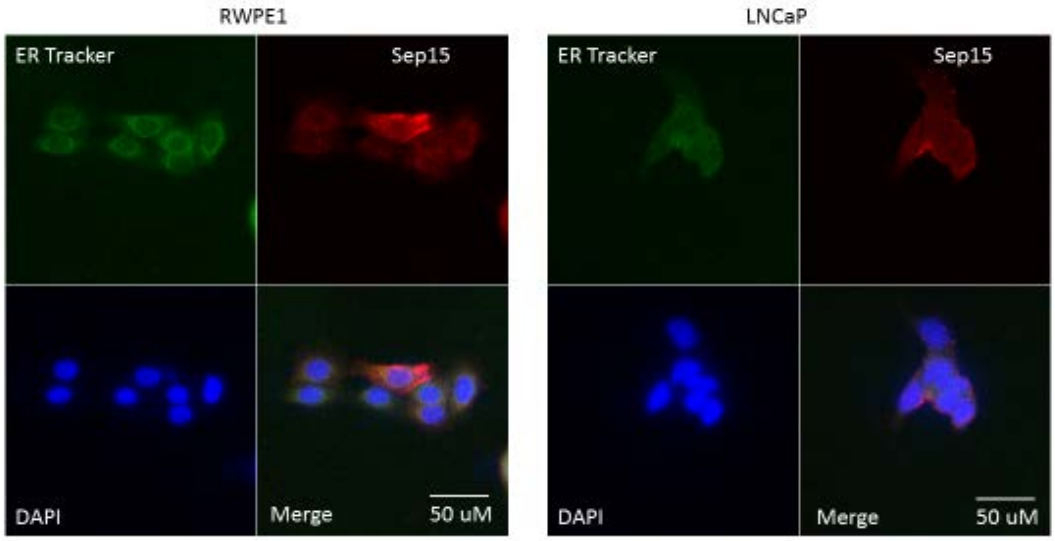
RWPE1
LNCaP
ER Tracker
Sep15
ER Tracker
Sep15
DAPI
Merge
50 uM
DAPI
Merge
50 uM

C

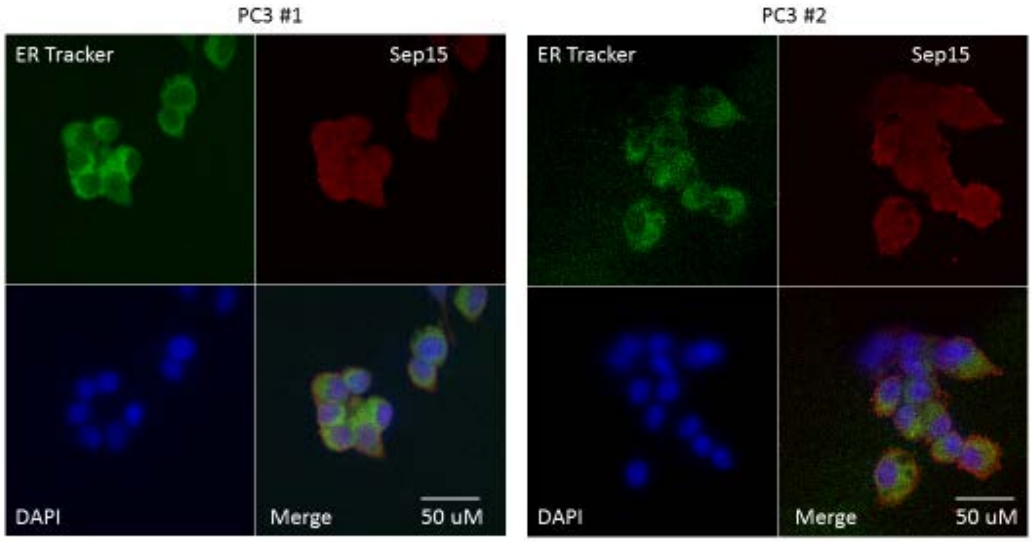

Figure 20. Localization of Sep15 to the ER. Localization of Sep15 (red fluorescence) was confirmed in the cell lines by immunofluorescence and subsequent confocal imaging, where Sep15 is exclusively co-localized with ER-Tracker (green florescence). Nuclei were counterstained with DAPI (blue fluorescence).

N. Sep15 is localized to the plasma membrane in prostate tissue and membrane localization of Sep15 is tissue specific.

To further investigate the rare membrane localization of Sep15 in some PC3 cells, tissue cores obtained from human prostates that were removed by prostatectomy were stained for Sep15 levels. All prostate tissue slides typically contained both cancer and adjacent histologically benign tissue. In all adjacent benign cores, Sep15 was expressed in epithelial cells but not the stroma, and although some cytoplasmic localization was observed, Sep15 was predominantly localized to the outer plasma membrane (Figure 21). This observation was unexpected given the established localization of Sep15 in the ER in previously published manuscripts [117]. Sep15 membrane localization and levels were reduced in cancer glands compared with benign glands (Figure 22). To assess whether membrane localization of the protein is prostate specific, Sep15 localization in human breast, colon and kidney tissues (5 benign and 5 cancer tissues) was assessed by immunohistochemistry. Sep15 was localized in the cytoplasm and its levels were reduced in cancer (Figure 23A). However, Sep15 membrane localization was also observed in benign human kidney tissue, specifically in distal tubules within that tissue (Figure 23A).

Sep15 is a closely related member of distinct family of ER resident selenoproteins that includes Selenoprotein M (SelM) with which it shares 31% sequence homology [178]. In order to determine whether membrane localization is specific to Sep15, SelM was also examined in human prostate, breast, colon and kidney (5 benign and 5 cancer tissues) and SelM localized to the ER and not the plasma membrane in non-cancerous human tissues (Figure 23B).

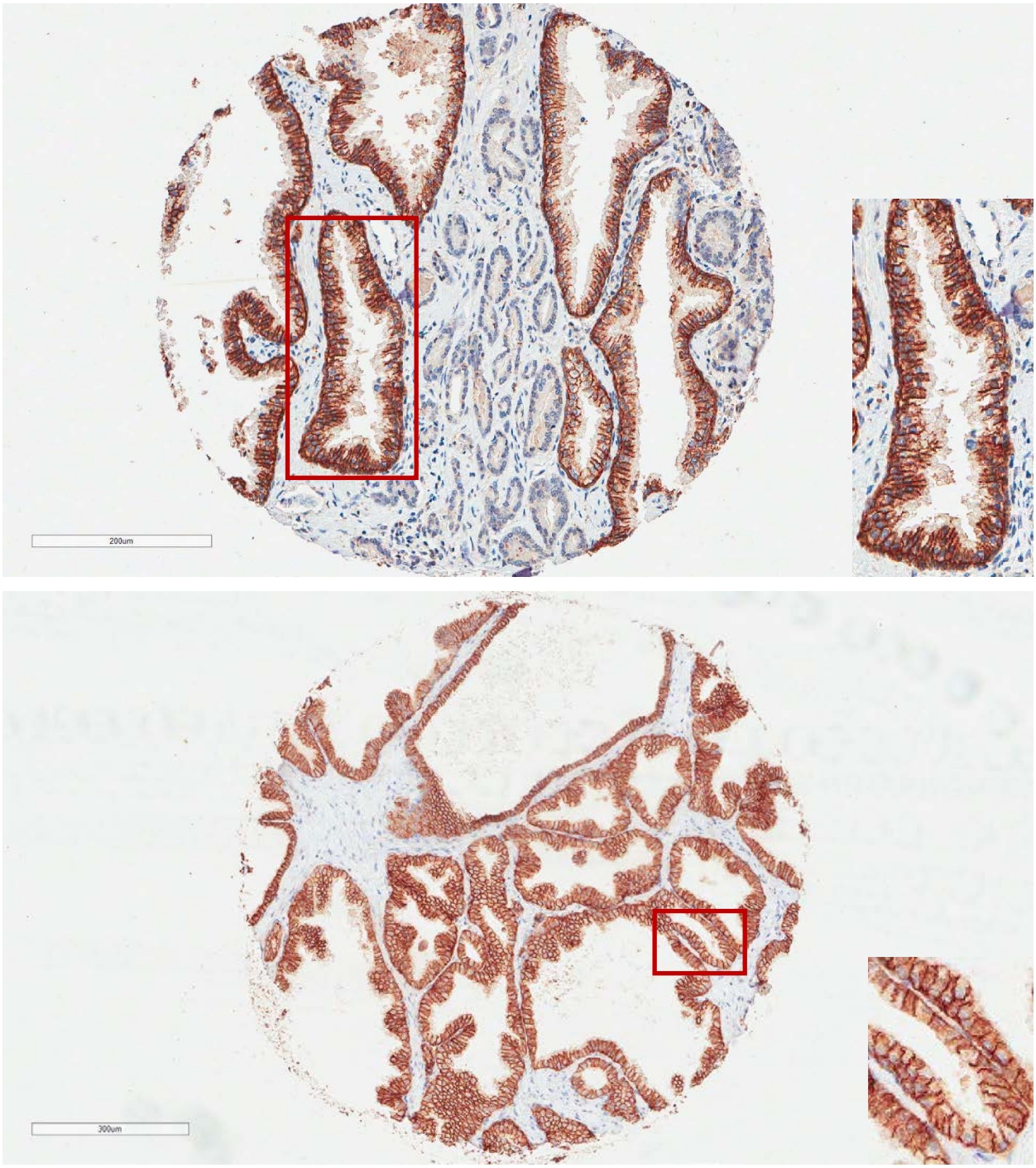

Figure 21. Sep15 is expressed in prostate epithelia and is predominantly localized to the plasma membrane in benign prostate. An example of a core from the outcome CPCTR tissue microarray assessed by immunohistochemistry and stained with anti-Sep15 antibody.Sep15 is expressed in prostate epithelia but not in stroma and ER localization is also observed.

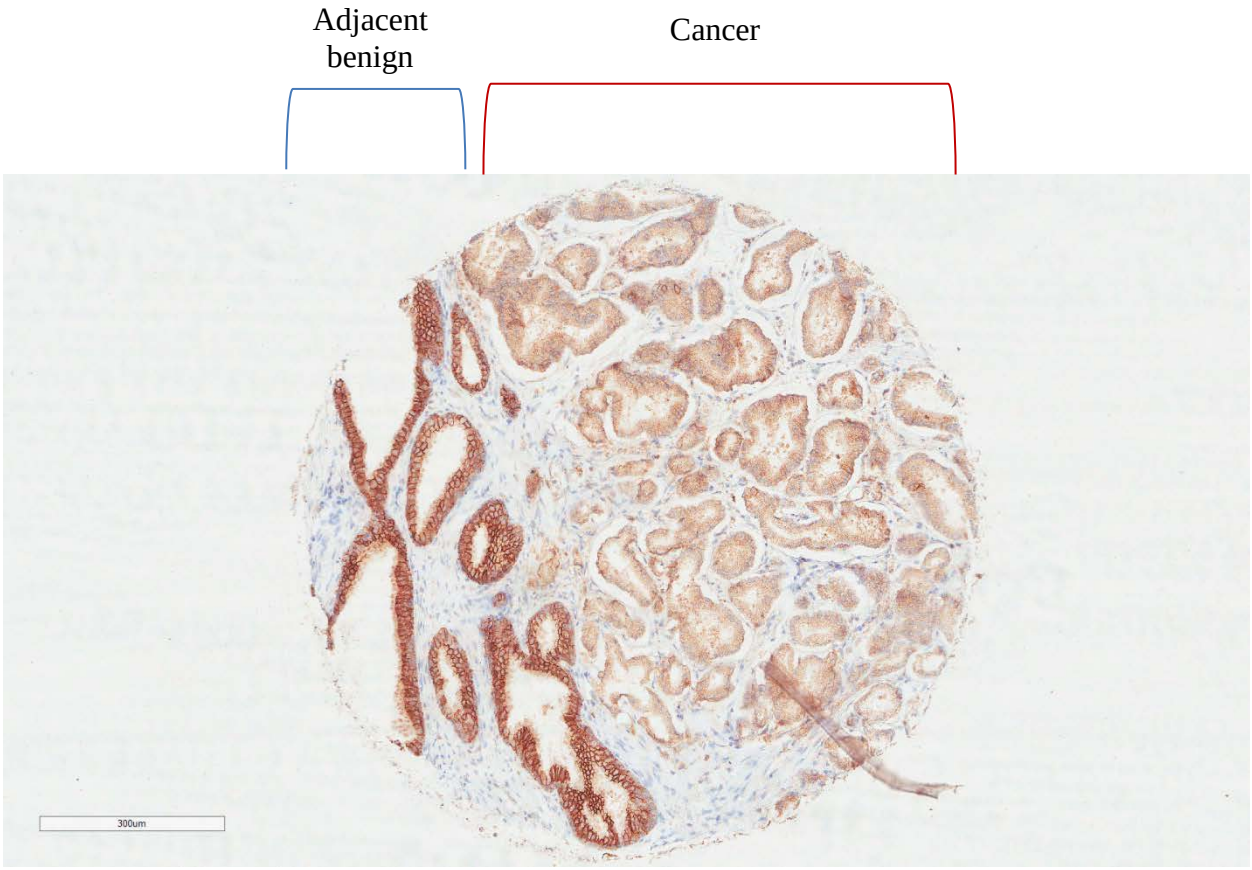

Figure 22. Sep15 levels and membrane localization are reduced in prostate cancer. Representative image of a core stained with anti-sep15 antibodies.

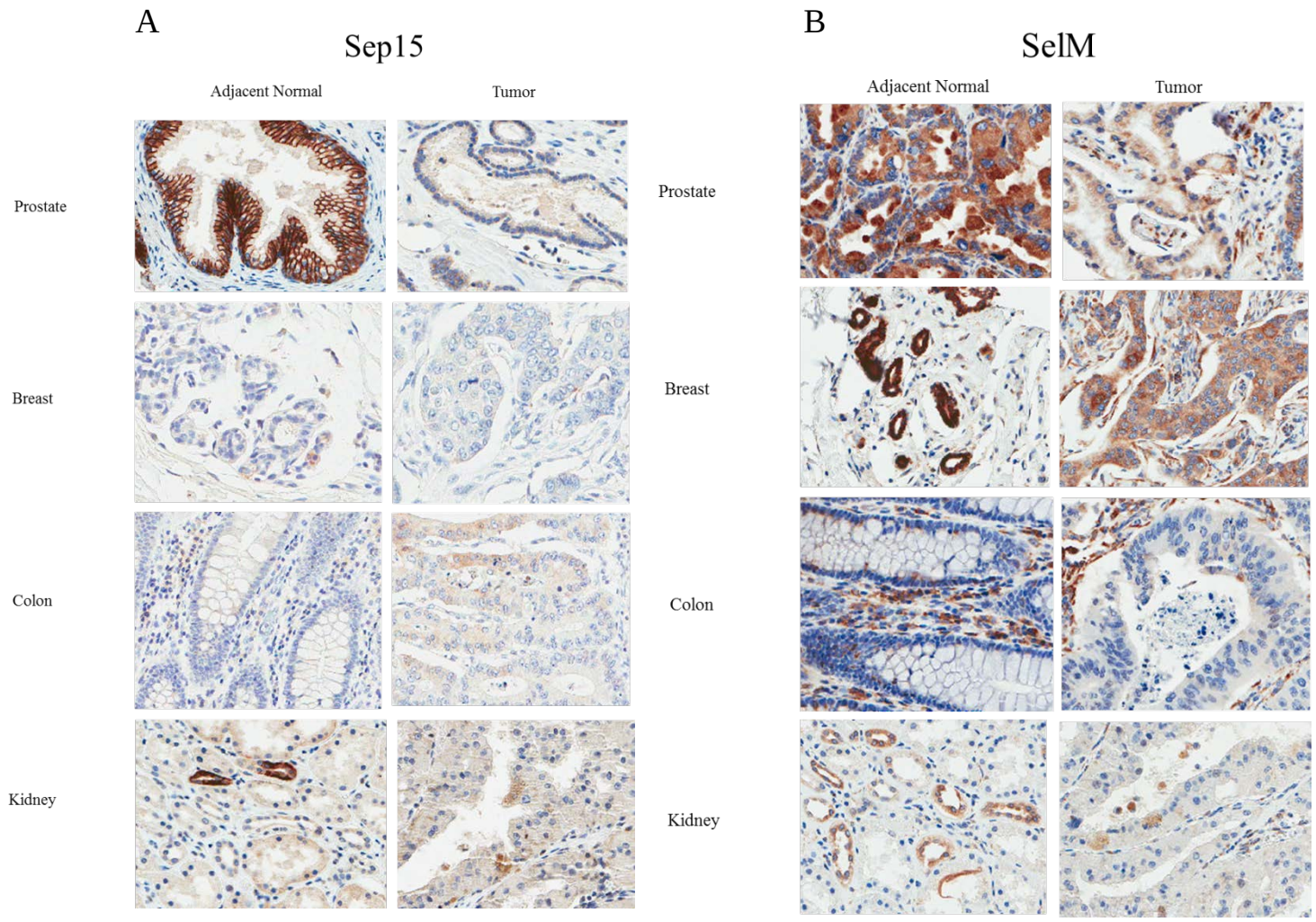

Figure 23. A. Sep15 localized in the ER in breast and colon tissues and in the plasma membrane in prostate and distal tubules in the kidney and its levels are reduced in tumors. Representative images of adjacent benign and tumor cores from prostate, breast, colon and kidney tissues stained with anti-sep15 antibodies. *B. SelM is localized to the ER in all tissues examined and its levels are reduced in tumors.* Representative images of adjacent benign and tumor cores from prostate, breast, colon and kidney tissues stained with anti-SelM antibodies.

O. Sep15 levels are not associated with Gleason grade of prostate cancer.

There is a statistically significant association between Sep15, plasma selenium levels and prostate cancer mortality, but not risk [141]. In order to assess whether Sep15 levels are associated with prostate cancer, a human prostatic tissue microarray from the CPCTR was used. The tissues including both cancer and adjacent benign tissue were examined by immunohistochemistry. In order to assess whether there is a relationship between Sep15 and advanced prostate cancer, the patients included in the tissue array were grouped by Gleason score. Patients with Gleason score 5 and 6 were grouped in GleasonCat 1 (n=79), Gleason score 7 (3+4) in GleasonCat 2 (n=171), and Gleason score 7 (4+3) and 8+ were in GleasonCat 3 (n=80). Patients with Gleason score 4+3 were included in GleasonCat 3 because the mortality rate of patients with this Gleason score is 3-fold higher than those with Gleason 3+4 score[179]. Sep15 levels in these tissues were analyzed using the VECTRA quantitative imaging system. Association between Sep15 levels and GleasonCat was determined using the Wilcoxon Rank Sum test and the distribution of scores were represented using box-and-whisker plots. The analysis indicated that Sep15 levels were not significantly associated with Gleason score, nor was there a significant difference between Gleason categories (Figure 24).

Category	Gleason Score	N	
1	≤6	79	
2	3+4	171	
3	4+3, ≥8	80	
		330	Total

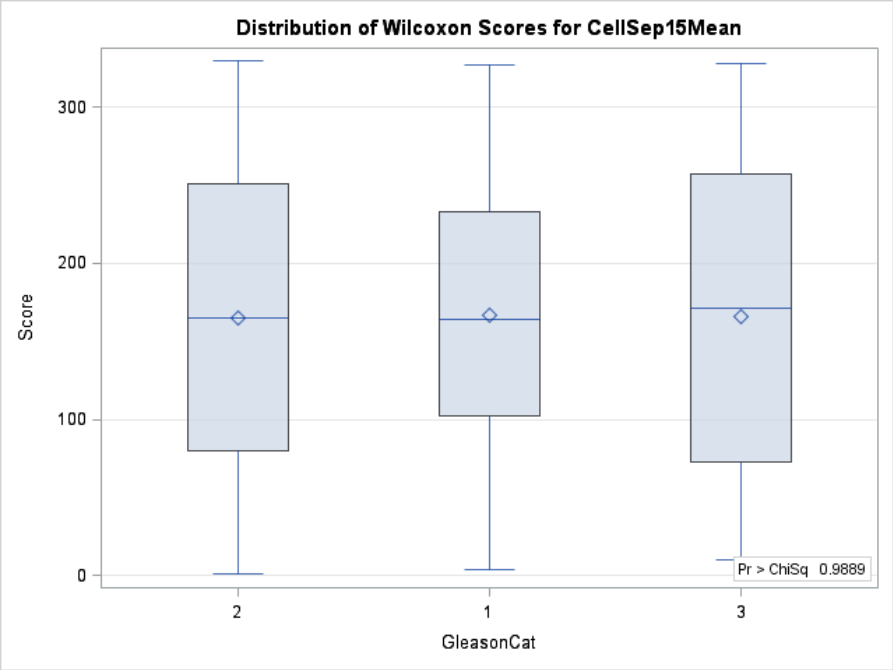

Figure 24. Sep15 levels are not associated with advanced prostate cancer. Tissues in the CPCTR prostate cancer outcome TMAs were distributed into 3 Gleason categories (GleasonCat) based on Gleason score (A). Mean tissue Sep15 levels were ranked for all cores and assigned a score from 1-330 based on relative Sep15 levels where the patient with the lowest tissue Sep15 received a score of 1 and the patient with the highest tissue Sep15 levels received a score of 330. Box-and-whisker plots represent the range of scores from patients in each category (vertical lines) and the range of the first and third quartiles in each category (boxes). The horizontal lines inside the box and the diamond represents the median and mean, respectively.

P. Levels of Sep15 are significantly reduced in prostate cancers compared to adjacent benign tissues.

Western analysis of prostate tissue showed high levels of Sep15. To determine whether Sep15 levels are reduced in cancers compared to adjacent benign tissue, 85 cores (CPCTR) having both cancer and benign adjacent tissue were analyzed. A paired t-test was used to determine the mean difference between benign and cancer which was statistically highly significant ($p<0.0001$) with adjacent benign having higher Sep15 levels (Table 5).

	Mean Difference (95% CL Mean) N=85	p-value
Cell Sep15 Mean	-0.06 (-0.08, -0.04)	**1.0E-07**
Total Tissue Sep15 Levels	-34.3005 (-47.41, -21.1910)	**1.4E-06**

Table 5. Sep15 levels are significantly lower in prostate cancers compared to benign adjacent tissue. Mean difference and 95% confidence limits for the mean (CL Mean) of total Sep15 in tissue cores of patients in the CPCTR prostate cancer outcome TMAs comparing levels in cancers and adjacent benign tissue (n=85). For each core with normal tissue and cancer tissue, the difference (cancer-normal) in each characteristic was taken. P-value is from a paired t-test of the difference within a core.

Q. Sep15 levels are significantly reduced in cancers of African American men compared to Caucasian men.

The Sep15 gene contains a haplotype in the 3'-UTR such that a C or *T* at residue 811 is always paired with a *G* or *T* at residue 1125. Compared to Caucasians, a 6-fold higher frequency of 31% for the at-risk *TT* allele is found among African Americans [130], who have both the highest incidence and mortality from prostate cancer [180]. Based on studies using reporter constructs, it was determined that the at-risk allele which is frequent in African Americans would be expected to result in lower levels of Sep15, an effect that is dependent on the serum or toenail Se levels. Among the CPCTR TMAs analyzed (n=328), 33 were obtained from African American men and 295 were Caucasians. The mean Sep15 levels in the cancer glands of African Americans were significantly lower (p=0.0179) compared to the levels of Sep15 in cancer glands from Caucasians (Table 6).

	Value (SD)		
	African American (n=33)	Caucasian (n=295)	Wilcoxon p-value
Total Sep15 Mean	**0.09** (0.04)	**0.10** (0.04)	**0.0179**

Table 6. Sep15 levels are significantly lower in prostate cancers of African American men compared to cancers of Caucasians. Mean and standard deviation of total Sep15 in tissue cores of patients in the CPCTR prostate cancer outcome TMAs comparing levels in African Americans (n=33) and Caucasians (n=295). Levels of Sep15 were assessed using the Wilcoxon Rank Sum test, two-tailed.

R. Se levels are reduced in sera of African American men compared to Caucasian men.

African American men have the highest total cancer incidence and mortality rates [181] with the greatest disparity observed for prostate cancer with 61% and 146% higher rates of incidence and mortality, respectively [181]. African Americans have lower serum Se levels when compared to Caucasians [182] and this difference is maintained when the Se levels are adjusted for geographical location [142]. In order to determine whether African Americans have lower serum Se levels than Caucasians, 129 serum samples were obtained from self-reported African-American and Caucasian men diagnosed with prostate adenocarcinoma and assessed for Se levels. Serum Se levels were significantly lower (17.2%) in African American men than Caucasians/others (Table 7).

	Value (SEM)		
	African American (n=27)	Caucasians/Others (n=102)	p-value
Total Se levels ng/mL	**115.24** (3.03803)	**139.177** (2.413743)	**0.0001**

Table 7. African Americans have 17.2% significantly lower Se levels compared to Caucasian/others. Levels of Se in sera samples was determined by graphite furnace atomic absorption spectrometry. There were statistically significant differences between means of serum Se for all patients grouped by ethnicity (Mann-Whitney test, two-tailed p=0.0001).

S. The presence of a *T* allele in Sep15 is associated with lower Se levels.

A 6-fold difference in frequency (31%) for the *TT* genotype was observed among African Americans who have both the highest incidence and mortality from prostate cancer and Caucasians [130]. To confirm whether the *T* allele is prevalent in African Americans and whether the presence of a T allele is associated with lower Se levels, 129 DNA samples obtained from the Chicago population was genotyped for Sep15. Of the 129 samples obtained, 126 DNA samples were successfully genotyped. A 13-fold difference in frequency for the *TT* genotype was observed among African Americans compared to Caucasians (Figure 25). In addition, the presence of a *T* allele was associated with lower Se levels (Figure 25).

A

	Percentage (n)	
Sep15 Genotype	African American (n=27)	Caucasians (n=99)
CC	**3.70** (1)	**60.6** (60)
CT	**55.5** (15)	**36.36** (36)
TT	**40.74** (11)	**3.03** (3)

B

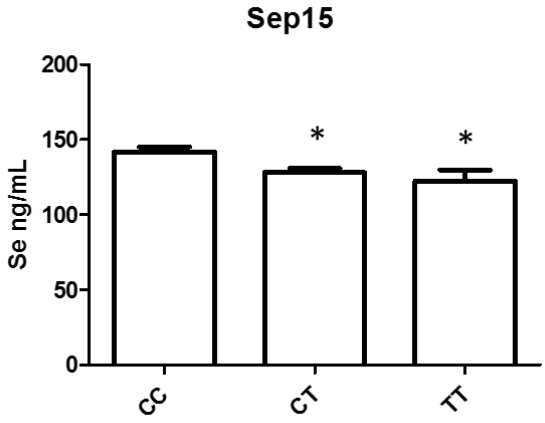

Figure 25 –African Americans have a 13-fold increased frequency for more likely to be homozygous for the TT Sep15allele and the presence of a T allele is associated with significantly lower serum Se levels (p<0.006). A. DNA was genotyped for Sep15. Genotype frequency was reported as percentage and the parenthesis are the number of individuals in each category.

B. There were statistically significant differences between means of serum Se for all patients grouped by Sep15 genotype. The *T* allele was associated with lower Se levels in the entire population (Kruskal-Wallis test p=0.0005, Dunn's Multiple Comparison Test *= p<0.05). Error bars represent the standard deviation of the mean.

T. Lower Se levels are associated with *SEPP1* genotype.

Selenoprotein P (SelP) , the plasma Se transporter which has been shown to confer increased risk of aggressive prostate cancer [109] was assessed for association between its functional polymorphisms and Se levels and Sep15 genotype. SEPP1-Ala234Thr (rs3877899) polymorphism was associated with a lower concentration of serum Se (Figure 26). Although SEPP1 rs3877899 AA allele was significantly associated with lower Se levels ($p < 0.05$), the allele distributions were similar when stratified by race (see appendix).

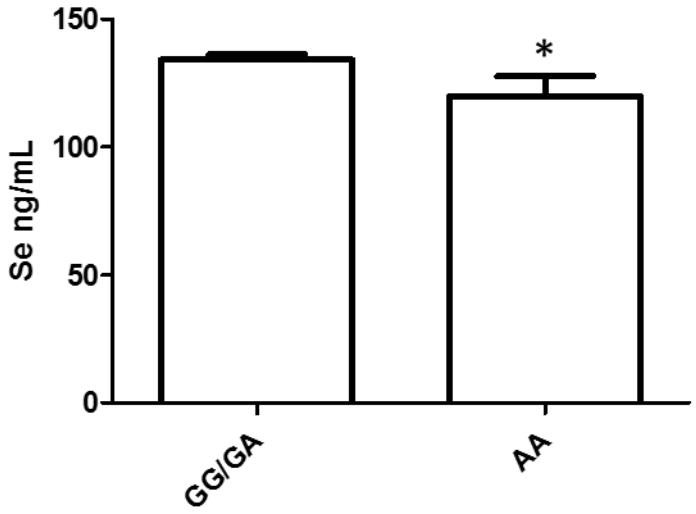

Figure 26 –Lower Se levels are associated with SEPP1 AA genotype. Se levels were analyzed by graphite furnace spectroscopy and DNAs (n=129) were genotyped for SEPP1 rs3877899. There were statistically significant differences between means of serum Se for all patients grouped by SEPP1 genotype (Mann-Whitney, two-tailed * = $p<0.05$). The error bars represent the standard error of the means.

Sep15 Summary

Sep15 levels are reduced in prostate cancers compared to benign tissue, as well as in cancer tissues of African American men compared to Caucasian men. However, Sep15 levels are not associated with advanced prostate cancer. Localization of Sep15 to the plasma membrane was observed in prostate tissue but its role has not yet been elucidated.

IV. DISCUSSION

Scientific debate on the association between Se and the risk of cancer has persisted for years. Originally viewed as a toxic agent, Se later gained a reputation as a chemopreventative agent which led to widespread epidemiological and supplementation studies aimed at assessing its efficacy. These initial studies produced conflicting findings perhaps due in part to underlining genetic factors that were not assessed, and thus were not successful in conclusively identifying an appropriate use of Se in cancer prevention in humans. In animal models, however, strong evidence was found in support of the ability of Se to reduce the incidence of cancer, and this effect likely occurs through selenoproteins. The data presented in this thesis elucidates novel roles of the selenoproteins GPx-1 and Sep15 in cancer and provides insight into how these selenoproteins may function to influence the biology and physiology of both benign and cancer cells.

The availability of Se in tissues is modulated by SEPP1 genotype

There is no consensus among studies regarding the validity of an association between allelic variations in GPx-1and the risk of cancer. The GPx-1 *Leu* allele is often referred to as the at-risk allele, but it was also found to be protective against carcinogenesis [86]. The inconsistent results of these studies may be attributed to both nutritional intake of Se and the influence of genetic variants in Se carrier protein SEPP1. SEPP1 binds 60% of total Se in the serum, and is the major form of selenium delivery to organs [183]. We showed that the rs3877899 polymorphism of SEPP1 is associated with lower Se levels (Figure 26) and may affect the levels of selenoproteins GPx-1 and Sep15, whose activities and levels are dependent on the intracellular availability of the micronutrient [47, 112, 184].

GPx-1 levels impact cellular ability to detoxify H_2O_2 generated by the mitochondrial antioxidant enzyme MnSOD. This interaction is made more complex by the association of SEPP1 polymorphisms with genetic variants in MnSOD [109], resulting in dual, contradictory mechanisms by which Se either prevents or promotes cancer through the same enzyme: GPx-1. High levels of GPx-1 in cells that have progressed to cancerous state may promote carcinogenesis, likely due to the inhibition of H_2O_2 mediated cell death [185].

Redox regulation in cancer is impacted by genetic variants in GPx-1 and MnSOD genes

The combined expression of *GPx-1*^{Leu} and *MnSOD*^{Ala} genotypes was significantly associated with increased risk of breast cancer [79]. The protein encoded by the *MnSOD*^{Ala} allele which is localized more readily to the mitochondria than the protein encoded by the *MnSOD*^{Val} allele [186], is thought to result in increased H_2O_2 production. Thus, the combined over-expression of MnSOD encoded by the *Ala* variant with a less enzymatically active GPx-1 encoded by the *Leu* variant (GPx-1^{A7L}) [58] may alter redox homeostasis. The investigation of this hypothesis was performed by examining the levels and genotypes of both proteins in a cell culture model using MCF-7 cells, which are null for GPx-1 and have negligible levels of MnSOD [110]. In these cells, there was a relationship between GPx-1 genotype and its location in the mitochondria and cytoplasm (Figure 3). The location of GPx-1^{A7L} protein almost exclusively in the cytoplasm was hypothesized to decrease its ability to effectively detoxify the elevated H_2O_2 generated by mitochondrial MnSOD^{Ala} protein and increase redox regulation in those cells by increasing the nuclear translocation of transcription factor Nrf2, the antioxidant defense system regulator. As expected, high MnSOD levels increased nuclear Nrf2 levels (Figure 10). Unexpectedly, GPx-1 also increased nuclear Nrf2 suggesting the MCF-7 GPx-1 transfected cells have high H_2O_2 levels even in the presence of GPx-1, and Nrf2 activation may not be

mediated solely through H_2O_2 levels (Figures 10, 14). The observation that *GPx-1*^{A7L} expression resulted in the highest levels of nuclear Nrf2 compared to *GPx-1* (Figure 14) indicates a reduced ability for GPx-1 encoded by the *A7L* allele to detoxify H_2O_2. Increased expression of *GPx-1* in combination with *MnSOD* does reduce nuclear Nrf2 to basal levels, except when *MnSOD*^{Val} is co-expressed with *GPx-1*^{A7L} suggesting that increased nuclear Nrf2 is likely due to H_2O_2 production. MnSOD encoded by either allele similarly increased nuclear Nrf2 which contradicts the reports that *MnSOD*^{Ala} expression uniquely results in higher MnSOD levels and activity and hence would have been expected to induce the greatest activation of Nrf2 of the two alleles. The ability of the interaction between *MnSOD*^{Ala} and *GPx-1*^{A7L} to maintain high levels of nuclear Nrf2 (Figures 10, 14) and the observation that either *MnSOD*^{Val} or *MnSOD*^{Ala} results in similar protein levels in breast tissues (Figure 17) does not resolve the conflict regarding which MnSOD encoded by the variants is more enzymatically active. Thus, the MnSOD genotype-activity relationship must be further explored.

<u>The interaction of GPx-1 and MnSOD affect molecular pathways implicated in cancer</u>

ROS have pleiotropic effects on cell survival and proliferation. Although high levels of ROS can lead to lipid peroxidation and membrane damage, low levels can activate transcription factors, protein kinases, as well as can lead to cell death [185, 187]. High levels of H_2O_2 as a result of MnSOD over-expression have been shown to contribute to the survival and proliferation of cancer cells [98], indicating that the detoxification of H_2O_2 or the expression of GPx-1 can promote apoptosis. The levels of the anti-apoptotic protein Bcl-2 are directly correlated with mitochondrial membrane potential, and a decrease in its levels leads to a pre-apoptotic state of cells [188, 189]. When the level of Bcl-2 was assessed in the MCF-7 cell lines, both *GPx-1* and

MnSOD, irrespective of genotype, decreased Bcl-2 (Figures 6, 12) indicating that either an elevation or reduction in H_2O_2 can promote apoptosis. Because Bcl-2 regulates mitochondrial potential by modulating the release of the pro-apoptogenic protein cytochrome c [189, 190], a decrease in Bcl-2 in these cells would decrease membrane potential. However, only *GPx-1*^{A7L}, *MnSOD*^{Val}, *MnSOD*^{Ala} and their combined expression significantly reduced membrane potential. Since high membrane potential is positively correlated with ATP production [191], ATP production would be reduced in these cells. A pro-survival phenotype of *MnSOD*^{Val} and *GPx-1* in increasing the levels of p-Akt but not decreasing Bcl-2 (Figures 6 and 7) indicate a dual role of these antioxidant enzymes in promoting apoptosis as well as promoting cell proliferation. Tumor suppressor E-Cadherin regulates proliferation, cell-cell adhesion and invasion of cells [192-194]. GPx-1 encoded by the *Pro* allele decreased E-Cadherin (Figure 5) indicating that GPx-1 may stimulate cells to a proliferative state while *GPx-1*^{A7L} attenuates the proliferative influence of GPx-1. The duality of GPx-1 and MnSOD to promote apoptosis and proliferation in the same cellular milieu likely contributes to both pro and anti-carcinogenic roles of these antioxidants.

<u>The role of the antioxidants in prostate cancer</u>

There have been conflicting findings regarding the association between genetic variants in *GPx-1* and prostate cancer. Similarly, some studies found that certain *MnSOD* polymorphisms convey significantly higher risk for early onset of prostate cancer while no association was found in other cohorts [99, 195]. The *16Ala* polymorphism has been associated with an increased risk of prostate cancer in men with the lowest intake level of dietary anti-oxidants, including carotenoids and Se [99, 100]. Together with the observation that higher MnSOD levels are associated with advanced progressing tumor stages [98], it is conceivable that the levels of these

proteins may predict prostate cancer recurrence after radical prostatectomy. However, neither GPx-1 nor MnSOD was found to predict recurrence of prostate cancer (Table 4), indicating that although they may play a role in cancer formation, they do not affect metastasis once the organ is removed.

The localization of GPx-1 in the nucleus infers a novel function

Selenium binding protein 1 (SBP1) is a non-Sec containing protein that is tightly associated with Se [196, 197]. An inverse relationship between the levels of GPx and SBP1 has been observed in human prostatic tissue and low nuclear SBP1 was an indicator of prostate cancer recurrence [198]. SBP1 co-localized with GPx-1 to the nucleus upon oxidative challenge of human hepatocellular carcinoma cells with H_2O_2 [199], indicating that GPx-1 localization to the nucleus may be induced by oxidative stress. SBP1 physically interacts with GPx-1 [200]. The observation that GPx-1, which is localized to the nucleus in benign prostate, is reduced in nuclear localization in prostate cancer (Figure18) as is SBP1 nuclear signal, indicate that nuclear localization of GPx-1 may be dependent on its physical interaction with SBP1. The presence of glutathione in the nucleus and the observation that reduction of nuclear glutathione prior to irradiation has been found to result in fragmentation of nuclear DNA and apoptosis suggest infers a role of GPx-1 in nuclear homeostasis [201]. Since SBP-1 levels are inversely associated with GPx-1 activity [200], the ratio of SBP1 and nuclear GPx-1 may impact genomic instability in the nucleus.

The role of plasma membrane localized Sep15 in prostate cancer

Research on the role of selenoproteins in cancer has indicated the importance of subcellular localization of selenoproteins, the impact their location has on their function, and the contribution of selenium to the etiology of cancer. The effect that allelic variations in the genes of selenoproteins have on their partitioning between cellular compartments [150] can lead to the discovery of potential novel functions of these proteins including Sep15. Although the function of Sep15 is not well characterized, Sep15 was found to be involved in protein folding given that it forms a stable complex with UGGT, an enzyme responsible for the proper folding of N-glycosylated proteins [116, 117]. The exclusive location of UGGT in the ER has led to the traditional thought that Sep15 is exclusively an ER resident protein, however, our examination of prostate tissue showed a novel location of the protein in the plasma membrane (Figure 21). The absence of SelM in the membrane (Figure 23B), indicates that the membrane localization of Sep15 is not a result of any of the shared sequences between the two proteins that could be recognized by antibodies used in immunohistochemistry. The role of Sep15 in the membrane has not yet been elucidated, and *in silico* analyses have not revealed any canonical plasma membrane targeting sequence, but reduced levels of Sep15 is a marker of cancer [115], suggesting that its localization either drives or is affected by carcinogenesis.

The argument for a role of Sep15 in the etiology of cancer is substantiated by its localization to a region on chromosome 1 that is often deleted in cancers of the breast, lung and cervix [202-204], the loss of heterozygosity at the Sep15 locus, and the presence of two polymorphic haplotype at position 811 (C/T) and 1125 (G/A) in the 3'-UTR, influencing the function of SECIS element in a Se-dependent manner[133] indicates that the allelic variants in conjunction with Se levels will influence Sep15 levels [133]. Indeed, the prevalence of the *811T* allele in African Americans, who are known to have higher incidence and mortality of prostate

cancer, was recapitulated (Figure 25), making it plausible that Sep15 levels are lower in this population. The notion that individuals homozygous for the *811T* allele will have lower Sep15 levels was not directly assessed. However, the comparison of prostatic tissue cores of Caucasians and African Americans who are 6x more likely to have the at-risk allele, demonstrated that African Americans indeed had significantly lower Sep15 levels (Table 6).Our study also confirmed that African Americans have significantly lower Se levels (Table 7) indicating that the interaction between Sep15 genotype and Sep 15 levels may be modulated by Se levels.

Given the observations made that the polymorphic variants of Sep15 are associated with death from prostate cancer [141], and with Sep15 being lower in prostate cancers than in benign tissue (Table 5), it is conceivable that the levels of Sep15 may predict prostate cancer recurrence. However, when cores obtained from cancer patients in the CPCTR outcome array were analyzed and categorized by Gleason score, Sep15 level was not predictive of advanced prostate cancer (Figure 24).

Considering these analyses together with the observed association between Se and prostate cancer risk in observational studies, there is strong evidence that Se may play a role in prostate cancer in males with genetic variants that influence the metabolism and transport of Se. Given the relationship between Se levels, genotypes in selenoproteins such as *SEPP*1, *GPx-1* and *Sep15*, and the interaction of Se with antioxidant protein MnSOD consideration should be given to genotyping individuals for genes encoding selenoproteins that require Se for their enzymatic activity as well as other proteins such as MnSOD and SBP1. This thesis project was accomplished in hopes of identifying a subset of the population identified by their genetic make-

up who have are at greater risk for prostate cancer and may benefit from Se supplementation for the prevention of cancer, specifically prostate cancer, while excluding those who would not.

Proposed mechanism of Se and cancer interaction

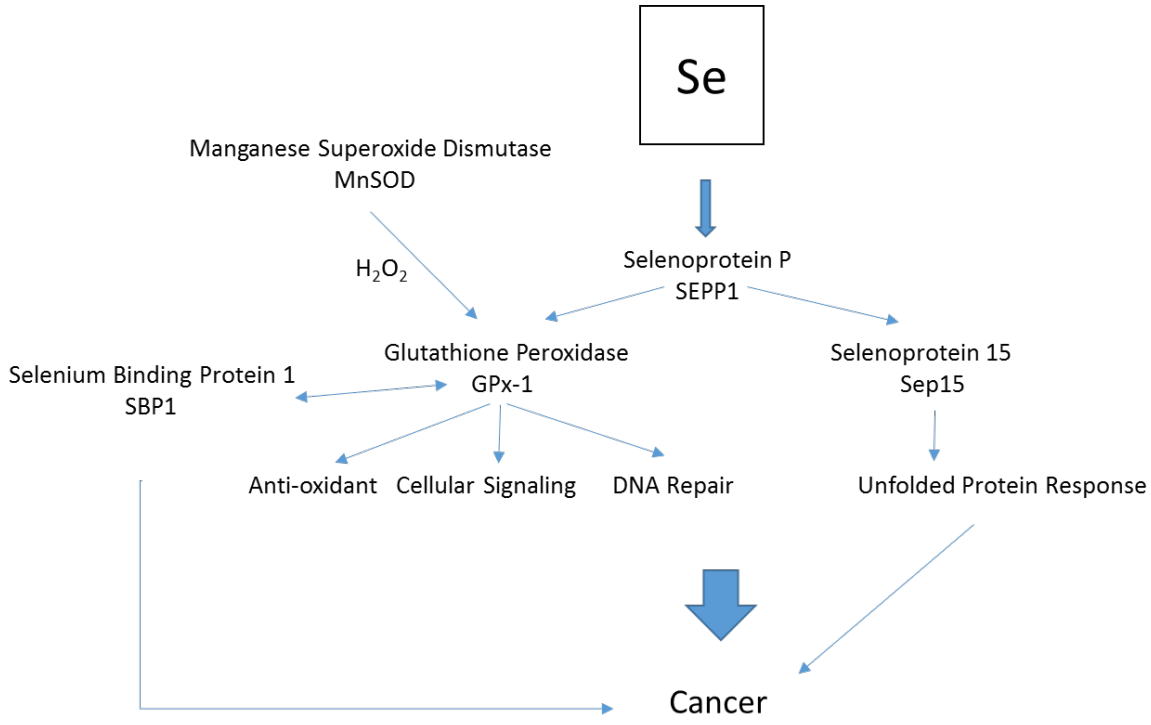

Figure 27 –Model for the impact of Se through selenoproteins in cancer. The incorporation of Se into Selenoprotein P (SEPP1), the Se carrier protein in the blood is affected by genotypes of SEPP1. Reduced levels of GPx-1, as a result of the polymorphisms in either *GPx-1* or *SEPP1* will increase the levels of H_2O_2 generated by MnSOD which can then modulate of cellular signaling and DNA repair pathways. The physical interaction between SBP-1, a protein whose levels are inversely associated with cancer incidence and poor outcome, and GPx-1 was shown to decrease GPx-1 activity and can limit its function as an anti-oxidant, all of which can lead to

cancer. Sep15 is involved in the unfolded protein response, a signaling pathway that regulates accumulation of unfolded proteins and is implicated in cancer.

V. CONCLUSIONS & FUTURE DIRECTIONS

Given the associations between cancer and the polymorphic variants in *GPx-1* and *Sep15* [86, 141], and considering that the risk of cancer may be modulated by Se in the body, a reasonable prediction was that these variants can be used as markers of recurrence The data provided by this study however does not establish an association between these selenoproteins and prostate cancer recurrence, but does indicate that a role may exist for these proteins in molecular pathways implicated in cancer. The localization of GPx-1 and Sep15 in different subcellular compartments than previously predicted presents an obstacle to pinpointing their function. However, these findings also provide opportunities to discover unknown functions of Se through its incorporation into these proteins.

Although GPx-1 was not a clinical biomarker of prostate cancer recurrence and Sep15 levels were not associated with tumor grade, investigating why low levels of Sep15 are observed in prostate cancers of African American men compared to Caucasian men, and as well as studying the presence of GPx-1 in the nucleus and its interaction with SBP1 may lead to further understanding of molecular changes that alters the levels of these proteins in malignant prostate tumors.

Allele specific effects of *GPx-1* were observed on the levels of proteins implicated in proliferation and apoptosis, and changes in mitochondrial membrane potential indicates a role of GPx-1 in cellular bioenergetics. Since increasing H_2O_2 levels as a result of increased MnSOD levels promote a more glycolytic phenotype [175], GPx-1 expression is expected to restore the oxidative phosphorylation capacity of these cells and this should be further studied.

Understanding the role of Sep15 in the membrane is made difficult by the fact that *in silico* analysis of its amino acid sequence does not contain any known plasma membrane

conserved sequences. A recent study indicates that Sep15 knockdown in Chang liver cells induced membrane blebbing due to reorganizing cytoskeletal proteins which inhibited migration as well as invasion [205]. Future studies investigating the role of Sep15 in plasma membrane of secreting glands will shed light into its biochemical function, which until now has only been suggested to aid in protein folding in the ER. Understanding the biology of Se and of GPx-1, and Sep15, the activities and levels of which are dependent upon the tissue levels of Se, will contribute to elucidating how selenium impacts carcinogenesis.

APPENDIX

1. Nrf2 and MnSOD levels in MCF-7 cell lines

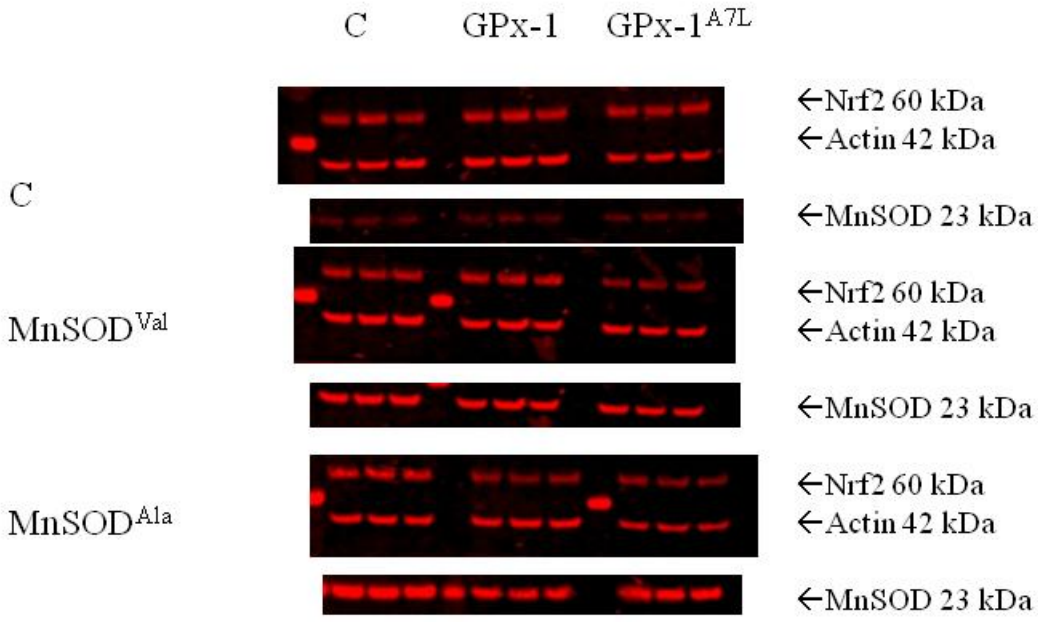

Figure 1. Nrf2 and MnSOD levels in MCF-7 cell lines. Lysates from MCF-7 transfected cells were analyzed for Nrf2 and MnSOD protein levels by western blot using anti-Nrf2 and anti-MnSOD antibodies. β-Actin was used as an endogenous protein loading control. Protein levels were quantified using fluorescence detection and normalized to β-Actin.

2. E-Cadherin and Sirt3 levels in MCF-7 cell lines

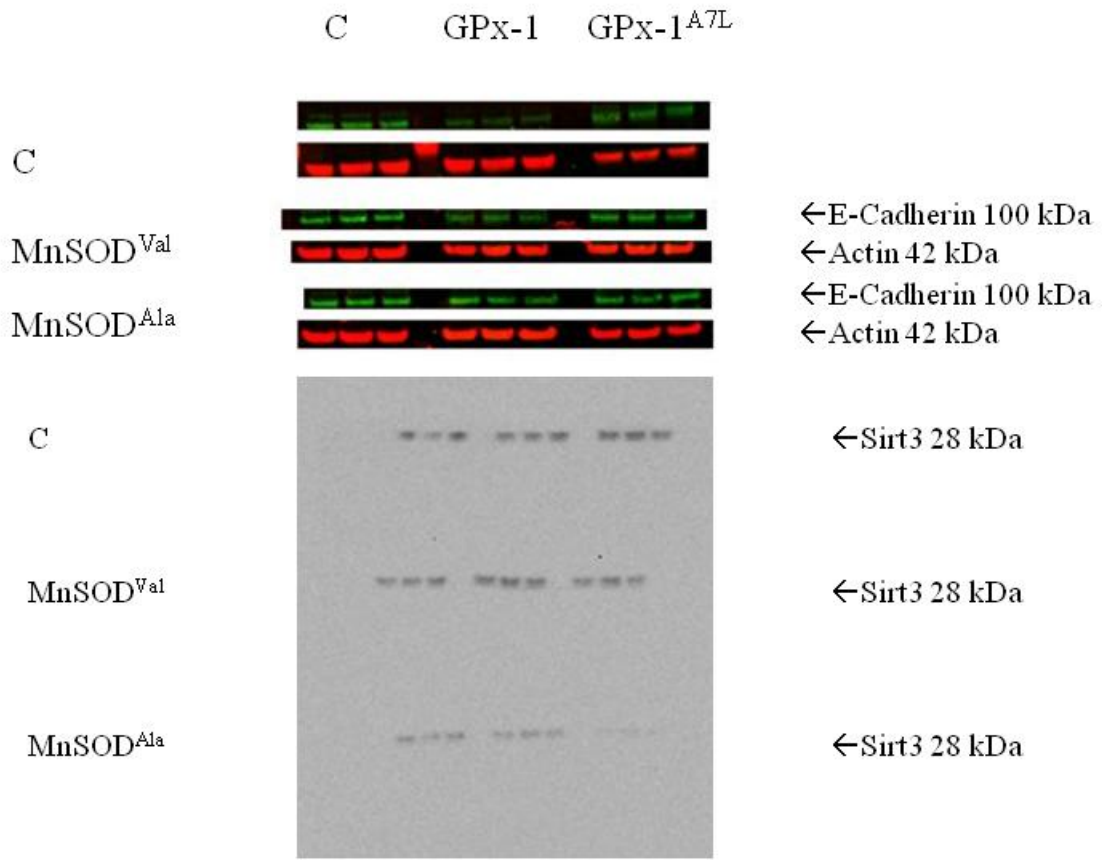

Figure 2. E-Cadherin and Sirt3 levels in MCF-7 cell lines. Lysates from MCF-7 transfected cells were analyzed for E-Cadherin and Sirt3 protein levels by western blot using anti-E-Cadherin and anti-Sirt3 antibodies. β-Actin was used as an endogenous protein loading control. Protein levels were quantified using fluorescence detection (E-Cadherin) or by densitometry (Sirt3) and normalized to β-Actin.

3. Levels of p-Akt and Bcl-2 in MCF-7 cell lines

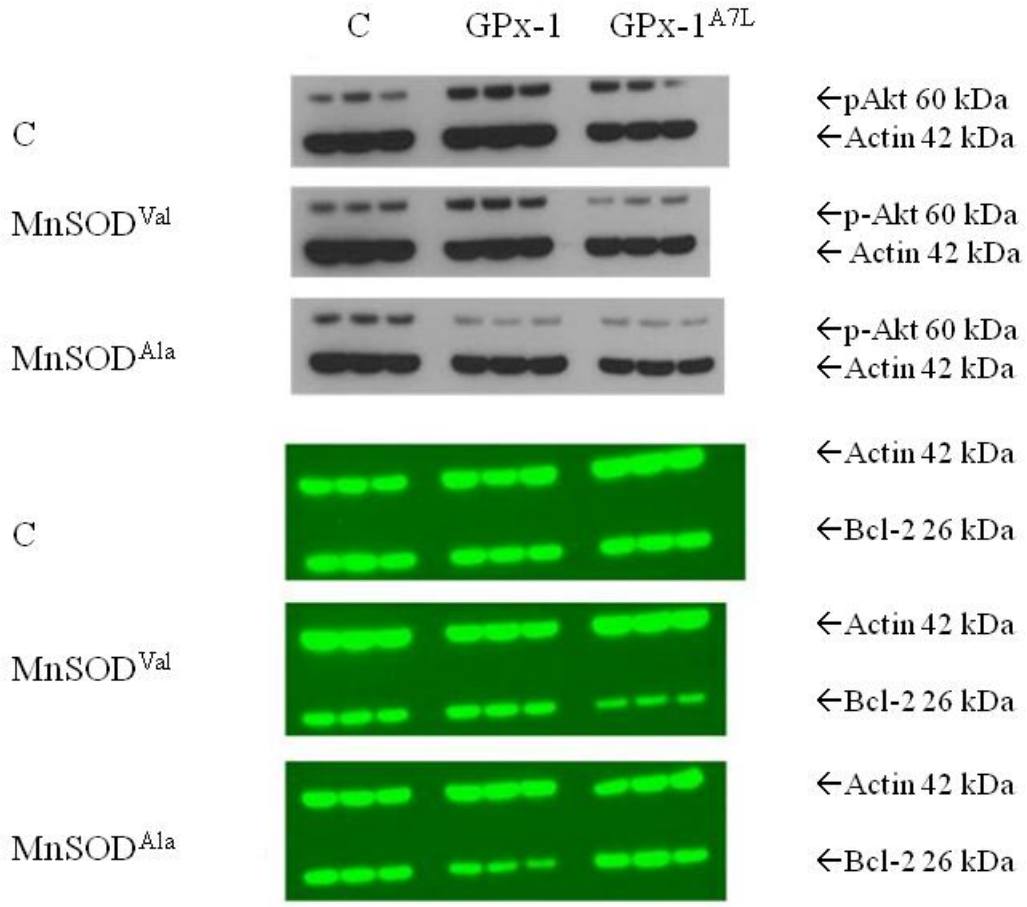

Figure 3. Levels of p-Akt and Bcl-2 in MCF-7 cell lines. Lysates from MCF-7 transfected cells were analyzed for p-Akt and Bcl-2 protein levels by western blot using anti-p-Akt and anti-Bcl-2 antibodies. β-Actin was used as an endogenous protein loading control. Protein levels were quantified by densitometry and normalized to β-Actin.

4. GPx-1 levels in MCF-7 cells

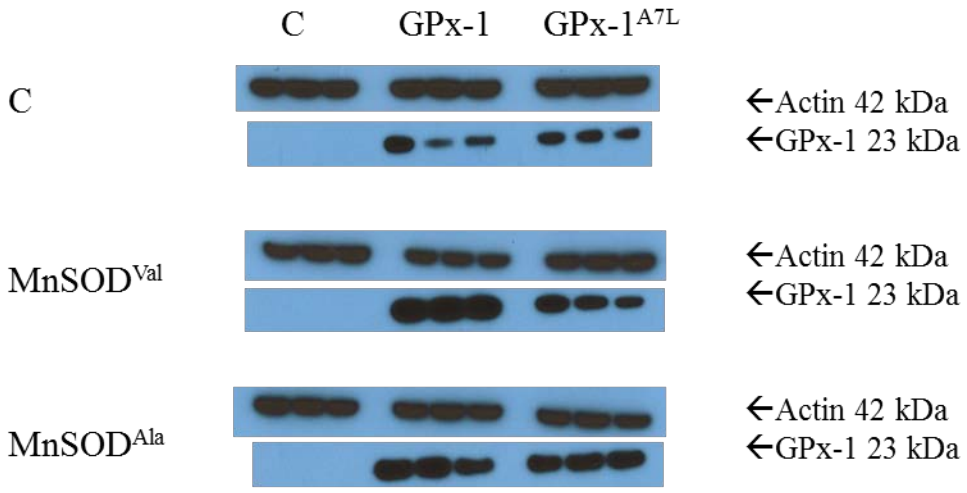

Figure 4. Levels of GPx-1 in MCF-7 cell lines. Lysates from MCF-7 transfected cells were analyzed for GPx-1 protein levels by western blot using anti-GPx-1 antibodies. β-Actin was used as an endogenous protein loading control.

5. Breast tissue patient demographics and tumor characteristics

Patient demographics and tumor characteristics

Characteristic	n	%	Missing
Ethnicity			
Black	20	67%	0
White	6	20%	
Other	4	13%	
Age			
20-39	4	13%	0
40-49	5	17%	
50-59	9	30%	
60-69	9	30%	
70-79	3	10%	
Diagnosis			
Ductal	8	27%	0
Ductal & DCIS	14	47%	
Lobular	3	10%	
Other	5	17%	
Subtype			
Hormone + (ER or PR)	18	67%	3
HER2 +	11	41%	
Triple Negative	3	11%	

Figure 6. Patient demographics and tumor characteristics. Patients are classified by ethnicity, age, diagnosis and breast cancer subtypes.

6. Breast tissue: *SEPP1* rs3877899, rs7579, and *GPx-1* genotype distribute non-randomly. *MnSOD* and *Sep15* (20 of 30 DNA samples were obtained from African American women) distributed randomly.

SEPP1		GG	GA	AA	Chi-Test
rs3877899 Genotype Frequency		60.00%	26.67%	13.33%	5.55E-05
	n	18	8	4	
Expected Genotype Frequency		25%	50%	25%	
	n	7.5	15	7.5	
SEPP1		GG	GA	AA	Chi-Test
rs 7579 Genotype Frequency		70.00%	30.00%	0.00%	3.75E-08
	n	21	9	0	
Expected Genotype Frequency		25%	50%	25%	
	n	7.5	15	7.5	
		CC	CT	TT	Chi-Test
SEP15 Genotype Frequency		26.67%	53.33%	20.00%	8.19E-01
	n	8	16	6	
Expected Genotype Frequency		25%	50%	25%	
	n	7.5	15	7.5	
		PP	PL	LL	Chi-Test
GPx-1 Genotype Frequency		60.00%	36.67%	3.33%	2.25E-05
	n	18	11	1	
GPx-1 Genotype Frequency		25%	50%	25%	
	n	7.5	15	7.5	
		VV	VA	AA	Chi-Test
MnSOD Genotype Frequency		20.00%	53.33%	26.67%	8.19E-01
	n	6	16	8	
Expected Genotype Frequency		25%	50%	25%	
	n	7.5	15	7.5	

Figure 5. Genotype Frequencies. DNAs obtained from breast tissue samples (n=30) were genotyped using gene specific primers. Observed genotype frequencies and expected genotype frequencies are reported (Chi-square test).

7. Genotypes of *GPx-1*, *MnSOD* and *Sep15* are not associated with breast tissue Se levels.

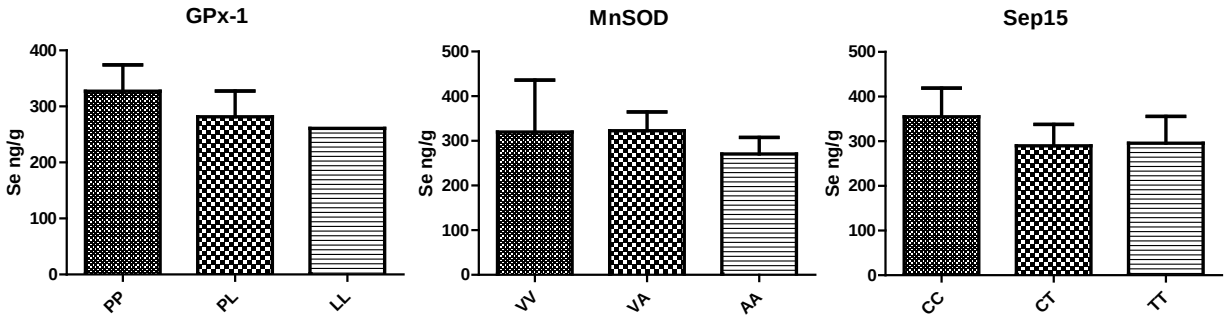

Figure 6. Se levels are not associated with GPx-1, MnSOD and Sep15 genotype. Se levels were analyzed by graphite furnace spectroscopy and DNAs (n=30) were genotyped for *GPx-1, MnSOD and Sep15*. There were no statistically significant differences between means of serum Se for all patients grouped by genotype (Mann-Whitney, two-tailed p>0.05).

8. SEPP1 rs3877899 not rs7579 is associated with serum Se levels

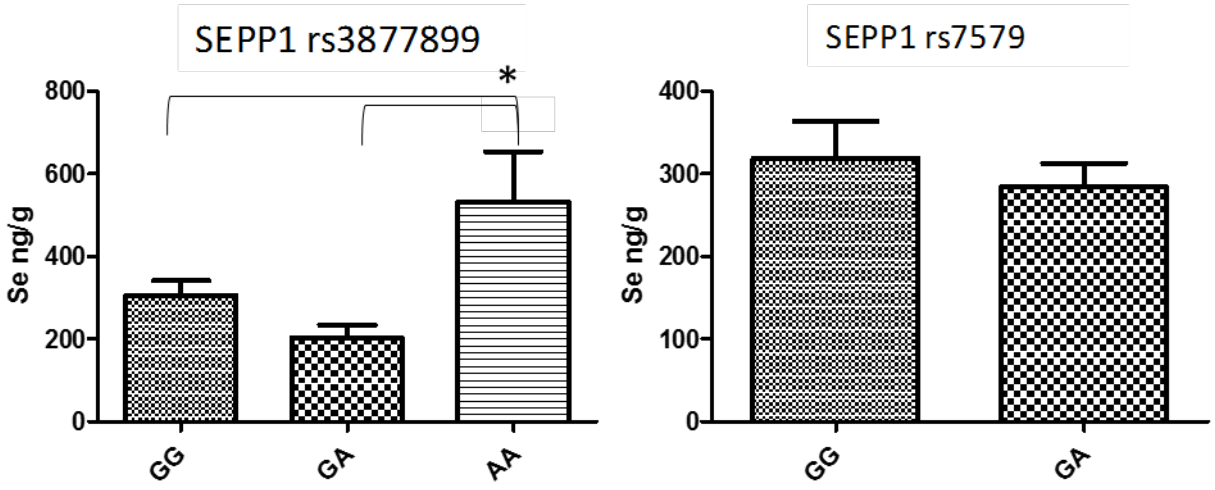

Figure 7. Higher Se levels in breast tissues are associated with SEPP1 rs 3877899 AA genotype. Tissue Se levels were analyzed by graphite furnace spectroscopy and DNAs (n=30) were genotyped for *SEPP1* rs3877899 and rs7579. There were statistically significant differences

between means of serum Se for all patients grouped by *SEPP1* rs 3877899 genotype (ANOVA One-way analysis of variance test $p<0.0057$, Tukey's Multiple Comparison Test *= $p<0.05$. The error bars indicate the standard error of the mean. There were no statistically significant differences between means of serum Se for patients grouped by *SEPP1* rs7579 (Mann-Whitney, two-tailed $p>0.05$)

9. *MnSOD Val16Ala* but not *GPx-1 Pro198Leu,* nor *SEPP1* rs3877899, rs7579 was in Hardy-Weinberg Equilibrium (HWE*)*

	PP	PL	LL	Chi-Test
GPx-1 Genotype Frequency	46.88%	45.31%	7.81%	1.88E-09
n	60	58	10	
GPx-1 Genotype Frequency	25%	50%	25%	
n	32	64	32	

	VV	VA	AA	Chi-Test
MnSOD Genotype Frequency	24.22%	52.34%	23.44%	0.862
n	31	67	30	
Expected Genotype Frequency	25%	50%	25%	
n	32	64	32	

SEPP1	GG	GA	AA	Chi-Test
rs3877899 Genotype Frequency	61.24%	32.56%	6.20%	4.17E-21
n	79	42	8	
Expected Genotype Frequency	25%	50%	25%	
n	32.25	64.5	32.25	

SEPP1	GG	GA	AA	Chi-Test
rs 7579 Genotype Frequency	56.59%	36.43%	6.98%	1.41E-16
n	73	47	9	
Expected Genotype Frequency	25%	50%	25%	
n	32.25	64.5	32.25	

Figure 8. Genotype Frequencies. DNAs obtained from white blood cells (n=129) were genotyped using gene specific primers. Observed genotype frequencies and expected genotype frequencies are reported (Chi-square test).

American Association for Cancer Research License Terms and Conditions

AMERICAN ASSOCIATION FOR CANCER RESEARCH LICENSE TERMS AND CONDITIONS

Jul 21, 2016

This Agreement between Dede N Ekoue ("You") and American Association for Cancer Research ("American Association for Cancer Research") consists of your license details and the terms and conditions provided by American Association for Cancer Research and Copyright Clearance Center.

License Number	3911940518901
License date	Jul 18, 2016
Licensed Content Publisher	American Association for Cancer Research
Licensed Content Publication	Cancer Discovery
Licensed Content Title	Natural Allelic Variations in Glutathione Peroxidase-1 Affect Its Subcellular Localization and Function
Licensed Content Author	Soumen Bera,Frank Weinberg,Dede N. Ekoue,Kristine Ansenberger-Fricano,Mao Mao,Marcelo G. Bonini,Alan M. Diamond
Licensed Content Date	2014-09-15
Licensed Content Volume Number	74
Licensed Content Issue Number	18
Type of Use	Thesis/Dissertation
Requestor type	author of the requested content
Format	print and electronic
Portion	figures/tables/illustrations
Number of figures/tables/illustrations	1
Will you be translating?	no
Circulation	999999
Territory of distribution	North America
Title of your thesis / dissertation	Selenoproteins in Cancer Etiology
Expected completion date	Jul 2016
Estimated size (number of pages)	130

CITED LITERATURE

1. Rayman, M.P., *The importance of selenium to human health.* Lancet, 2000. **356**(9225): p. 233-41.
2. James, L.F., et al., *Suspected phytogenic selenium poisoning in sheep.* J Am Vet Med Assoc, 1982. **180**(12): p. 1478-81.
3. James, L.F., K.V. Van Kampen, and W.J. Hartley, *Astragalus bisulcatus--a cause of selenium or locoweed poisoning?* Vet Hum Toxicol, 1983. **25**(2): p. 86-9.
4. Baker, D.C., et al., *Toxicosis in pigs fed selenium-accumulating Astragalus plant species or sodium selenate.* Am J Vet Res, 1989. **50**(8): p. 1396-9.
5. Allan, C.B., G.M. Lacourciere, and T.C. Stadtman, *Responsiveness of selenoproteins to dietary selenium.* Annu Rev Nutr, 1999. **19**: p. 1-16.
6. Ermakov, V.V., *Biogeochemical regioning problems and the biogeochemical selenium provinces in the former USSR.* Biol Trace Elem Res, 1992. **33**: p. 171-85.
7. Ge, K. and G. Yang, *The epidemiology of selenium deficiency in the etiological study of endemic diseases in China.* Am J Clin Nutr, 1993. **57**(2 Suppl): p. 259S-263S.
8. Chen, X., et al., *Studies on the relations of selenium and Keshan disease.* Biol Trace Elem Res, 1980. **2**(2): p. 91-107.
9. Yang, G., et al., *Endemic selenium intoxication of humans in China.* American Journal of Clinical Nutrition, 1983. **37**: p. 872-881.
10. Yang, G.Q., et al., *The role of selenium in Keshan disease.* Adv Nutr Res, 1984. **6**: p. 203-31.
11. Monsen, E.R., *Dietary reference intakes for the antioxidant nutrients: vitamin C, vitamin E, selenium, and carotenoids.* J Am Diet Assoc, 2000. **100**(6): p. 637-40.
12. Nelson AA, F.O., Calvery HO, *Liver tumors following cirrhosis caused by selenium in rats.* Cancer Res, 1943. **3 :230– 236**.
13. Shamberger, R.J. and D.V. Frost, *Possible protective effect of selenium against human cancer.* Can Med Assoc J, 1969. **100**(14): p. 682.
14. Vinceti, M., et al., *Selenium for preventing cancer.* Cochrane Database Syst Rev, 2014. **3**: p. CD005195.
15. Clark, L.C., et al., *Effects of selenium supplementation for cancer prevention in patients with carcinoma of the skin. A randomized controlled trial. Nutritional Prevention of Cancer Study Group.* JAMA, 1996. **276**(24): p. 1957-63.
16. Duffield-Lillicoe, A., et al., *Baseline characteristics and the effect of selenium supplementation on cancer incidence in a randomized clinical trial: a summary report of the Nutritional Prevention of Cancer Trial.* Cancer Epidemiol Biomarkers Prev., 2002. **11**(7): p. 630-639.
17. Lippman, S.M., et al., *Designing the Selenium and Vitamin E Cancer Prevention Trial (SELECT).* Journal of National Cancer Institute, 2005. **97**: p. 94-102.
18. Lippman, S.M., et al., *Effect of selenium and vitamin E on risk of prostate cancer and other cancers: the Selenium and Vitamin E Cancer Prevention Trial (SELECT).* JAMA, 2009. **301**(1): p. 39-51.
19. Klein, E.A., et al., *Vitamin E and the risk of prostate cancer: the Selenium and Vitamin E Cancer Prevention Trial (SELECT).* Jama, 2011. **306**(14): p. 1549-56.
20. Schrauzer, G.N., *Selenomethionine: a review of its nutritional significance, metabolism and toxicity.* J Nutr, 2000. **130**(7): p. 1653-6.
21. Larsen, E.H., et al., *Speciation and bioavailability of selenium in yeast-based intervention agents used in cancer chemoprevention studies.* J AOAC Int, 2004. **87**(1): p. 225-32.
22. Waters, D.J., et al., *Prostate cancer risk and DNA damage: translational significance of selenium supplementation in a canine model.* Carcinogenesis, 2005.

23. Waters, D.J., et al., *Noninvasive prediction of prostatic DNA damage by oxidative stress challenge of peripheral blood lymphocytes.* Cancer Epidemiol Biomarkers Prev, 2007. **16**(9): p. 1906-10.
24. Waters, D.J., et al., *Prostatic response to supranutritional selenium supplementation: comparison of the target tissue potency of selenomethionine vs. selenium-yeast on markers of prostatic homeostasis.* Nutrients, 2012. **4**(11): p. 1650-63.
25. Hesketh, J., *Nutrigenomics and selenium: gene expression patterns, physiological targets, and genetics.* Annu Rev Nutr, 2008. **28**: p. 157-77.
26. Hesketh, J. and C. Meplan, *Transcriptomics and functional genetic polymorphisms as biomarkers of micronutrient function: focus on selenium as an exemplar.* Proc Nutr Soc, 2011: p. 1-9.
27. Dennert, G., et al., *Selenium for preventing cancer.* Cochrane Database Syst Rev, 2011(5): p. CD005195.
28. Vinceti, M., et al., *Selenium for preventing cancer.* Cochrane Database Syst Rev, 2014(3): p. CD005195.
29. Ip, C., Y. Dong, and H. Ganther, *New concepts in selenium chemoprevention.* Cancer Metastasis Rev, 2002. **21**(3-4): p. 281-289.
30. Zhang, Z., M. Kimura, and Y. Itokawa, *The decrement of carcinogenesis by dietary selenium and expression of placental form of glutathione-S-transferase in rat glioma.* Biol Trace Elem Res, 1997. **57**(2): p. 147-55.
31. Hurst, R., et al., *Selenium and prostate cancer: systematic review and meta-analysis.* Am J Clin Nutr, 2012. **96**(1): p. 111-22.
32. Kryukov, G.V., et al., *Characterization of mammalian selenoproteomes.* Science, 2003. **300**(5624): p. 1439-43.
33. Bock, A., et al., *Selenocysteine: the 21st amino acid.* Mol Microbiol, 1991. **5**(3): p. 515-520.
34. Bock, A., et al., *Selenoprotein synthesis: an expansion of the genetic code.* Trends Biochem Sci, 1991. **16**(12): p. 463-7.
35. Hatfield, D.L. and V.N. Gladyshev, *How selenium has altered our understanding of the genetic code.* Mol Cell Biol, 2002. **22**(11): p. 3565-76.
36. Hatfield, D.L., et al., *Selenium and selenocysteine: roles in cancer, health, and development.* Trends Biochem Sci, 2014. **39**(3): p. 112-20.
37. Berry, M.J., et al., *Recognition of UGA as a selenocysteine codon in Type I deiodinase requires sequences in the 3' untranslated region.* Nature, 1991. **353**: p. 273-276.
38. Lee, B.J., et al., *Identification of a selenocysteyl-tRNA(Ser) in mammalian cells that recognizes the nonsense codon, UGA.* J Biol Chem, 1989. **264**(17): p. 9724-7.
39. Driscoll, D.M. and P.R. Copeland, *Mechanism and regulation of selenoprotein synthesis.* Annu Rev Nutr, 2003. **23**: p. 17-40.
40. Copeland, P., et al., *A novel RNA binding protein, SBP2, is required for the translation of mammalian selenoprotein mRNAs.* EMBO J., 2000. **19**(2): p. 306-314.
41. Xu, X.M., et al., *Biosynthesis of selenocysteine on its tRNA in eukaryotes.* PLoS Biol, 2007. **5**(1): p. e4.
42. Diamond, A.M., et al., *Dietary Selenium Affects Methylation of the Wobble Nucleoside in the Anticodon of Selenocysteine tRNA$^{(Ser)Sec}$.* Journal of Biological Chemistry, 1993. **268**(19): p. 14215-14223.
43. Chittum, H.S., et al., *Replenishment of selenium deficient rats with selenium results in redistribution of the selenocysteine tRNA population in a tissue specific manner.* Biochim Biophys Acta, 1997. **1359**(1): p. 25-34.
44. Hatfield, D., et al., *Selenium induces changes in the selenocysteine tRNA[Ser]Sec population in mammalian cells.* Nucleic Acids Res, 1991. **19**(4): p. 939-43.

45. Budiman, M.E., et al., *Eukaryotic initiation factor 4a3 is a selenium-regulated RNA-binding protein that selectively inhibits selenocysteine incorporation.* Mol Cell, 2009. **35**(4): p. 479-89.
46. Sun, X., et al., *Nonsense-mediated decay of mRNA for the selenoprotein phospholipid hydroperoxide glutathione peroxidase is detectable in cultured cells but masked or inhibited in rat tissues.* Mol Biol Cell, 2001. **12**(4): p. 1009-17.
47. Moriarty, P.M., C.C. Reddy, and L.E. Maquat, *Selenium deficiency reduces the abundance of mRNA for Se-dependent glutathione peroxidase 1 by a UGA-dependent mechanism likely to be nonsense codon-mediated decay of cytoplasmic mRNA.* Mol Cell Biol, 1998. **18**(5): p. 2932-9.
48. Lei, X.G., et al., *Glutathione peroxidase and phospholipid hydroperoxide glutathione peroxidase are differentially regulated in rats by dietary selenium.* J Nutr, 1995. **125**(6): p. 1438-46.
49. Behne, D., et al., *Evidence for specific selenium target tissues and new biologically important selenoproteins.* Biochim Biophys Acta, 1988. **966**(1): p. 12-21.
50. Hill, K.E., P.R. Lyons, and R.F. Burk, *Differential regulation of rat liver selenoprotein mRNAs in selenium deficiency.* Biochem Biophys Res Commun, 1992. **185**(1): p. 260-3.
51. Hafeman, D.G., R.A. Sunde, and W.G. Hoekstra, *Effect of dietary selenium on erythrocyte and liver glutathione peroxidase in the rat.* Journal of Nutrition, 1974. **104**: p. 580-587.
52. Rotruck, J.T., et al., *Selenium: biochemical role as a component of glutathione peroxidase.* Science, 1973. **179**(4073): p. 588-90.
53. Rotruck, J.T., et al., *Prevention of oxidative damage to rat erythrocytes by dietary selenium.* J Nutr, 1972. **102**(5): p. 689-96.
54. Utsunomiya, H., et al., *Exact ultrastructural localization of glutathione peroxidase in normal rat hepatocytes: advantages of microwave fixation.* J Histochem Cytochem, 1991. **39**(9): p. 1167-74.
55. Asayama, K., et al., *Purification and immunoelectron microscopic localization of cellular glutathione peroxidase in rat hepatocytes: quantitative analysis by postembedding method.* Histochemistry, 1994. **102**(3): p. 213-9.
56. Esworthy, R.S., Y.S. Ho, and F.F. Chu, *The Gpx1 gene encodes mitochondrial glutathione peroxidase in the mouse liver.* Arch Biochem Biophys, 1997. **340**(1): p. 59-63.
57. Brigelius-Flohe, R., *Tissue-specific functions of individual glutathione peroxidases.* Free Radic Biol Med, 1999. **27**(9-10): p. 951-65.
58. Hu, Y.J. and A.M. Diamond, *Role of glutathione peroxidase 1 in breast cancer: loss of heterozygosity and allelic differences in the response to selenium.* Cancer Res, 2003. **63**(12): p. 3347-51.
59. Moscow, J.A., et al., *Loss of heterozygosity of the human cytosolic glutathione peroxidase I gene in lung cancer.* Carcinogenesis, 1994. **15**(12): p. 2769-73.
60. Gladyshev, V.N., et al., *Contrasting patterns of regulation of the antioxidant selenoproteins, thioredoxin reductase, and glutathione peroxidase, in cancer cells.* Biochem Biophys Res Commun, 1998. **251**(2): p. 488-493.
61. Cullen, J.J., F.A. Mitros, and L.W. Oberley, *Expression of antioxidant enzymes in diseases of the human pancreas: another link between chronic pancreatitis and pancreatic cancer.* Pancreas, 2003. **26**(1): p. 23-7.
62. Liu, J., et al., *Redox regulation of pancreatic cancer cell growth: role of glutathione peroxidase in the suppression of the malignant phenotype.* Hum Gene Ther, 2004. **15**(3): p. 239-50.
63. Baliga, M.S., et al., *Selenium and GPx-1 overexpression protect mammalian cells against UV-induced DNA damage.* Biol Trace Elem Res, 2007. **115**(3): p. 227-42.
64. Baliga, M.S., et al., *Selenoprotein deficiency enhances radiation-induced micronuclei formation.* Mol Nutr Food Res, 2008. **52**(11): p. 1300-4.

65. Lu, Y.P., et al., *Enhanced skin carcinogenesis in transgenic mice with high expression of glutathione peroxidase or both glutathione peroxidase and superoxide dismutase.* Cancer Res, 1997. **57**(8): p. 1468-74.
66. Cheng, W.H., et al., *Cellular glutathione peroxidase is the mediator of body selenium to protect against paraquat lethality in transgenic mice.* J Nutr, 1998. **128**(7): p. 1070-6.
67. Esworthy, R.S., et al., *Mice with combined disruption of Gpx1 and Gpx2 genes have colitis.* Am J Physiol Gastrointest Liver Physiol, 2001. **281**: p. G848-G855.
68. Chu, F.-F., et al., *Bacteria-induced intestinal cancer in mice with disrupted Gpx1 and Gpx2 genes.* Cancer Research, 2004. **64**(962-968).
69. Foster, C.B., et al., *Polymorphism analysis of six selenoprotein genes: support for a selective sweep at the glutathione peroxidase 1 locus (3p21) in Asian populations.* BMC Genet, 2006. **7**: p. 56.
70. Kote-Jarai, Z., et al., *Association between the GCG polymorphism of the selenium dependent GPX1 gene and the risk of young onset prostate cancer.* Prostate Cancer Prostatic Dis, 2002. **5**(3): p. 189-92.
71. Jablonska, E., et al., *Association between GPx1 Pro198Leu polymorphism, GPx1 activity and plasma selenium concentration in humans.* Eur J Nutr, 2009. **48**(6): p. 383-6.
72. Yang, P., et al., *Glutathione pathway genes and lung cancer risk in young and old populations.* Carcinogenesis, 2004. **25**(10): p. 1935-44.
73. Ratnasinghe, D., et al., *Glutathione peroxidase codon 198 polymorphism variant increases lung cancer risk.* Cancer Res, 2000. **60**(22): p. 6381-3.
74. Lee, C.H., et al., *[Effects of oxidative DNA damage and genetic polymorphism of the glutathione peroxidase 1 (GPX1) and 8-oxoguanine glycosylase 1 (hOGG1) on lung cancer].* J Prev Med Pub Health, 2006. **39**(2): p. 130-4.
75. Ravn-Haren, G., et al., *Associations between GPX1 Pro198Leu polymorphism, erythrocyte GPX activity, alcohol consumption and breast cancer risk in a prospective cohort study.* Carcinogenesis, 2006. **27**(4): p. 820-5.
76. Sutton, A., et al., *Genetic polymorphisms in antioxidant enzymes modulate hepatic iron accumulation and hepatocellular carcinoma development in patients with alcohol-induced cirrhosis.* Cancer Res, 2006. **66**(5): p. 2844-52.
77. Chen, J., et al., *GPx-1 polymorphism (rs1050450) contributes to tumor susceptibility: evidence from meta-analysis.* J Cancer Res Clin Oncol, 2011. **137**(10): p. 1553-61.
78. Anand, P., et al., *Cancer is a preventable disease that requires major lifestyle changes.* Pharm Res, 2008. **25**(9): p. 2097-116.
79. Cox, D.G., R.M. Tamimi, and D.J. Hunter, *Gene x Gene interaction between MnSOD and GPX-1 and breast cancer risk: a nested case-control study.* BMC Cancer, 2006. **6**: p. 217.
80. Meplan, C., et al., *Genetic polymorphisms in the human selenoprotein P gene determine the response of selenoprotein markers to selenium supplementation in a gender-specific manner (the SELGEN study).* FASEB J, 2007. **21**(12): p. 3063-74.
81. Cao, C., et al., *Glutathione peroxidase 1 is regulated by the c-Abl and Arg tyrosine kinases.* J Biol Chem, 2003. **278**(41): p. 39609-14.
82. Shepard, B.D., D.J. Tuma, and P.L. Tuma, *Chronic ethanol consumption induces global hepatic protein hyperacetylation.* Alcohol Clin Exp Res, 2010. **34**(2): p. 280-91.
83. Fritz, K.S., et al., *Mitochondrial acetylome analysis in a mouse model of alcohol-induced liver injury utilizing SIRT3 knockout mice.* J Proteome Res, 2012. **11**(3): p. 1633-43.
84. Weisiger, R.A. and I. Fridovich, *Superoxide dismutase. Organelle specificity.* J Biol Chem, 1973. **248**(10): p. 3582-92.
85. Fridovich, I., *Superoxide dismutases.* Annu Rev Biochem, 1975. **44**: p. 147-59.

86. Lubos, E., J. Loscalzo, and D.E. Handy, *Glutathione peroxidase-1 in health and disease: from molecular mechanisms to therapeutic opportunities.* Antioxid Redox Signal, 2011. **15**(7): p. 1957-97.
87. Li, J.J., et al., *Phenotypic changes induced in human breast cancer cells by overexpression of manganese-containing superoxide dismutase.* Oncogene, 1995. **10**(10): p. 1989-2000.
88. Xu, Y., et al., *An intronic NF-kappaB element is essential for induction of the human manganese superoxide dismutase gene by tumor necrosis factor-alpha and interleukin-1beta.* DNA Cell Biol, 1999. **18**(9): p. 709-22.
89. Koch, O.R., et al., *Ethanol treatment up-regulates the expression of mitochondrial manganese superoxide dismutase in rat liver.* Biochem Biophys Res Commun, 1994. **201**(3): p. 1356-65.
90. Perera, C.S., D.K. St Clair, and C.J. McClain, *Differential regulation of manganese superoxide dismutase activity by alcohol and TNF in human hepatoma cells.* Arch Biochem Biophys, 1995. **323**(2): p. 471-6.
91. Fukai, T. and M. Ushio-Fukai, *Superoxide dismutases: role in redox signaling, vascular function, and diseases.* Antioxid Redox Signal, 2011. **15**(6): p. 1583-606.
92. Sutton, A., et al., *The Ala16Val genetic dimorphism modulates the import of human manganese superoxide dismutase into rat liver mitochondria.* Pharmacogenetics, 2003. **13**(3): p. 145-57.
93. Nishida, S., et al., *Manganese superoxide dismutase content and localization in human thyroid tumours.* J Pathol, 1993. **169**(3): p. 341-5.
94. Oberley, T.D., et al., *Immunogold analysis of antioxidant enzymes in human renal cell carcinoma.* Virchows Arch, 1994. **424**(2): p. 155-64.
95. Baker, S.J., et al., *Suppression of human colorectal carcinoma cell growth by wild-type p53.* Science, 1990. **249**(4971): p. 912-5.
96. Sun, G.G., et al., *Novel cancer suppressor gene for esophageal cancer: manganese superoxide dismutase.* Dis Esophagus, 2011. **24**(5): p. 346-53.
97. Landriscina, M., et al., *The level of MnSOD is directly correlated with grade of brain tumours of neuroepithelial origin.* Br J Cancer, 1996. **74**(12): p. 1877-85.
98. Hart, P.C., et al., *MnSOD upregulation sustains the Warburg effect via mitochondrial ROS and AMPK-dependent signalling in cancer.* Nat Commun, 2015. **6**.
99. Mikhak, B., et al., *Manganese superoxide dismutase (MnSOD) gene polymorphism, interactions with carotenoid levels and prostate cancer risk.* Carcinogenesis, 2008. **29**(12): p. 2335-40.
100. Li, H., et al., *Manganese superoxide dismutase polymorphism, prediagnostic antioxidant status, and risk of clinical significant prostate cancer.* Cancer Res, 2005. **65**(6): p. 2498-504.
101. Woodson, K., et al., *Serum insulin-like growth factor I: tumor marker or etiologic factor? A prospective study of prostate cancer among Finnish men.* Cancer Res, 2003. **63**(14): p. 3991-4.
102. Ambrosone, C.B., et al., *Manganese superoxide dismutase (MnSOD) genetic polymorphisms, dietary antioxidants, and risk of breast cancer.* Cancer Res, 1999. **59**(3): p. 602-6.
103. Mitrunen, K., et al., *Association between manganese superoxide dismutase (MnSOD) gene polymorphism and breast cancer risk.* Carcinogenesis, 2001. **22**(5): p. 827-9.
104. Tamimi, R.M., et al., *Manganese superoxide dismutase polymorphism, plasma antioxidants, cigarette smoking, and risk of breast cancer.* Cancer Epidemiol Biomarkers Prev, 2004. **13**(6): p. 989-96.
105. Cai, Q., et al., *Genetic polymorphism in the manganese superoxide dismutase gene, antioxidant intake, and breast cancer risk: results from the Shanghai Breast Cancer Study.* Breast Cancer Res, 2004. **6**(6): p. R647-55.
106. Egan, K.M., et al., *MnSOD polymorphism and breast cancer in a population-based case-control study.* Cancer Lett, 2003. **199**(1): p. 27-33.

107. Ansenberger-Fricano, K., et al., *The peroxidase activity of mitochondrial superoxide dismutase.* Free Radic Biol Med, 2013. **54**: p. 116-24.
108. Cox, D.G., et al., *No association between GPX1 Pro198Leu and breast cancer risk.* Cancer Epidemiol Biomarkers Prev, 2004. **13**(11 Pt 1): p. 1821-2.
109. Cooper, M.L., et al., *Interaction between single nucleotide polymorphisms in selenoprotein P and mitochondrial superoxide dismutase determines prostate cancer risk.* Cancer Res, 2008. **68**(24): p. 10171-7.
110. Esworthy, R.S., M.A. Baker, and F.F. Chu, *Expression of selenium-dependent glutathione peroxidase in human breast tumor cell lines.* Cancer Res, 1995. **55**(4): p. 957-62.
111. Zhuo, P., et al., *Molecular consequences of genetic variations in the glutathione peroxidase 1 selenoenzyme.* Cancer Res, 2009. **69**(20): p. 8183-90.
112. Novoselov, S.V., et al., *Selenoprotein deficiency and high levels of selenium compounds can effectively inhibit hepatocarcinogenesis in transgenic mice.* Oncogene, 2005. **24**(54): p. 8003-11.
113. Kalcklosch, M., et al., *A new selenoprotein found in the glandular epithelial cells of the rat prostate.* Biochem Biophys Res Commun, 1995. **217**(1): p. 162-70.
114. Gladyshev, V.N., et al., *A new human selenium-containing protein. Purification, characterization and cDNA sequence.* The journal of biological chemistry, 1998. **273**(15): p. 8910-8915.
115. Kumaraswamy, E., et al., *Structure-expression relationships of the 15-kDa selenoprotein gene. Possible role of the protein in cancer etiolgy.* J Biol Chem, 2000. **275**(45): p. 35540-35547.
116. Labunskyy, V.M., et al., *Sep15, a thioredoxin-like selenoprotein, is involved in the unfolded protein response and differentially regulated by adaptive and acute ER stresses.* Biochemistry, 2009. **48**(35): p. 8458-65.
117. Korotkov, K.V., et al., *Association between the 15-kDa selenoprotein and UDP-glucose:glycoprotein glucosyltransferase in the endoplasmic reticulum of mammalian cells.* J Biol Chem, 2001. **276**(18): p. 15330-6.
118. Ron, D. and P. Walter, *Signal integration in the endoplasmic reticulum unfolded protein response.* Nat Rev Mol Cell Biol, 2007. **8**(7): p. 519-29.
119. Hammond, C., I. Braakman, and A. Helenius, *Role of N-linked oligosaccharide recognition, glucose trimming, and calnexin in glycoprotein folding and quality control.* Proc Natl Acad Sci U S A, 1994. **91**(3): p. 913-7.
120. Helenius, A. and M. Aebi, *Roles of N-linked glycans in the endoplasmic reticulum.* Annu Rev Biochem, 2004. **73**: p. 1019-49.
121. Baird, M., et al., *The unfolded protein response is activated in Helicobacter-induced gastric carcinogenesis in a non-cell autonomous manner.* Lab Invest, 2013. **93**(1): p. 112-22.
122. Yan, M., et al., *Endoplasmic reticulum stress and unfolded protein response in Atm-deficient thymocytes and thymic lymphoma cells are attributable to oxidative stress.* Neoplasia, 2008. **10**(2): p. 160-7.
123. Vandewynckel, Y.P., et al., *The paradox of the unfolded protein response in cancer.* Anticancer Res, 2013. **33**(11): p. 4683-94.
124. Matsuo, K., et al., *The endoplasmic reticulum stress marker, glucose-regulated protein-78 (GRP78) in visceral adipocytes predicts endometrial cancer progression and patient survival.* Gynecol Oncol, 2013. **128**(3): p. 552-9.
125. Papalas, J.A., et al., *Patterns of GRP78 and MTJ1 expression in primary cutaneous malignant melanoma.* Mod Pathol, 2010. **23**(1): p. 134-43.
126. Wu, M.J., et al., *Elimination of head and neck cancer initiating cells through targeting glucose regulated protein78 signaling.* Mol Cancer, 2010. **9**: p. 283.

127. Bartkowiak, K., et al., *Discovery of a novel unfolded protein response phenotype of cancer stem/progenitor cells from the bone marrow of breast cancer patients.* J Proteome Res, 2010. **9**(6): p. 3158-68.
128. Uramoto, H., et al., *Expression of endoplasmic reticulum molecular chaperone Grp78 in human lung cancer and its clinical significance.* Lung Cancer, 2005. **49**(1): p. 55-62.
129. Lee, A.S., *GRP78 induction in cancer: therapeutic and prognostic implications.* Cancer Res, 2007. **67**(8): p. 3496-9.
130. Hu, Y., et al., *Distribution and functional consequences of nucleotide polymorphisms inthe 3'-untranslated region of the human Sep 15 gene.* Cancer Res., 2001. **61**: p. 2307-2310.
131. Kumaraswamy, E., et al., *Genetic and functional analysis of mammalian Sep15 selenoprotein.* Methods Enzymol, 2002. **347**: p. 187-97.
132. Nasr, M.A., Y.J. Hu, and A.M. Diamond, *Allelic loss at the Sep15 locus in breast cancer.* Cancer Therapy, 2003. **1**: p. 293-298.
133. Hu, Y.J., et al., *Distribution and functional consequences of nucleotide polymorphisms in the 3'-untranslated region of the human Sep15 gene.* Cancer Res, 2001. **61**(5): p. 2307-10.
134. Sutherland, A., et al., *Polymorphisms in the selenoprotein S and 15-kDa selenoprotein genes are associated with altered susceptibility to colorectal cancer.* Genes Nutr, 2010. **5**(3): p. 215-23.
135. Meplan, C., et al., *Genetic variants in selenoprotein genes increase risk of colorectal cancer.* Carcinogenesis, 2010. **31**(6): p. 1074-9.
136. Jablonska, E., et al., *Lung cancer risk associated with selenium status is modified in smoking individuals by Sep15 polymorphism.* Eur J Nutr, 2008. **47**(1): p. 47-54.
137. Gresner, P., et al., *Expression of selenoprotein-coding genes SEPP1, SEP15 and hGPX1 in non-small cell lung cancer.* Lung Cancer, 2009. **65**(1): p. 34-40.
138. Irons, R., et al., *Deficiency in the 15-kDa selenoprotein inhibits tumorigenicity and metastasis of colon cancer cells.* Cancer Prev Res (Phila), 2010. **3**(5): p. 630-9.
139. Tsuji, P.A., et al., *Deficiency in the 15 kDa selenoprotein inhibits human colon cancer cell growth.* Nutrients, 2011. **3**(9): p. 805-17.
140. Tsuji, P.A., et al., *Knockout of the 15 kDa selenoprotein protects against chemically-induced aberrant crypt formation in mice.* PLoS One, 2012. **7**(12): p. e50574.
141. Penney, K.L., et al., *A large prospective study of SEP15 genetic variation, interaction with plasma selenium levels, and prostate cancer risk and survival.* Cancer Prev Res (Phila Pa), 2010. **3**(5): p. 604-10.
142. Vogt, T.M., et al., *Racial differences in serum selenium concentration: analysis of US population data from the Third National Health and Nutrition Examination Survey.* Am J Epidemiol, 2007. **166**(3): p. 280-8.
143. Samuels, B.A., et al., *Increased glutathione peroxidase activity in human sarcoma cell line with inherent doxorubicin resistance.* Cancer Research, 1991. **51**: p. 521-527.
144. Handy, D.E., et al., *Glutathione peroxidase-1 regulates mitochondrial function to modulate redox-dependent cellular responses.* J Biol Chem, 2009. **284**: p. 11913-21.
145. Tobe, R., et al., *High error rates in selenocysteine insertion in mammalian cells treated with the antibiotic doxycycline, chloramphenicol, or geneticin.* J Biol Chem, 2013. **288**(21): p. 14709-15.
146. Melamed, J., et al., *The cooperative prostate cancer tissue resource: a specimen and data resource for cancer researchers.* Clin Cancer Res, 2004. **10**(14): p. 4614-21.
147. Kajdacsy-Balla, A., et al., *Practical aspects of planning, building, and interpreting tissue microarrays: the Cooperative Prostate Cancer Tissue Resource experience.* J Mol Histol, 2007. **38**(2): p. 113-21.
148. Freeman, V.L., et al., *Racial differences in survival among men with prostate cancer and comorbidity at time of diagnosis.* Am J Public Health, 2004. **94**(5): p. 803-8.

149. Li, S., et al., *The role of cellular glutathione peroxidase redox regulation in the suppression of tumor cell growth by manganese superoxide dismutase.* Cancer Res, 2000. **60**(14): p. 3927-39.
150. Bera, S., et al., *Natural allelic variations in glutathione peroxidase-1 affect its subcellular localization and function.* Cancer Res, 2014. **74**(18): p. 5118-26.
151. van Roy, F. and G. Berx, *The cell-cell adhesion molecule E-cadherin.* Cell Mol Life Sci, 2008. **65**(23): p. 3756-88.
152. Liu, Z., et al., *Manganese superoxide dismutase induces migration and invasion of tongue squamous cell carcinoma via H2O2-dependent Snail signaling.* Free Radic Biol Med, 2012. **53**(1): p. 44-50.
153. Onder, T.T., et al., *Loss of E-cadherin promotes metastasis via multiple downstream transcriptional pathways.* Cancer Res, 2008. **68**(10): p. 3645-54.
154. Kowalski, P.J., M.A. Rubin, and C.G. Kleer, *E-cadherin expression in primary carcinomas of the breast and its distant metastases.* Breast Cancer Res, 2003. **5**(6): p. R217-22.
155. Cheng, J.C., C. Klausen, and P.C. Leung, *Hydrogen peroxide mediates EGF-induced down-regulation of E-cadherin expression via p38 MAPK and snail in human ovarian cancer cells.* Mol Endocrinol, 2010. **24**(8): p. 1569-80.
156. Taylor, J.M., et al., *Diminished Akt phosphorylation in neurons lacking glutathione peroxidase-1 (Gpx1) leads to increased susceptibility to oxidative stress-induced cell death.* J Neurochem, 2005. **92**(2): p. 283-93.
157. Brunet, A., et al., *Akt promotes cell survival by phosphorylating and inhibiting a Forkhead transcription factor.* Cell, 1999. **96**(6): p. 857-68.
158. Ayala, G., et al., *High levels of phosphorylated form of Akt-1 in prostate cancer and non-neoplastic prostate tissues are strong predictors of biochemical recurrence. .* Clinical Cancer Research, 2004. **10**: p. 6572-6578.
159. Kreisberg, J.I., et al., *Phosphorylation of Akt (Ser473) is an excellent predictor of poor clinical outcome in prostate cancer.* Cancer Research, 2004. **64**: p. 5232-5236.
160. Choi, J.H., et al., *Potential inhibition of PDK1/Akt signaling by phenothiazines suppresses cancer cell proliferation and survival.* Ann N Y Acad Sci, 2008. **1138**: p. 393-403.
161. Li, M., et al., *Down-regulation of manganese-superoxide dismutase through phosphorylation of FOXO3a by Akt in explanted vascular smooth muscle cells from old rats.* J Biol Chem, 2006. **281**(52): p. 40429-39.
162. Suzuki, Y.J., H.J. Forman, and A. Sevanian, *Oxidants as stimulators of signal transduction.* Free Radic Biol Med, 1997. **22**(1-2): p. 269-85.
163. Lindsay, J., M.D. Esposti, and A.P. Gilmore, *Bcl-2 proteins and mitochondria--specificity in membrane targeting for death.* Biochim Biophys Acta, 2011. **1813**(4): p. 532-9.
164. Hockenbery, D.M., *bcl-2 in cancer, development and apoptosis.* J Cell Sci Suppl, 1994. **18**: p. 51-5.
165. Hockenbery, D.M., et al., *Bcl-2 functions in an antioxidant pathway to prevent apoptosis.* Cell, 1993. **75**(2): p. 241-51.
166. Giralt, A. and F. Villarroya, *SIRT3, a pivotal actor in mitochondrial functions: metabolism, cell death and aging.* Biochem J, 2012. **444**(1): p. 1-10.
167. Kim, H.S., et al., *SIRT3 is a mitochondria-localized tumor suppressor required for maintenance of mitochondrial integrity and metabolism during stress.* Cancer Cell, 2010. **17**(1): p. 41-52.
168. Bell, E.L., et al., *SirT3 suppresses hypoxia inducible factor 1alpha and tumor growth by inhibiting mitochondrial ROS production.* Oncogene, 2011. **30**(26): p. 2986-96.
169. Tao, R., et al., *Sirt3-mediated deacetylation of evolutionarily conserved lysine 122 regulates MnSOD activity in response to stress.* Mol Cell, 2010. **40**(6): p. 893-904.
170. Ma, Q., *Role of nrf2 in oxidative stress and toxicity.* Annu Rev Pharmacol Toxicol, 2013. **53**: p. 401-26.

171. Itoh, K., et al., *Keap1 represses nuclear activation of antioxidant responsive elements by Nrf2 through binding to the amino-terminal Neh2 domain.* Genes Dev, 1999. **13**(1): p. 76-86.
172. Itoh, K., et al., *An Nrf2/small Maf heterodimer mediates the induction of phase II detoxifying enzyme genes through antioxidant response elements.* Biochem Biophys Res Commun, 1997. **236**(2): p. 313-22.
173. Sekhar, K.R., G. Rachakonda, and M.L. Freeman, *Cysteine-based regulation of the CUL3 adaptor protein Keap1.* Toxicol Appl Pharmacol, 2010. **244**(1): p. 21-6.
174. Ye, X.Q., et al., *Mitochondrial and energy metabolism-related properties as novel indicators of lung cancer stem cells.* Int J Cancer, 2011. **129**(4): p. 820-31.
175. Hart, P.C., et al., *MnSOD upregulation sustains the Warburg effect via mitochondrial ROS and AMPK-dependent signalling in cancer.* Nat Commun, 2015. **6**: p. 6053.
176. McAtee, B.L. and J.D. Yager, *Manganese superoxide dismutase: effect of the ala16val polymorphism on protein, activity, and mRNA levels in human breast cancer cell lines and stably transfected mouse embryonic fibroblasts.* Mol Cell Biochem, 2010. **335**(1-2): p. 107-18.
177. Jardim, B.V., et al., *Glutathione and glutathione peroxidase expression in breast cancer: an immunohistochemical and molecular study.* Oncol Rep, 2013. **30**(3): p. 1119-28.
178. Novoselov, S.V., et al., *Identification and characterization of Fep15, a new selenocysteine-containing member of the Sep15 protein family.* Biochem J, 2006. **394**(Pt 3): p. 575-9.
179. Stark, J.R., et al., *Gleason score and lethal prostate cancer: does 3 + 4 = 4 + 3?* J Clin Oncol, 2009. **27**(21): p. 3459-64.
180. Siegel, R., et al., *Cancer statistics, 2011: the impact of eliminating socioeconomic and racial disparities on premature cancer deaths.* CA Cancer J Clin. **61**(4): p. 212-36.
181. Jemal, A., et al., *Cancer statistics, 2006.* CA Cancer J Clin, 2006. **56**(2): p. 106-30.
182. Niskar, A.S., et al., *Serum selenium levels in the US population: Third National Health and Nutrition Examination Survey, 1988-1994.* Biol Trace Elem Res, 2003. **91**(1): p. 1-10.
183. Moschos, M.P., *Selenoprotein P.* Cell Mol Life Sci, 2000. **57**(13-14): p. 1836-45.
184. Baker, R.D., et al., *Selenium regulation of glutathione peroxidase in human hepatoma cell line Hep3B.* Arch Biochem Biophys, 1993. **304**(1): p. 53-7.
185. Levine, A., et al., *H2O2 from the oxidative burst orchestrates the plant hypersensitive disease resistance response.* Cell, 1994. **79**(4): p. 583-93.
186. Sutton, A., et al., *The manganese superoxide dismutase Ala16Val dimorphism modulates both mitochondrial import and mRNA stability.* Pharmacogenet Genomics, 2005. **15**(5): p. 311-9.
187. Sundaresan, M., et al., *Requirement for generation of H2O2 for platelet-derived growth factor signal transduction.* Science, 1995(270): p. 296-299.
188. Dispersyn, G., et al., *Bcl-2 protects against FCCP-induced apoptosis and mitochondrial membrane potential depolarization in PC12 cells.* Biochim Biophys Acta, 1999. **1428**(2-3): p. 357-71.
189. Harris, M.H. and C.B. Thompson, *The role of the Bcl-2 family in the regulation of outer mitochondrial membrane permeability.* Cell Death Differ, 2000. **7**(12): p. 1182-91.
190. Chen, Y.B., et al., *Bcl-xL regulates mitochondrial energetics by stabilizing the inner membrane potential.* J Cell Biol, 2011. **195**(2): p. 263-76.
191. Gross, A., J.M. McDonnell, and S.J. Korsmeyer, *BCL-2 family members and the mitochondria in apoptosis.* Genes Dev, 1999. **13**(15): p. 1899-911.
192. Beavon, I.R., *Regulation of E-cadherin: does hypoxia initiate the metastatic cascade?* Mol Pathol, 1999. **52**(4): p. 179-88.
193. Le Bivic, A., et al., *Vectorial targeting of an endogenous apical membrane sialoglycoprotein and uvomorulin in MDCK cells.* J Cell Biol, 1990. **110**(5): p. 1533-9.
194. Stockinger, A., et al., *E-cadherin regulates cell growth by modulating proliferation-dependent beta-catenin transcriptional activity.* J Cell Biol, 2001. **154**(6): p. 1185-96.

195. Arsova-Sarafinovska, Z., et al., *Manganese superoxide dismutase (MnSOD) genetic polymorphism is associated with risk of early-onset prostate cancer.* Cell Biochem Funct, 2008. **26**(7): p. 771-7.
196. Bansal, M.P., et al., *DNA sequencing of a mouse liver protein that binds selenium: implications for selenium's mechanism of action in cancer prevention.* Carcinogenesis, 1990. **11**(11): p. 2071-3.
197. Bansal, M.P., et al., *Evidence for two selenium-binding proteins distinct from glutathione peroxidase in mouse liver.* Carcinogenesis, 1989. **10**(3): p. 541-6.
198. Ansong, E., et al., *Evidence that Selenium Binding Protein 1 is a Tumor Suppressor in Prostate Cancer.* PLoS One, 2015. **Under Review**.
199. Huang, C., et al., *Decreased Selenium-Binding Protein 1 Enhances Glutathione Peroxidase 1 Activity and Downregulates HIF-1alpha to Promote Hepatocellular Carcinoma Invasiveness.* Clin Cancer Res, 2012. **18**: p. 3042-53.
200. Fang, W., et al., *Functional and physical interaction between the selenium-binding protein 1 (SBP1) and the glutathione peroxidase 1 selenoprotein.* Carcinogenesis, 2010. **31**(8): p. 1360-6.
201. Morales, A., et al., *Oxidative damage of mitochondrial and nuclear DNA induced by ionizing radiation in human hepatoblastoma cells.* Int J Radiat Oncol Biol Phys, 1998. **42**(1): p. 191-203.
202. Apostolou, S., et al., *Growth inhibition and induction of apoptosis in mesothelioma cells by selenium and dependence on selenoprotein SEP15 genotype.* Oncogene, 2004. **23**(29): p. 1-9.
203. Nagai H., N.M., Carter S. L., Gillum D. R., Rosenberg A. L., Schwartz G. F., Croce C. M., *Detection and Cloning of a Common Region of Loss of Heterozygosity at Chromosome 1p in Breast Cancer.* Cancer Res, 1995. **55:1752–1757**.
204. Cheung T. H., C.T.K., Poon C. S., Hampton G. M., Wang V. W., Wong Y. F. , *Allelic loss on chromosome 1 is associated with tumor progression of cervical carcinoma.* Cancer Genet, 1999. **86:1294–1298**.
205. Bang, J., et al., *Deficiency of the 15-kDa selenoprotein led to cytoskeleton remodeling and non-apoptotic membrane blebbing through a RhoA/ROCK pathway.* Biochem Biophys Res Commun, 2015. **456**(4): p. 884-90.

VITAE

Dede N. Ekoue

Education

2011-Present Ph.D., University of Illinois at Chicago, in progress

2007 B.S., Molecular and Cellular Biology, University of Illinois at Urbana-Champaign

Research Experience

2011-Present Ph.D. Candidate, Department of Pathology, University of Illinois at Chicago

2006 Ronald E. McNair/Summer Research Opportunity Program, Microbiology & Molecular Genetics, Michigan State University

2005 Undergraduate Mentoring in Environmental Biology, Spatial Epidemiology, University Of Illinois at Urbana-Champaign

Academic and Professional Honors

2015-Present Research Supplement to Promote Diversity in Health-Related Research Pre-Doctoral Fellowship, National Institute of Health (3R21CA182103-02W1)

2016 Federation of American Societies for Experimental Biology (FASEB) Maximizing Access to Research Careers (MARC) Travel Grant, Experimental Biology, San Diego, CA

2015 Federation of American Societies for Experimental Biology (FASEB) Maximizing Access to Research Careers (MARC) Travel Grant, Experimental Biology, Boston, MA

2015 Chancellor's Student Service and Leadership Award (CSSLA), University of Illinois at Chicago

2014-2015 Center for Clinical and Translational Science (UIC CCTS) Pre-Doctoral Education for Clinical and Translational Scientists (PECTS) Fellowship, University of Illinois at Chicago

Research Papers

1. **Ekoue DE**, Ansong E, Macias V, Deaton R, Kajdacsy-Balla A, Li L, Picklo M, Freeman VL, Gann PH, Diamond AM. The Sep15 Selenoprotein Localizes to the Outer Plasma Membrane in Human Prostatic Tissue and Its Levels are Reduced in Prostate Cancer. Manuscript in preparation.
2. **Ekoue DE**, Bera S, Ansong E, Hart PC, Dorman F, Bonini M, Diamond AM. Polymorphisms in the Genes Encoding MnSOD and GPx-1 Interact to Affect Gene Expression and Energy Metabolism. Manuscript in preparation.
3. Ansong E, Ying Q, **Ekoue DN**, Deaton R, Hall AR, Kajdacsy-Balla A, Yang W, Gann PH, Diamond AM. Evidence that selenium binding protein 1 is a tumor suppressor in prostate cancer. PLoS One. 2015.
4. Hart PC, Mao M, de Abreu AL, Ansenberger-Fricano K, **Ekoue DN**, Ganini D, Kajdacsy-Balla A, Diamond AM, Minshall RD, Consolaro ME, Santos JK,

Bonini MG. MnSOD upregulation sustains the Warburg effect via mitochondrial ROS and AMPK-dependent signaling in cancer. Nat Commun. 2015.

5. Bera S, Weinber F, **Ekoue DN**, Ansenberger-Fricano K, Mao M, Bonini MG, Diamond AM. Natural allelic variations in glutathione peroxidase-1 affect its subcellular localization and function. Cancer Res. 2014.
6. Reinke EN, **Ekoue DN**, Bera S, Mahmud N, Diamond AM. Translational regulation of GPx-1 and Gpx-4 by the mTOR pathway. PloS One. 2014.

Reviews

Ekoue DN, Diamond AM. It takes 2 antioxidants to tango: the interaction between manganese superoxide dismutase and glutathione peroxidase-1. Turkish Journal of Biology. 2014.

Abstracts

1. **Oral presentation**, Disease Associated Polymorphisms in MnsOD and GPx-1 Affect Metabolism, Mitochondrial Membrane Potential and Expression of Signaling Proteins, Experimental Biology, San Diego, CA, 2016.
2. **Poster presentation**, Allelic Variations in the Gene for Glutathione Peroxidase-1 Differentially Affect Cell Migration as well as the Levels of pAkt and E-Cadherin, Experimental Biology, San Diego, CA, 2016.
3. **Poster presentation**, Biochemical Interactions between Allelic Variations in the MnSOD and GPx-1 Affects Cancer Related Pathways, Translational Science, Washington DC, 2015.
4. **Poster presentation**, Disease-Associated Variations in Glutathione Peroxidase-1 Affect Its Subcellular Localization and Function, Experimental Biology, Boston, MA, 2015.
5. **Poster presentation**, Genotype and Cellular Localization Affect GPx-1 Function, College of Medicine Research Symposium, University of Illinois at Chicago, 2013.

Complete List of Published Work in MyBibliography:
http://www.ncbi.nlm.nih.gov/sites/myncbi/10mmHWlrEtrk_/bibliograpahy/49914333/public/?sort=date&direction=ascending